AD-A035 217 GOLDSWORTHY ENGINEERING INC TORRANCE CALIF F/G 11/4
MM AND T-PULTRUDED COMPOSITE STRUCTURAL ELEMENTS.(U)
DEC 76 B H JONES, W JAKWAY DAAJ02-74-C-0053
UNCLASSIFIED USAAMRDL-TR-76-5 NL

1 OF 2
ADA035217



AD A035217

USAAMRDL-TR-76-5

12
5c

MM&T - PULTRUDED COMPOSITE STRUCTURAL ELEMENTS

Goldsworthy Engineering, Inc.
2917 Lomita Blvd.
Torrance, CA 90505

December 1976

Final Report

DDC
RECEIVED
FEB 4 1977
A

Approved for public release;
distribution unlimited.

Prepared for

U. S. ARMY AVIATION SYSTEMS COMMAND
P. O. Box 209
St. Louis, Mo. 63166

EUSTIS DIRECTORATE
U. S. ARMY AIR MOBILITY RESEARCH AND DEVELOPMENT LABORATORY
Fort Eustis, Va. 23604

391379

EUSTIS DIRECTORATE POSITION STATEMENT

This manufacturing methods and technology project has been accomplished as part of the U. S. Army Aviation Systems Command Production Engineering Missions Program. This report identifies the application of pultruded structural elements, provides design allowables data, and establishes a fabrication technology base. Results of this contract are being integrated with other R&D efforts at the Eustis Directorate to improve the characteristics of future Army aircraft systems.

Robert L. Rodgers of the Technology Applications Division served as technical monitor for this effort.

DISCLAIMERS

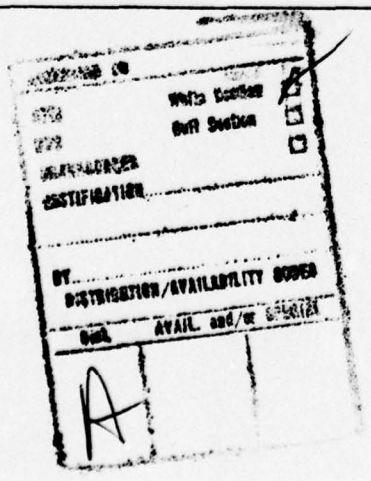
The findings in this report are not to be construed as an official Department of the Army position unless so designated by other authorized documents.

When Government drawings, specifications, or other data are used for any purpose other than in connection with a definitely related Government procurement operation, the United States Government thereby incurs no responsibility nor any obligation whatsoever; and the fact that the Government may have formulated, furnished, or in any way supplied the said drawings, specifications, or other data is not to be regarded by implication or otherwise as in any manner licensing the holder or any other person or corporation, or conveying any rights or permission, to manufacture, use, or sell any patented invention that may in any way be related thereto.

Trade names cited in this report do not constitute an official endorsement or approval of the use of such commercial hardware or software.

DISPOSITION INSTRUCTIONS

Destroy this report when no longer needed. Do not return it to the originator.



UNCLASSIFIED

SECURITY CLASSIFICATION OF THIS PAGE (When Data Entered)

REPORT DOCUMENTATION PAGE	READ INSTRUCTIONS BEFORE COMPLETING FORM
1. REPORT NUMBER: USAAMRDL-TR-76-5	2. GOVT ACCESSION NO. / 3. RECIPIENT'S CATALOG NUMBER
4. TITLE (and Subtitle): MMAT - PULTRUDED COMPOSITE STRUCTURAL ELEMENTS.	5. TYPE OF REPORT & PERIOD COVERED: FINAL Rept. 1
	6. PERFORMING ORG. REPORT NUMBER
7. AUTHOR(s): Brian H. Jones, William Jakway, (Appendix C - William Jakway)	8. CONTRACT OR GRANT NUMBER(s): DAAJ02-74-C-0053 new
9. PERFORMING ORGANIZATION NAME AND ADDRESS: Goldsworthy Engineering, Inc., 2917 Lomita Blvd., Torrance, CA 90505.	10. PROGRAM ELEMENT, PROJECT, TASK AREA & WORK UNIT NUMBERS
11. CONTROLLING OFFICE NAME AND ADDRESS: U.S. Army Aviation Systems Command, St. Louis, Missouri 63166.	12. REPORT DATE: December 1976
	13. NUMBER OF PAGES: 123 (12) 124 p.
14. MONITORING AGENCY NAME & ADDRESS (if different from Controlling Office): Eustis Directorate, U.S. Army Air Mobility R&D Laboratory, Fort Eustis, Virginia 23604	15. SECURITY CLASS. (of this report): Unclassified
	15a. DECLASSIFICATION/DOWNGRADING SCHEDULE

16. DISTRIBUTION STATEMENT (of this Report)

Approved for public release; distribution unlimited.

17. DISTRIBUTION STATEMENT (of the abstract entered in Block 20, if different from Report)

18. SUPPLEMENTARY NOTES

19. KEY WORDS (Continue on reverse side if necessary and identify by block number)

Pultrusion
Composites
Graphite/Epoxy
Post Forming Graphite/Epoxy Pultrusions
Pultrusion Design Allowables

20. ABSTRACT (Continue on reverse side if necessary and identify by block number)

The objectives of this program were to establish the manufacturing technology base in order to pultrude with a range of resin matrices and reinforcing forms, to investigate the post-forming capability of epoxy matrix pultrusions, and to derive a representative range of static and fatigue mechanical property design allowables. Additionally, structural efficiency studies were performed to evaluate the potential advantages of using pultruded substructural elements.

DD FORM 1 JAN 73 1473 EDITION OF 1 NOV 65 IS OBSOLETE

UNCLASSIFIED

SECURITY CLASSIFICATION OF THIS PAGE (When Data Entered)

391 379

bpg

20. ABSTRACT - Continued

It was concluded that even using existing epoxy systems, pultrusion is a highly viable process that results in structures possessing good mechanical properties at potentially low cost. Post-forming operations may be readily carried out, which further enhances the potential application areas for the technique.

PREFACE

This investigation of manufacturing technology for pultruded composite structural elements was performed under Contract DAAJ02-74-C-0053 for the Eustis Directorate, U.S. Army Air Mobility Research and Development Laboratory, Fort Eustis, Virginia and was under the general technical cognizance of Mr. R.L. Rodgers of the Technical Applications Division.

The authors acknowledge contributions to this program by Messrs William Pao, Robert Zark, and Dennis Waldemar of Goldsworthy Engineering. They also acknowledge gratefully the interest shown by Mr. Thomas Mazza of USAAMRDL and Mr. Robert Vollmer of AVSCOM, St. Louis.

TABLE OF CONTENTS

	Page
PREFACE	3
LIST OF ILLUSTRATIONS	7
LIST OF TABLES	11
INTRODUCTION	13
GENERAL DESCRIPTION OF THE PULTRUSION PROCESS	15
Process Considerations	16
RESIN SELECTION	20
Polymerization Thermochemistry - Polyesters and Epoxies	20
Use of Mold Releases in Pultrusion	21
Resin Evaluation - Polyester	24
Resin Evaluation - Epoxy	25
FIBER SELECTION	42
Graphite Fibers Evaluated	43
Fiberglass Fibers Evaluated	44
Kevlar Fibers Evaluated	44
DETERMINATION OF DESIGN ALLOWABLES	45
Results of Mechanical Property Evaluations	47
Discussion of Test Results	59
DESIGN ALLOWABLES EVALUATION	64
PRODUCTION AND TEST OF DEMONSTRATION ARTICLE	71
APPLICATION STUDIES	81
Parametric Studies	81
Manufacturing Cost Studies	94
CONCLUSIONS	96
RECOMMENDATIONS	98

PRECEDING PAGE BLANK-NOT FILMED

Page

REFERENCES CITED..... 99

APPENDIXES

A. Chemical Considerations for Epoxy Resins When Being Used in Pultrusion..... 101

B. Chemical Considerations for Polyester Resins When Being Used in Pultrusion..... 107

C. Derivation of Structural Efficiency Equations.... 111

LIST OF SYMBOLS..... 122

LIST OF ILLUSTRATIONS

Figure		Page
1	Pultrusion Process.....	13
2	Typical Pultruder Using Augmented Cure on Multiple Product Streams.....	17
3	Adjustable Pultrusion Die.....	29
4	Effects of Various Hardeners and Diluents on the Interlaminar Shear Strength of Epoxy Resins..	32
5	Tank Life for Epoxy Resins With 14 phr MPDA and 15 phr BGE.....	34
6	Tank Life for Epoxy Resins With 16 phr MPDA and 10 phr BGE.....	35
7	Tank Life for Epoxy Resins With 23 phr RF-45 and BGE.....	36
8	Tank Life for Epoxy Resins With 14 phr MPDA and DMF.....	36
9	Tensile Test Specimens for 0° and Off-Axis Fiber Orientation.....	48
10	Tensile Test Specimens for 90° Fiber Orientation.....	48
11	Loading Fixture to Maintain Alignment for 90° Tension Tests.....	49
12	Compression Specimens.....	49
13	Compression Test Fixture Showing Load Introduction and Supports.....	55
14	Tension Fatigue Specimens.....	55
15	Shear Stress Distribution in a Rectangular Shaft.....	56
16	0° Tensile Stress-Strain Relationships of Hercules AS With Various Resins.....	61

LIST OF ILLUSTRATIONS (continued)

Figure		Page
17	90° Tensile Stress-Strain Relationships of Hercules AS With Various Resins.....	61
18	0° Tensile Stress-Strain Relationships of OC HTS-904 Fiberglass With Various Resins.....	61
19	90° Tensile Stress-Strain Relationships of OC HTS-904 Fiberglass With Various Resins.....	61
20	0° Compression Stress-Strain Relationships of Hercules AS With Various Resins.....	62
21	90° Compression Stress-Strain Relationships of Hercules AS With Various Resins.....	62
22	0° Compression Stress-Strain Relationships of OC HTS-904 Fiberglass With Various Resins.....	62
23	90° Compression Stress-Strain Relationships of OC HTS-904 Fiberglass With Various Resins.....	62
24	Short Beam Interlaminar Shear Strength Comparison.....	63
25	S-N Curve for Hercules AS/Shell 826 Unidirectional Laminate Tested in 0° Direction in Tensile Fatigue.....	65
26	S-N Curve for OC HTS-904/Shell 826 Unidirectional Laminate Tested in 0° Direction in Tensile Fatigue.....	65
27	S-N Curve for Hercules AS/Shell 826 ($\pm 45_C$) Laminate in Tensile Fatigue.....	66
28	S-N Curve for Hercules AS/Shell 826 ($0, \pm 45_S$) Laminate in Tensile Fatigue.....	66
29	S-N Curve for OC HTS-904/Shell 826 ($\pm 20_C$) Laminate in Tensile Fatigue.....	67
30	S-N Curve for OC HTS-904/Shell 826 ($0, \pm 20_S$) Laminate in Tensile Fatigue.....	67
31	S-N Curve for Hercules AS/Shell 826 Unidirectional Laminate in Torsional Fatigue.....	68

LIST OF ILLUSTRATIONS (continued)

Figure		Page
32	S-N Curve for OC HTS-904/Shell 826 Unidirectional Laminate in Torsional Fatigue.....	68
33	One-Sided Tolerance Limits and Sample Size for the Normal Distribution.....	69
34	Demonstration Article-Integrally Stiffened Panel.....	72
35	Pultrusion of Demonstration Article.....	73
36	Entrance to Resin Tank.....	74
37	Entrance to Pultrusion Die.....	74
38	Postforming Tool.....	75
39	Section of Postformed Material.....	75
40	Panel Undergoing Buckling Tests.....	77
41	Load Deflection Relationships Obtained During Buckling Tests.....	77
42	Crippling Stress of (0,$\pm$45) Hybrid Composite.....	80
43	Webcore Panel-Dimensions and Coordinate System...	83
44	Single-Face Corrugated Skin Panel-Dimensions and Coordinate System.....	83
45	Minimum Weight Curves for Structural Efficiency Analysis.....	86
46	Webcore Designs Analyzed.....	86
47	Structural Weight Relation for Webcore Panel.....	88
48	Distribution of Plies in Single-Face Corrugated Panels.....	88
49	Fiberglass Versus Graphite for Angle Ply Layers With Single-Face Corrugated Panels.....	90

LIST OF ILLUSTRATIONS (continued)

Figure		Page
50	Thickness Effect in Single-Face Corrugated Panels.....	90
51	Modulus Effect in Single-Face Corrugated Panels.....	91
52	Orientation Effect of Fibers for Single-Face Corrugated Panels.....	91
53	Material Comparison for Single-Face Corrugated Panels.....	92
54	Characteristic Die Costs	93

LIST OF TABLES

Table		Page
1	Interlaminar Shear Strength of Hercules AS Graphite Fiber With Various Polyester Resins.....	25
2	Fiber, Resin, and Hardener Combinations Evaluated for Die Adhesion Characteristics.....	30
3	Effects of Diluents on Resin Viscosity at Room Temperature.....	32
4	Flexural Strength at 170°F and Interlaminar Shear Strength at Room Temperature (Hercules AS Graphite/Epoxy).....	33
5	Interlaminar Shear Strength of Various Intermediate Grades of Graphite Fiber With Shell 826/MPDA/DMF.....	43
6	Tension Test Result Averages.....	50
7	Compression Test Result Averages.....	51
8	In-Plane Shear Test Result Averages.....	53
9	Four Point Flexural Test Result Averages.....	53
10	Short Beam Interlaminar Shear Test Result Averages.....	54
11	Tensile Fatigue Test Results With Hercules AS Fiber/826 Resin, Fiber Oriented 0° to Load.....	57
12	Tensile Fatigue Test Results With OC HTS-904/ 826 Resin, Fiber Oriented 0° to Load.....	58
13	Torsional Fatigue of Hercules AS/826 Unidirectional Composite.....	60
14	Torsional Fatigue of S-Glass/826 Unidirectional Composite.....	60
15	Design Allowables (B-Value) for Pultruded Composite.....	70

LIST OF TABLES (continued)

Table		Page
16	Crippling Test Results of Elements From Final Article.....	78
17	Unidirectional Properties of Composite Materials Used in Efficiency Analysis.....	79

INTRODUCTION

Over the past seven years, a large number of research and development programs have been conducted by the Government and private industry to study the potential of advanced composites for use in aircraft structures. While these studies have shown that the use of high-stiffness, high-strength composites (such as graphite-epoxy) can reduce structural weight, widespread application has not generally occurred. The high cost of the basic fibers has been only partly responsible for this; another reason has been the generally uneconomic costs of structural fabrication. It is being increasingly recognized that the use of advanced composites will only become viable provided consideration is given to developing cost-effective manufacturing procedures which minimize the labor content inherent in producing the structure.

One production technology that holds considerable promise for reducing fabrication costs to a realistic level is that known as pultrusion - the forming of structural shapes by pulling preimpregnated oriented filaments through a heated die (Figure 1). Pultrusion is one of the few basic processes in the reinforced plastics industry that converts primary raw materials directly into a finished product, continuously and automatically.

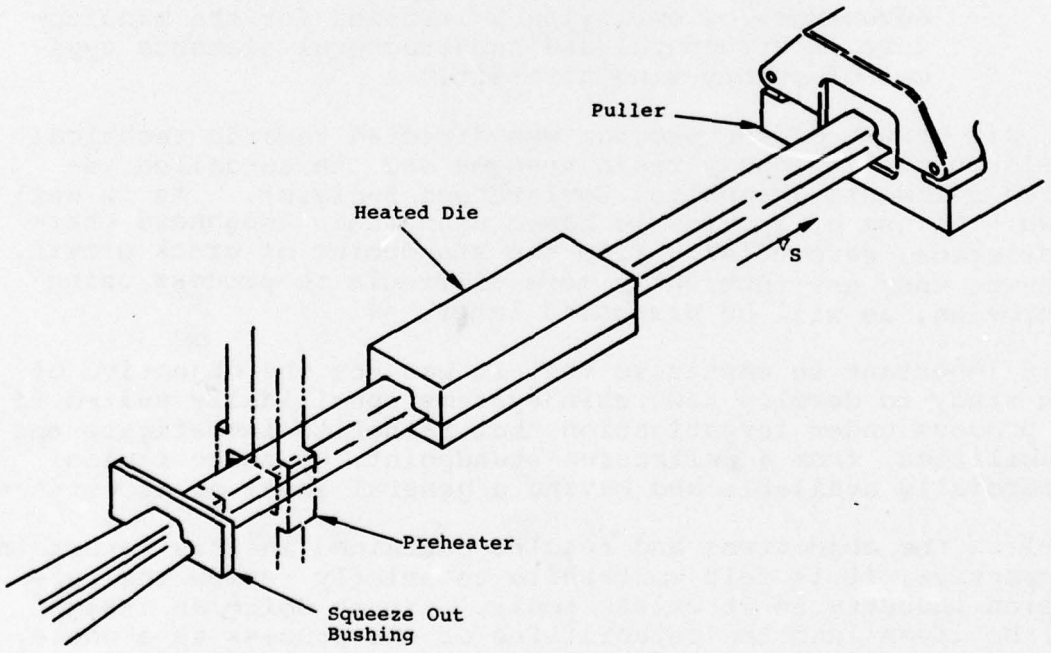


Figure 1. Pultrusion Process.

For some time, it has been recognized that the use of pultruded composite elements in aerospace structures offers the potential for realizing highly cost-effective designs.[1] This is particularly evident in the case of rotary-wing vehicles, where the generally favorable geometric and loading conditions suggest many design concepts highly suited to a pultruded approach. However, in order that adequate designs can be established, a data base of material properties must be available and the processing conditions must be capable of realistic definition. The purpose of this program was to provide such information.

Investigations were conducted in three phases:

1. To define the fabrication technology base for the pultrusion of cured and partially-cured structural shapes with the objective of enhancing the design potential of the pultrusion technique for a variety of structural configurations.

2. To provide initial design allowables data (static and dynamic) for pultruded structural materials to form a base for a design philosophy and criterion.

3. To identify the potential economic and performance advantages of employing pultrusion for the manufacture of structural and substructural elements typical of rotary-wing aircraft.

The main thrust of the program was directed towards technical developments with epoxy resin systems and the so-called advanced filaments (graphite, Kevlar® and S-glass). As is well known, the use of epoxies is based upon their toughness characteristics, particularly from the standpoint of crack growth. However, they are inherently more difficult to process using pultrusion, as will be discussed later.

It is important to emphasize that it was not the objective of this study to develop new resin systems specifically suited to the process under investigation, but rather to investigate the capabilities, from a pultrusion standpoint, of those resins commercially available and having a general level of acceptance.

To place the objectives and results contained in this report in perspective, it is felt worthwhile to briefly review the pultrusion industry as it exists today. In so doing, an insight will be given into the capabilities of the process as a whole.

GENERAL DESCRIPTION OF THE PULTRUSION PROCESS

The pultrusion process can be performed by up to 12 machine type variations, [2] characterized by

(a) intermittent or continuous pulling

(b) horizontal or vertical mounting

(c) tractor or reciprocating - clamp pullers

(d) conductive, dielectric or inductive curing (or combinations thereof.)

The thermosetting matrix is polymerized by the addition of heat, which may be added prior to entering the die in addition to during passage through the die. When heat is added during both periods, the cure is described as being augmented. [3] The die material is generally made of suitably plated steel, but fluoroplastics and ceramics may also be used. [3] With other than dielectric or inductive preheating, production rates are ultimately set by the thermal conductivity of the resin system. [4] Suitable preheating systems can increase production rates significantly, the limits being set by the onset of thermal cracks due to mass effect and degraded surface finish.

It is often erroneously assumed that pultrusion employs only unidirectional reinforcements. This is not the case; almost every accepted form (roving, tow, mat, cloth, braiding), from all types of filaments (glass, graphite, Kevlar, boron, steel, nylon, etc) may be used. Consideration must, however, be given to:

(a) intrinsic strength and stiffness of the impregnated material (adequate axial strength must be present to sustain instantaneous pulling forces.)

(b) thermal conductivity and specific heat (second order-effects, influencing rate of heat transmitted from die, etc.)

(c) volume ratio of reinforcing-to-matrix (controls mass effect during curing.)

If some form of dielectric or inductive preheating (injection of heat prior to final cure in the die) is being used, the electrical properties of the filaments (dielectric constant, loss tangent, etc.) become significant.

A pultrusion machine having continuous pulling capability

employing reciprocating clamp pullers together with augmented cure using radio-frequency dielectric augmented cure is shown in Figure 2.

The material properties required in the finished product can dictate that angle plies of fibers are necessary. Fibers oriented in the direction of pulling are best against the die surface. A cloth pulled in the warp direction will have the fill yarns displaced due to the friction of the die. The displacement will not normally be sufficient to cause jamming in the die, but continuous filament mat with a binder of low solubility in the resin can be used against the die surface. When other than random (mat) or 0°, 90° (cloth) fiber orientations are required, then braided fabric tapes can be used. Since they are fabrics, the orientations are balanced, i.e., $\pm$ 20°, $\pm$ 45°, etc.

The general requirements of the pultrusion process can be combined in a variety of ways to provide an economical solution to the fabrication of composite products while maintaining consistent quality, material properties and high production rates.

PROCESS CONSIDERATIONS

The process of pultrusion is concerned essentially with:

(a) ensuring that the resin matrix is subjected to a temperature-time history sufficient to ensure an adequate level of polymerization prior to being gripped by the puller system. At the same time, the combined effects of thermal and mechanical stress gradients caused by heating, cooling, shrinkage and pulling must not cause unacceptable material property degradation.

(b) ensuring that the impregnated material, during passage through the die, does not create shear forces that give rise to pulling requirements in excess of the intrinsic strength of the part or that cause surface spalling.

Obviously, (a) is a function of the level of preheat (if augmented cure is being employed), resin reactivity (due to hardeners, accelerators, and catalysts), die temperature, die length, stock speed, stock dimensions, mass effects and stock transverse thermal conductivity. Shear forces arise from:

1. Viscous shear - a function of temperature and the amount of diluent used. As the impregnated mass enters the heated die, the viscosity first drops and

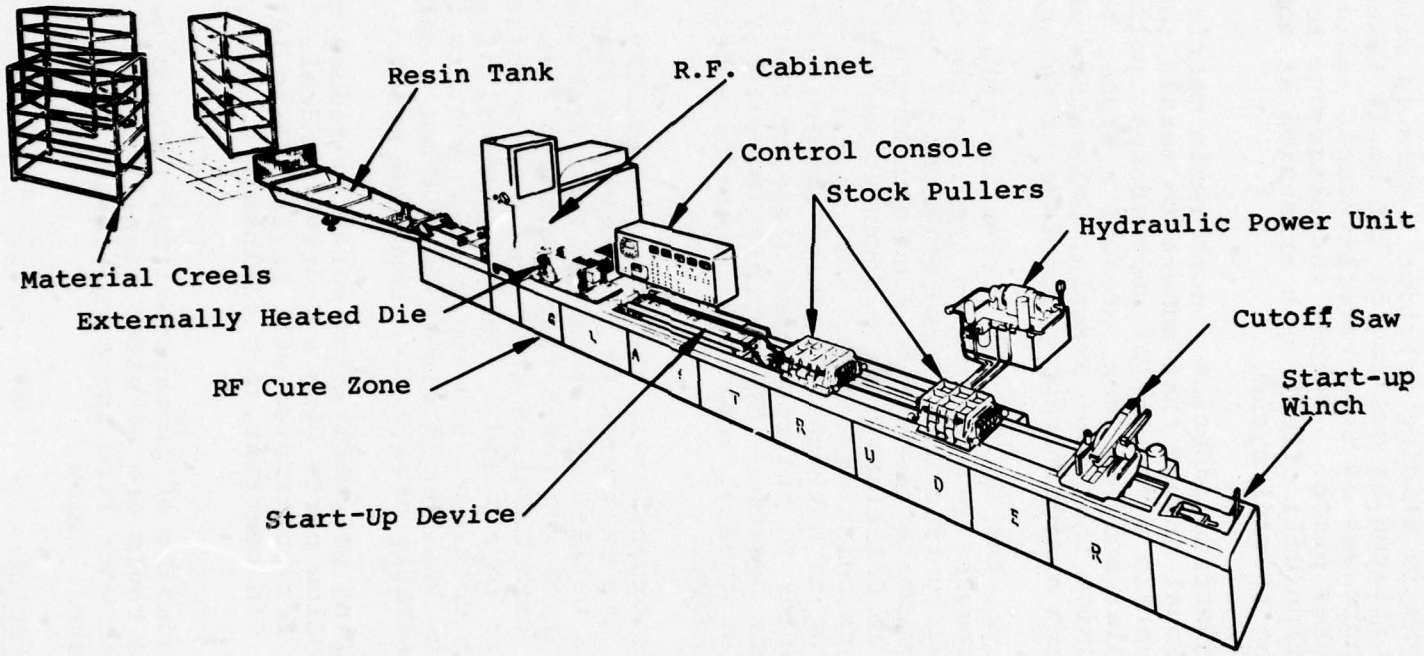


Figure 2. Typical Pultruder Using Augmented Cure on Multiple Product Streams.

then rises again as polymerization proceeds.

2. Dynamic sliding friction - this is assumed to be initiated as gelling of the resin takes place and increases as temperature-induced radial expansion takes place. Volume shrinkage due to polymerization will offset such expansion at some point in the thermal cycle.

3. Interface adhesion - most resin matrices have functional groups that adhere to metals (epoxy molecules contain a variety of such groups, polar and nonpolar and, as such, produce a higher level of adhesion than, for example, polyesters which do not have a significant percentage of polar groups).

As noted above, the frictional forces are related to the level of radial stresses (which are, in turn, mainly dependent upon the expansion/contraction characteristics of the resin), the effective composite restrained modulus,and the instantaneous coefficient of friction.Since pultrusion generally results in some filaments being exposed to sliding frictional effects, it is interesting to note that graphite reinforcements are fundamentally easier to pultrude than glass or Kevlar when using the same resin system. This occurs in spite of the transverse coefficient of thermal expansion of graphite being of the order 20×10^{-6} in/in/°F.

Resin thermal expansion in the die is initially relieved by backflow. The expansion in the composite that increases die forces occurs between gellation and exit from the die. The characteristic of the resin that minimizes this effect is a sharp temperature level at which gel occurs followed by rapid polymerization to a solid. This is typical of polyester resin systems. In contrast, the epoxy resin systems typically exhibit a steady buildup in viscosity without a definite gel point and generally have slower reaction rates.

Shrinkage during polymerization works to reduce the die forces, except for hollow parts with a central mandrel. Typical polyester resins for pultrusion will shrink 7% to 10% during polymerization. In contrast, the shrinkage of epoxy resins is 1% to 6%.

From the standpoint of processability, three other characteristics of the resin are of vital significance, viz., filament wetting, resin work life and cure time. These aspects are discussed separately below.

Viscosity Effects

During wet impregnation of the fiber stream, the viscosity of

the resin system is a primary factor in wet-out and a secondary factor in controlling resin content. Basically, wetting of the fibers is a function of the relative surface energies of the solid and liquid involved. The fiberglass and graphite fibers have finishes or surface treatments to ensure good wetting; the Kevlar® fibers generally do not. In addition, the viscosity of the resin must be sufficiently low to ensure that the wetting is not transport limited. At the same time, it must have a high enough viscosity to prevent excessive draining from the fiber-resin stream after leaving the wet-out bath.

Experience has shown that, in general, good wetting will be obtained with viscosities below 1200 centipoise and excessive drainage will not occur at viscosities above 200 centipoise. Special techniques can be employed to operate outside this viscosity range. The resin can be heated to lower the viscosity below 200 centipoise, then the fiber-resin stream cooled after leaving the bath to increase the viscosity and prevent drainage. For higher viscosities, the rate of pulling can be reduced or the bath length increased.

Above about 15,000 to 20,000 centipoise, the viscous drag of the resin at the squeeze-out bushings, guides, or the die entrance may become high enough to commence breaking the filaments at the surface of the stream.

Resin Work Life

The pultrusion process is an automated, high-production process that realizes its greatest economies through continuous operation. A resin system, to be compatible with this type of operation, should have a long pot life or gel time at bath temperatures. Then, large batches of resin can be prepared that will be usable for a protracted period of time.

A work life of 1 week is desirable, 8 hours is acceptable, and as a minimum, it can be equal to the time required to pass the resin volume in the impregnation tank through the die at operating speeds. This latter time will allow fresh resin to be added to the bath as the level is drawn down, thereby allowing continuous operation.

Cure Time

In the pultrusion process, a fast cure time permits higher production rates and/or shorter dies. There is an upper limit on pulling speed, depending upon each resin-fiber-die combination. Since the polymerization of epoxy and polyester resins is an exothermic reaction, the polymerization will continue after leaving the die. In practice, a full cure is not required before the part leaves the die. It is only necessary that the

resin be hard enough to maintain its shape, and possess sufficient tensile and compressive strength to resist the forces exerted by the gripping/pulling system.

RESIN SELECTION

As has been emphasized previously, it was not one of the objectives of this program to evolve the optimum resin system for pultrusion, but rather to evaluate the pultrusion capabilities of those resin systems that were commercially available and which had a reasonable level of aerospace acceptance. The latter requirement demanded attention be directed primarily toward epoxies (intended for wet impregnation and preimpregnation) and secondarily toward polyesters (liquid and solid at room temperature).

Recent experience with epoxy matrix composites has indicated a tendency to absorb water in such a manner as to subsequently affect mechanical strength at elevated temperature [5]. As a consequence, attention is being directed toward the potential of high-performance polyesters.

For each resin type, level of compatability with the filamentary reinforcements used for aerospace application, i.e., graphite, Kevlar and S-glass, were quantified. The factors evaluated included:

(a) Tendency to die adherence, assessed only from the standpoint of acceptable/unacceptable. Actual levels of adherence were not measured.

(b) Change of viscosity with temperature, time and amount of diluent.

(c) Mechanical properties, evaluated in terms of interlaminar shear strength (considered to be a sensitive indicator of intrinsic resin performance, wet-out and processing control).

POLYMERIZATION THERMOCHEMISTRY - POLYESTERS AND EPOXIES

To aid evaluation of the results to be presented, it is proposed to briefly review the thermochemistry of both polyesters and epoxies as it applies to the pultrusion process. A more detailed discussion is to be found in Appendixes A and B of this report.

Polyesters

The unsaturated polyesters generally used in reinforced plastics consist of an ester dissolved in polymerizable monomer which

provides three-dimensional chain cross-linking.

The solution is generally polymerized under the influence of heat and/or peroxide catalyst (more correctly an initiator) to produce an infusible thermoset. Under the influence of the energy imparted by the heat, the catalyst breaks down into free radicals which initiate polymerization. A chain reaction then occurs whereby molecules are caused to react and unite. The higher the temperature, the faster the rate of catalyst decomposition. The rate of polymerization can therefore be controlled by regulating the temperature and also the amount of catalyst used.

Theoretically, the reaction should proceed to the point where all unbroken double bonds of the original unsaturated mixture are reacted by the free radicals.

In fact, about 92-95% of unsaturation is converted.[6] Gelation occurs when about 35-40% of unsaturation has taken place, the gel hardening with a reduction of volume. An incomplete cure exists when a total of approximately 80% of the unsaturation has been utilized.

Epoxies

Of the three major types of epoxy in commercial use, the epichlorohydrin/bisphenol A resins are most readily suited to pultrusion. The epoxy novalacs, used frequently as the basis for prepregs, may be used for wet impregnation pultrusion processing only,with some difficulty.

In the pultrusion process, curing agents (rather than catalysts) are generally used as the hardener, amines and acid anhydrides finding the greatest range of suitability. Aliphatic amines will give tight fast cures at room temperature but usually have a short pot life and yield products with low heat deflection temperatures. Aromatic amines result in a product with good heat deflection characteristics and chemical resistance, in addition to having a reduced tendency to adhere to the die wall when compared to anhydrides. The suggested chemical reason for this is established in Appendix A.

While anhydrides yield products with high heat deflection temperatures, good chemical resistance, low exotherms, etc., their increased tendency to die adhesion is viewed as a significant disadvantage. As indicated below, the use of internal mold releases to offset such adhesive tendencies is not recommended.

USE OF MOLD RELEASES IN PULTRUSION

Mold releases are typically fatty acids or waxes that are sol-

uble in the liquid resin, but come out of solution during polymerization. The use of these internal mold releases was evaluated for the pultrusion process by a two-step procedure carried out on stainless steel, a material known to have low tendencies for adhesion:

Step 1. A 304 stainless steel plate was wet sanded with No. 600 sandpaper to simulate the honed surface of a pultrusion die. Half of the plate was buffed to a mirror surface and then oxidized by heating to 350°F for 2 hours. One-half of the honed and mirrored surface was coated with carnuba wax and held at 250°F for 2 hours to treat the surface. A second 304 plate was prepared by sanding and buffing to a mirror surface, then oxidized at 350°F for 2 hours.

Step 2. Stainless steel tubing, 0.25 inch I.D., was cut 24 inches long and one end flared. The bore of the tubing was honed to remove ripples and any draw marks. The tubes were mounted in a square aluminum holder for use as dies.

Mold Releases Investigated

Various mold releases were combined with an epoxy resin system that had been used for pultrusion, though with problems of adherence to the die. The resin system was Ciba 6010 Epoxy with NMA Hardener (nodic methyl anhydride) 72 phr., Ciba Accelerator 062 (benzyldimethylamine) 3 phr., and Ciba Reactive Diluent RD-2 (1, butanediol diglycidl ether) 16 phr. The following mold releases were tested by adding 2% by weight to the resin:

1. Atlas Chemical Ind., Inc.
   Atmul 84

2. Argus Chemical Corp.
   Stearone

3. Glyco Chemicals, Inc.
   Acrawax C Atomized

4. Ram Chemicals
   Moldgard X

5. Axel Plastics Res. Labs., Inc.
   Mold Wiz No. INT-18E
   Mold Wiz. No. INT-18-36
   Mold Wiz. No. INT-114-NO

6. Contour Chemical Co.

Results Obtained Using Mold Releases

The first plate was heated to 350°F, and each of the resin solutions containing the mold releases was dropped on the four surface treatments. In all cases the resin was a soft gel in about 1-1/2 minutes and a hard gel in about 3 minutes, showing no inhibiting action from any of the mold releases. With the plates at 350°F, the resins were scraped to check for release properties from the surfaces. The release was poorer from the carnuba wax-treated surface than from the clean metal. As expected,the highly polished stainless steel surface released better than the sanded surface. The best release was obtained with the Mold Wiz No. INT-18E.

To further evaluate the Mold Wiz No. INT-18E, the resin was prepared with 0, 1, 2 and 3 percent mold release. The second plate was heated to 350°F, and spots of each of the resin solutions were poured on the plate. After curing for 5 minutes, the spots were scraped off and tested for adhesion and residue left on the plates. Almost perfect release and minimal residue were left on the plate with 3% mold release.

Evaluation of the mold release under dynamic pultrusion conditions was next evaluated with the 0.25-inch I.D. tube die. The initial set of runs were made without mold release added to the resin and using E-glass, graphite and Kevlar® fibers.

Runs were made with both Hercules A-S and Thornel 300 graphite fibers. There was no discernable difference between these fibers. They could be pultruded continuously, but after running 30 to 40 feet the surfaces showed spalling of the resin. After a stop in the run, of only 30 seconds, it was impossible to restart. The addition of 3% Mold Wiz No. INT-18E to the resin had no effect on the results and was not deemed successful.

The E-glass and Kevlar® behaved the same during the trial runs. In both cases, without mold release, the resin adhered to the die and surface fibers began breaking out. After 20 to 30 feet of material had been run, the amount of fibers broken had reduced the cross-sectional area of the rod sufficiently so that it broke from the pulling force. The addition of mold release to the resin reduced the adherence of the resin sufficiently to allow a continuous run. However, the same spalling and degradation of the surface was observed as with the graphite fibers.

Conclusions Reached From Mold Release Tests

The results of the testing demonstrated that internal mold releases slightly improve the pultrusion characteristics of epoxy resins in concentrations of approximately 3% by weight. Use of mold releases in concentrations above 1% by weight can degrade the resin properties. Therefore, solutions to die sticking were sought by changes in the epoxy resin system and hardener used.

RESIN EVALUATION - POLYESTER

The pultrusion process has predominately used polyester resins due to their lower viscosity at room temperature, faster cures, longer pot lives, and lower cost. However, the use of polyester with graphite is typified by low mechanical properties, especially compression and shear. The interlaminar shear strength is in the range of 6,000 to 7,500 psi.

Approach

The influence of different polyester resins and a fiber size on the mechanical properties of graphite-polyester composites was evaluated by molding unidirectional bar specimens and then testing for interlaminar shear strength.

Polyester Resins Investigated

The resins selected were as follows:

1. Silmar 685 - a liquid isophtalic-styrene resin developed for pultrusion.

2. Lubrizol 24161 - a solid isophtalic-acrylic resin with about 6% shrinkage.

3. Pittsburgh Plate Glass F34-117 - a solid, crystalline, fusible, aromatic resin with about 3% shrinkage. This resin also has a 264 psi heat distortion temperature greater than 500°F.

To improve adhesion between the graphite filaments of main interest and the polyesters, the filaments were coated with a special size, as described below.

Sizing of graphite filaments for use with polyester

The size for the graphite fibers was a special clear epoxy primer BC-401, developed by Glidden to improve adhesion of unsaturated polyester laminating resins to surfaces. Hercules AS graphite fibers were used in the test. It was found that

pulling the fibers through a mixture of 3 parts primer to 1000 parts epoxy thinner left a very light film of the primer on the fibers. The sized fibers were left to air-dry overnight.

Testing and Results

Using filaments that were sized and unsized, two test specimens 0.80 X 0.250 X 6.0 inches were match-die molded from each resin. The resins were catalyzed with 1.5% benzoyl peroxide and cured at 300°F for 1 hour. The fiber content of the bars was 60 v/o. The specimens were cut into test coupons and tested for interlaminar shear strength, in accordance with ASTM D-2344 -72, at a span-to-depth ratio of 4. The results of the tests are presented in Table 1.

TABLE 1. INTERLAMINAR SHEAR STRENGTH OF HERCULES AS GRAPHITE FIBER WITH VARIOUS POLYESTER RESINS

RESIN	CONTROL		SIZED		% of
	ILS (PSI)	C.V. (%)	ILS (PSI)	C.V. (%)	Change
Silmar 685	7,500	5.1	9,300	6.0	+24
Lubrizol 24161	7,600	6.6	8,200	5.2	+ 8
PPG F34-117	7,800	1.6	12,000	3.2	+54

Conclusions

It will be noted that for all resins the sized fibers resulted in higher composite interlaminar shear strengths. Also, the new class of aromatic polyester resins showed a marked improvement in strength and can be expected to show major improvements in the other mechanical properties.

RESIN EVALUATION - EPOXY

Selecting a resin system involved a consideration of various chemical, physical and mechanical properties. Pultrusion requires the resin system to have low viscosity, stability at impregnation bath temperatures, fast gel time, good wet-out of the fibers, and good mechanical properties. High-performance aircraft applications require the resin system to be moisture resistant, weather well, have temperature capabilities in the 175°F to 200°F range and exhibit good toughness. Two basic groups were investigated, the first conventional liquid, the second resins formulated for prepregging.

Liquid Resins

The resins were evaluated primarily for low viscosity and good all-round properties. Also considered was the data base available on the resin regarding their properties, reactions and general use. The resins selected were:

1. Shell Epon 828 - a 11,000 to 15,000 centipoise viscosity bisphenol A - epichlorohydrin type epoxy resin.

2. Shell Epon 815 - a 500 to 700 centipoise viscosity version of Epon 828 with butyldiglycidylether diluent added to lower viscosity.

3. Shell Epon 826 - a 6,500 to 9,500 centipoise viscosity epoxy resin.

4. Ciba Araldite 6010 - a 12,000 to 16,000 centipoise viscosity bisphenol A - epichlorhydrin type epoxy resin.

5. Dow DER-332 - a 4,000 to 6,000 centipoise viscosity bisphenol A - epichlorohydrin type epoxy resin.

Other manufacturers have similar resins, but with the above there is extensive data on their performance with various hardeners, accelerators, and diluents. These resins are widely used and with the proper hardeners have good properties at elevated temperatures.

Hardeners Used With Liquid Resins

The hardeners were reviewed with respect to their ability to minimize die adherence, to reduce the viscosity of the resins, to influence gel time, to influence pot life, and to influence elevated temperature properties. The hardeners selected were:

1. Nadic methyl anhydride (NMA) - a low-viscosity liquid. The anhydride hardeners are frequently used in adhesive formulations to promote the adhesion of epoxy resins.

2. Aromatic diamine (Shell Y) - a medium-viscosity liquid used at 30 phr.

3. Aromatic diamine (Shell Z) - a medium-viscosity liquid used at 20 phr.

4. Menthane diamine (E.V. Roberts RF-45) - a low-viscosity liquid used at 22 phr.

5. Metaphenylene diamine (MPDA) - a solid that, when

heated to 150°F, becomes liquid and is used at 14 phr.

6. Linear polyamide (Versamid 140)- a medium-viscosity liquid used at 30 phr.

7. Polymeric diamine (Furane 9231) - a high-viscosity liquid used at 12 phr.

Compared to amine curing agents, anhydrides react at a slower rate with epoxy resins in addition to requiring higher cure temperatures and longer cure time. Due to the low solubility of the anhydrides in the resin, special techniques are necessary to ensure uniform dispersion. While increased solubility can be obtained by increasing temperatures, this will usually result in shorter pot life. Anhydrides such as methyl nadic anhydride are liquid at room temperature and therefore exhibit improved solubility. In Europe, eutectic mixtures of anhydrides or the higher melting point dianhydrides are sometimes used for pultrusion processing.

Of the amines, the aromatics are generally preferred for pultrusion since they give a good pot life in addition to high heat distortion temperature and chemical resistance.

When using a primary amine, the reaction involves opening the epoxide ring through an electronegative attack by nitrogen to form an alcohol without formation of by-products. For the anhydride, reaction is initiated by the formation of an ester through the anhydride and an hydroxyl group present in the amine.

Any oxide present on the die surface will electronegatively attack epoxide groups and produce adhesion. Tendency to die sticking appears slightly greater with anhydrides than with amines, since the metal oxides or metal hydroxyl groups attack the epoxide ring in a similar manner to the secondary alcohol in the anhydride case.

Diluents Used With Liquid Resins

The diluents investigated were of two types: reactive and unreactive. They were selected for their ability to reduce the viscosity of the epoxy resins. Diluents tend to reduce the mechanical properties of the cured epoxy resins. Therefore, the intent was to add the smallest amount of diluent possible. The diluents selected were:

1. Butyl glycidyl ether (BGE)

2. 1, 4 - butanediol diglycidyl ether (BDE)

3. Dimethylformamide (DMF)

Process Evaluation - Liquid Epoxies

Evaluation of the resin involved:

(a) Investigating the level of die adherence.

(b) Determining the extent to which the viscosity of the resin was to be modified by application of heat or diluents in order to attain adequate wet out.

(c) Establishing characteristic curing rates while pultruding a circular rod.

(d) Testing the pultruded product to determine mechanical properties in terms of interlaminar shear strength, flexural strength and modulus.

The level of general process control was evaluated by determining the coefficient of variation observed in the mechanical properties data.

Die Adherence

Die adherence phenomena were investigated by control of die surface characteristics (treatment, finish) and by variation of the polymerization process involved in cross-linking the resin.

From the tests carried out into the influence of internal mold releases, it was determined that the most advantageous conditions to minimize die sticking would be attained using stainless steel, since this material does not readily form an oxide that possesses high electron attracting characteristics (high surface energy), was readily capable of being finished to produce low surface roughness under protracted use, and would not require replating (as would be the case with a steel/chrome plated die).

The stainless steel die, 24 inches long, is shown in Figure 3, and was designed with the objective of enabling specimens of various widths and thicknesses to be pultruded. The die, when pinned and bolted together, can form cavities with thicknesses of either 0.08, 0.10 or 0.125 inch and widths of 0.25 or 0.50 inch. The cover plates were 304 stainless steel and the shim spacers were steel chrome plated. A hole drilled into the upper cover plate to the centerline of the die accommodated a thermocouple probe that was attached to a temperature controller. After polishing, the die surfaces were conditioned by holding them at 350°F for 4 hours. Following this, one end of the die was plugged then filled with molten carnuba wax and held at 250°F for 24 hours.

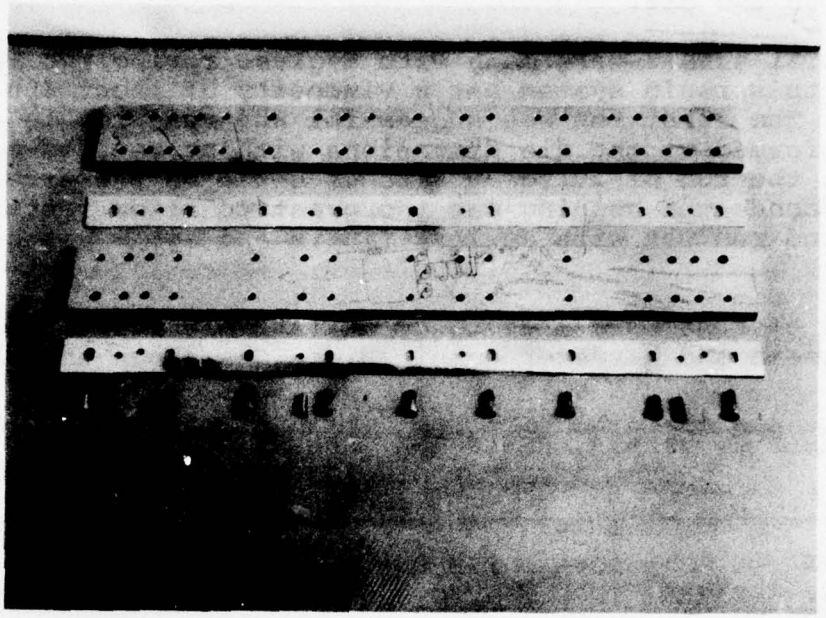


Figure 3. Break-Apart Adjustable Stainless Steel Die - 24 Inches Long.

Four 1000-watt strip heaters were attached to the cover plates, two on top and two on the bottom.

Initial trials through the die with E-glass roving and the Ciba 6010/NMA resin system all resulted in die adherence and termination of the run. The die was opened after the runs and it could be seen that a resin buildup was occurring on the die surface, about two-thirds of the way from the entrance. By opening the die immediately following a run, while the die was still hot, it could be seen that a resin buildup was occurring at the point of initial gellation of the resin. The resin buildup reduced the die opening and caused the product to jam in the die.

The second approach was to vary the type of hardener. As reviewed earlier, the anhydride hardeners react by activating the

hydroxyl groups on the epoxy resin and proceed in a chain reaction. The activated hydroxyl groups, at the mold surface, can promote bonding. Conversely, the amine hardeners react with the terminal epoxide groups. The result is less tendency to bond to the die.

The initial trials were made with E-glass roving and Epon 815/RF45 as this resin system has a viscosity of about 600 centipoise. The first run was successful and resulted in a part that conformed to the die dimensions without rounded corners. Stops in the run of 20 to 30 seconds could be restarted, but at 60 seconds the bonding was too great to allow restarting. The second run was with Kevlar® fibers and again was successful.

A series of runs were made to quantitatively evaluate different fiber, resin and hardener combinations, as shown in Table 2.

TABLE 2. FIBER, RESIN AND HARDENER COMBINATIONS EVALUATED FOR DIE ADHESION CHARACTERISTICS

RUN NO.	FIBER	# OF ROV-INGS	FIBER V/O	RESIN	HARDENER	DIE TEMP. °F
1	E-Glass	5	60	Epon 815	RF-45	400
2	Kevlar®	5	60	Epon 815	RF-45	400
3	Herc.-AS	15	55	Epon 815	RF-45	400
4	Herc.-AS	15	55	Epon 815	Shell Z	350
5	E-Glass	5	60	Epon 815	RF-45	400
6	E-Glass	5	60	Epon 828	RF-45	400
7	E-Glass	5	60	Epon 815	Shell Z	350
8	E-Glass	5	60	Epon 815	MPDA	400
9	E-Glass	5	60	Epon 828	MPDA	400
10	E-Glass	5	60	Epon 828	MPDA	400
11	E-Glass	5	60	Epon 815	Furane 9231	400
12	E-Glass	5	60	Epon 828	Furane 9231	400
13	E-Glass	5	60	Epon 828	Furane 9231	400
14	E-Glass	5	60	Epon 828	Shell Z	350

Run No. 5 was made with the Mold Wiz INT-18E added to the 815/RF45 resin. There was no change that could be discerned between this run and No. 1 without the mold release. The higher viscosity resin systems were run in a heated impregnating bath to reduce resin viscosity to between 1000 and 2000 centipoise.

During these runs, the die temperature was set initially at 350°F, then the pull rate was adjusted until the fiber-resin stream emerging from the die was just solid. If the pull rate was then below 10 to 12 inches per minute, the die temperature was increased to 400°F and the pulling speed readjusted. If the resin system showed signs of being burned, the die temperature was reduced.

From these runs it was concluded that, in general, epoxy resin with amine hardeners could be successfully pultruded without sticking in the die with fiberglass, Kevlar® or graphite fibers.

Viscosity Investigations

The viscosity of the resin in the impregnation tank is of prime importance in controlling fiber wetting, resin content, air entrapment and voids. From the prior runs it was established that a practical upper limit on the viscosity of the resin should be about 1000 centipoise. From experience with polyester resins, the lower limit was set between 300 and 500 centipoise. A viscosity above 1000 centipoise requires additional attention from the machine operator to ensure wetting and a smooth fiber flow. Entrapped air in the fiber-resin stream is normally removed at the squeeze-out bushings and the die entrance. A viscosity below 300 or 400 centipoise allows air to reenter the fiber-resin stream.

All the epoxy resins selected for development have viscosities above 1000 centipoise, except the Shell Epon 815. However, this latter resin is identical to Epon 828 with about 15 phr butyl glycidyl ether as a diluent to adjust the viscosity to 500 to 700 centipoise. Therefore, the Epon 815 was dropped from the investigation.

The MPDA and RF-45 hardeners have the greatest effect on lowering the viscosity of the epoxy resins and give good elevated temperature mechanical properties. The viscosity of all the resins with these hardeners was above 1000 centipoise. The viscosities were then lowered by the addition of both butyl glycidyl ether (BGE) and dimethylformamide (DMF) to the resins. The results are given in Table 3. The viscosities were measured with a Brookfield Viscometer using a No. 1 spindle.

To evaluate these resin systems, a series of pultrusion runs were made with seven rovings of E-glass in a .10-x.25-inch die. The material from the run could then be cut into lengths for short beam interlaminar shear tests. The results of the interlaminar shear tests on the composite from the runs is shown in Figure 4. In reviewing the data it will be noted that with

TABLE 3. EFFECT OF DILUENTS ON RESIN VISCOSITY AT ROOM TEMPERATURE

	Viscosity - Centipoise							
	Shell 828		Shell 826		Ciba 6010		Dow 332	
Diluent phr	MPDA	RF45	MPDA	RF45	MPDA	RF45	MPDA	RF45
BGE 15	600	-	-	-	510	-	-	-
BGE 10	-	-	750	-	-	400	500	-
BGE 7.5	-	-	-	400	-	-	-	-
DMF 5	-	-	-	-	800	630	-	-
DMF 2.5	-	-	650	550	-	-	-	-
DMF 2	-	-	-	-	-	-	-	525

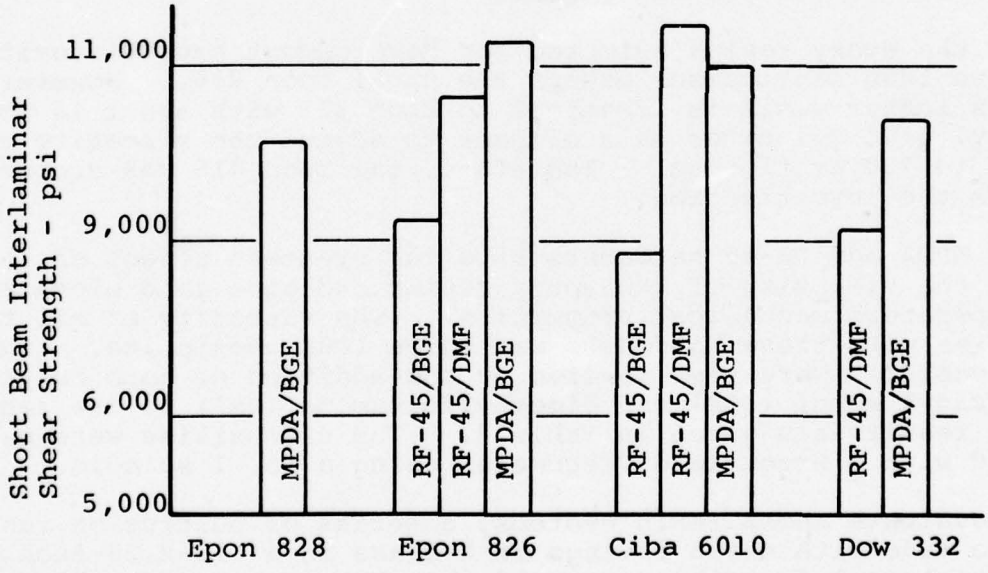


Figure 4. Effects of Various Hardeners and Diluents on the Interlaminar Shear Strength of Epoxy Resins.

the same hardener, the DMF diluent gave higher strenths, and of the two hardeners, the MPDA gave better values. Based on these results, two final pultrusion runs were made using Thornel 300 graphite fibers in the 0.10-x 0.25-inch die. To produce 60 volume percent graphite, 88 tows of the 3000 filament tows were required. Two resin systems were chosen for these runs as follows:

1.	Shell Epon 826	100 parts
	MPDA	14 phr
	DMF	5 phr
	Viscosity @ 100°F	500 cps
2.	Ciba 6010	100 parts
	MPDA	14 phr
	DMF	7.5 phr
	Viscosity @ 100°F	500 cps

The runs were made with a heated and thermostatically controlled impregnating tank maintained between 100°F and 120°F.

The results of short beam interlaminar shear tests on the graphite-epoxy material from the runs were almost identical, with the Epon 826 system being 11,700 psi and the Ciba 6010 system being 11,400 psi. The respective coefficients of variation were 7.6% and 3.3%. These results, in themselves, were not considered sufficiently conclusive to enable resin selection to be confidently made. Since, in general, the addition of diluents decreases the elevated temperature strength of epoxy resins it was felt desirable, therefore, to make two additional pultrusion runs using Hercules AS graphite fiber with 10,000 filaments per tow for four-point flexure testing at 170°F together with interlaminar shear strength at room temperature. The test results are shown in Table 4.

TABLE 4. FLEXURAL STRENGTH AT 170°F AND INTERLAMINAR SHEAR STRENGTH AT ROOM TEMPERATURE (HERCULES AS GRAPHITE/EPOXY)

Resin System	170°F Flexural strength (PSI)	Interlaminar shear strength (PSI)
826/MPDA/DMF	145,000	14,300
6010/MPDA/DMF	113,000	12,300

These tests identified the advantage of the lower diluent percentage possible with the Shell Epon 826 resin. As a result of this testing, the choice of the liquid epoxy resin system for the program was 826/MPDA/DMF.

Tank Life

In a continuous process, the work life of the resin ideally should be several days. However, if the impregnating bath volume can be kept small in relation to the resin being withdrawn, it is practical to have work lives for the resin of the order of 3 to 4 hours. Less than this time causes problems in mixing small batches and is too time-consuming. The working life of a resin system varies with the type of hardener, temperature of the bath and mass of the sample.

To evaluate the tank life of the resin-hardener-diluent systems studied for viscosity effects, a 1-quart sample of each of the resin systems was held at 77°F, and the viscosity of the mixture was tested each hour for 8 hours. The criterion used to establish the usable tank life was that the viscosity could not exceed 1000 centipoise. The viscosity was measured with a Brookfield Viscometer using a No. 1 spindle.

The results of the test at room temperature for the Shell 828/MPDA and Ciba 6010/MPDA, both with 15 phr of BGE, are shown in Figure 5.

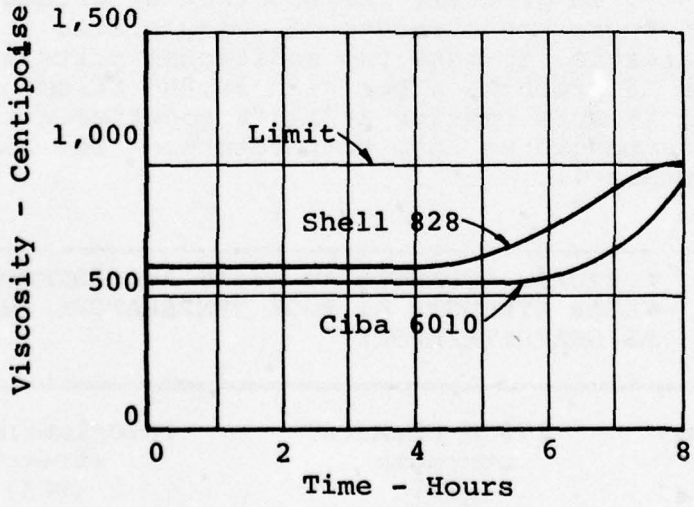


Figure 5. Tank Life for Epoxy Resins With 14 phr MPDA and 15 phr BGE.

The results for the other resin systems at room temperature are shown in Figures 6, 7 and 8. The tank life of the

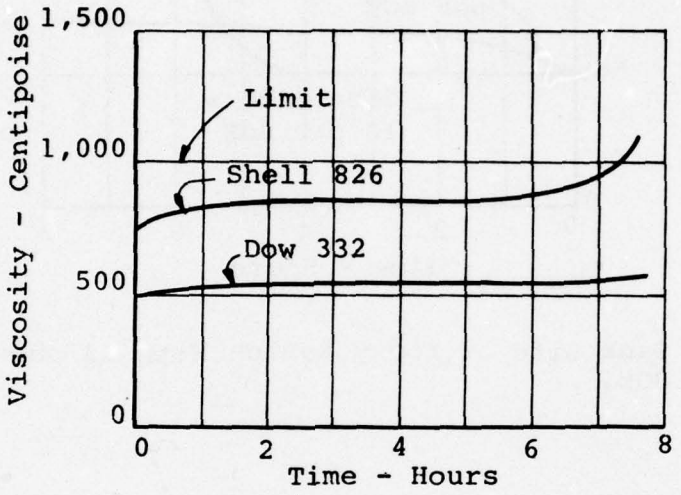


Figure 6. Tank Life for Epoxy Resins With 16 phr MPDA and 10 phr BGE.

Shell 826/MPDA/DMF system, shown in Figure 7, indicates 6 hours to reach a viscosity of 1000 centipoise at room temperature and 4 hours at 120°F. These items are acceptable for a production system.

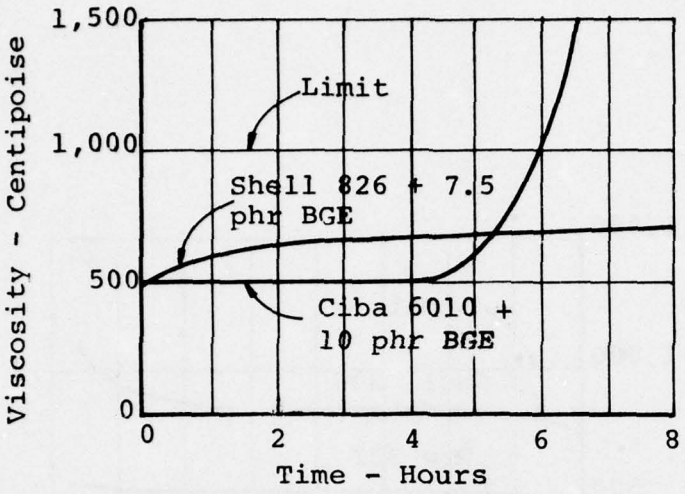


Figure 7. Tank Life of Epoxy Resins With 23 phr RF-45 and BGE.

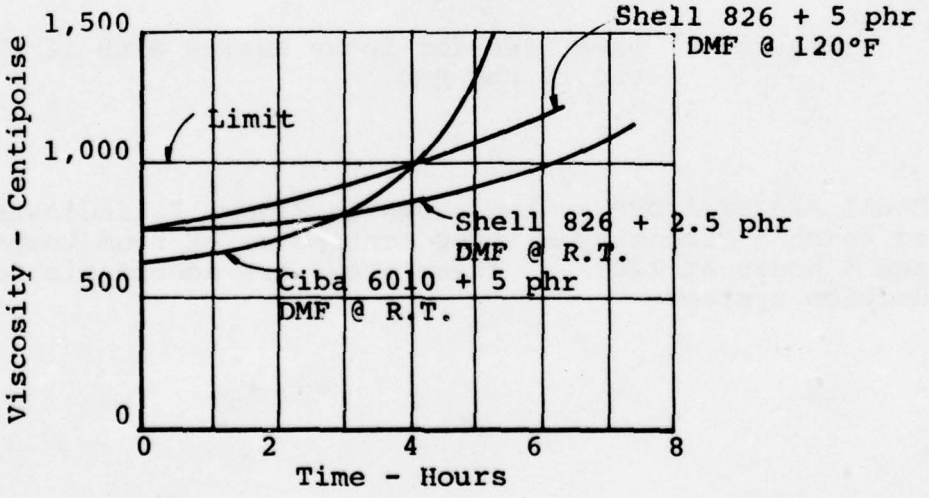


Figure 8. Tank Life of Epoxy Resins With 14 phr MPDA and DMF

Cure Time Characteristics

The extremely fast epoxy resin and hardener systems that give cure times in the order of minutes also have very short work lives. As a result, this type of epoxy system is not suitable for pultrusion. The more stable epoxy systems that also are effective matrices in structural composites have extended cure times and cure schedules normally including various phases for applying vacuum and pressure to the system as well as definite temperature and time steps. (For the Shell 826/MPDA/DMF resin system, a typical cure cycle would be to hold the part at 100 psi pressure for 30 minutes at 300°F followed by removal from the mold and postcure either 1 hour at 400°F or 2 hours at 300°F.)

In pultrusion, the exposure of the resin matrix to a thermal cycle is a function of the die length and part pulling speed. Since the force required to pull a part through a pultrusion die is a direct function of die length and surface area, the practical limit to die length may be set by the tensile strength of the fiber-resin stream and the cross sectional area of the part. In this program, die length was limited to 24 inches because of the greater sticking tendency of the epoxy resins. The pulling speeds were varied from 6 inches per minute to 24 inches per minute. Below 6 inches per minute pulling speed, the part progressed in an irregular manner through the die. Therefore, speeds below 6 inches per minute were not used. The upper limit of 24 inches per minute was set by the general cure requirements of the resin.

At a die temperature of 400°F, a speed of 24 inches per minute could be obtained with the Shell 826/MPDA/DMF epoxy with any of the fibers identified earlier. The resin went from a soft gel to a hard gel in the final 8 inches of the die, giving a "cure time" of 20 seconds. By using either induction preheat with graphite-epoxy or RF preheat with fiberglass-epoxy, soft gel could be attained just inside the die entrance; under such conditions, a 24-inch die would allow a maximum pull speed of about 60 inches per minute.

The Shell 826/MPDA/DMF resin system will advance to about a 90% cure after 30 minutes at 300°F under pressure, or 2 hours at 175°F at atmospheric pressure. An additional postcure is required for maximum properties. Based on these times and temperatures, it can be appreciated that the resin coming out of the die is just advanced in polymerization past the B stage and is essentially in a hard gel state. Also, the pultrusion process can not be operated slow enough to realize a complete cure during pultrusion. Advantage can be taken of this situation where postforming of the pultruded part is desirable.

Postforming Evaluation

A series of experiments was performed on the 826/MPDA/DMF resin system to determine its potential for being postformed. Using 0.04-inch-thick by 2.25-inch-wide sheets of unidirectional graphite/epoxy, a series of tests were run to postform transverse to the filaments over radii of 2, 3.5 and 4 inches. The first attempts were made using a vacuum bag and holding the part in an oven at 175°F for one-half hour. Another set was taken through 2 hours at 175°F followed by 2 hours at 300°F, the normal cure cycle. In neither case did the part postform. By preheating the parts to 325°F to 335°F for 3 to 5 minutes, then transferring to a jig and applying pressure, the parts readily formed. It was determined that the parts had to be maintained in the jig throughout the cure cycle in order to maintain the curvature. Consistent forming could be accomplished down to a radius of curvature-to-thickness ratio (R/t) of 50 without cracking. A slight spring back was noted after release of jig pressure. Experiments performed trying to postform with radius of curvature longitudinal to the filaments were unsuccessful. Neither preheating to 325°F to 335°F prior to forming nor forming at room temperature prior to heating was successful. The specimens that were bent cold and then heated for curing experienced compressive failures on the inner surface. Specimens that were heated and bent slowly into shape could be cured successfully when R/t was greater than 250. However, on release from the jig they sprang back to an essentially flat condition.

Discussion - Liquid Epoxy Resins

From this series of experiments, an epoxy resin system has been defined that is compatible with the parameters required for the pultrusion process. The Shell 826/MPDA/DMF resin system has the following advantages:

1. Die adherence is minimum, and long runs can be made. It will permit short stoppages of 20 to 30 seconds.
2. The resin can be used with fiberglass, Kevlar® and graphite fibers with equal ease.
3. The viscosity of 500 to 1000 centipoise gives good wet-out of the fiber streams.
4. The tank life of about 4 hours is sufficient for continuous operation of the process.
5. The product that leaves the die is in a solid enough state to enable cutting and reasonable

handling until it is cured.

6. The 2 feet per minute pulling speed for heated dies is adequate. However, for parts with large cross sections and for higher pulling speeds, auxiliary heating sources should be used to achieve speeds for up to 5 feet per minute.

7. Postforming transverse to the filaments is possible at R/t = 50 or greater for unidirectional or angle plied composites.

The resin system has the following disadvantages:

1. Die adherence will possibly occur for stops longer than 30 seconds, requiring the string-up procedure to be repeated.

2. While the work life is adequate under certain conditions, it is not as long as would be required for general usage.

3. The cure of the resin is not complete when the product exits the die, necessitating a postcure. This postcure may, of course, be carried out without further application of pressure or containment within tooling.

Process Evaluation - Prepreg Resins

As will be discussed later in this report, the suitability of available prepreg resins was evaluated in the form of: (1) a conventional prepreg (resin previously applied to graphite filaments), and (2) a bulk resin (supplied in such a manner as to inhibit polymerization by being packed in dry ice).

With the exception of Narmco Materials, no companies involved in prepregging were willing to supply bulk resin. Through the cooperation of Narmco, the following resins were made available in both conventional and bulk form:

1. Rigidite 5209 - a 250°F service temperature resin with a fast cure cycle and 150°F liquid point.

2. Rigidite 5208 - 350°F service temperature resin with a slower cure cycle and 225°F liquid point.

The Narmco 5208 and 5209 resin systems are widely used in prepreg form for graphite-epoxy aircraft parts. As a result,

there is extensive data available on the composite mechanical properties when cured in an autoclave. Both 5208 and 5209 resins at room temperature have the same form, being slightly tacky semisolids. However, the 5209 is a 250°F service temperature resin. The 5209 melts at a low temperature and cures faster than the 5208.

Prepreg Graphite-epoxy Tapes

Thornel 300 prepreg tapes, 3 inches wide, were obtained of both 5208 and 5209 resin. The trials with these tapes were made with a 0.10 x 0.25 cross section die. The tapes were slit into 0.50-inch-wide ribbons for feeding into the die. It was calculated that 8 ribbons would give a fiber volume content of 56%. In practice, only 6 ribbons could be strung through the die; it was planned to add the remaining 2 ribbons after the runs were started.

The first run was with Narmco 5209. The die was heated to 200°F and then the tape was pulled slowly till the die reached 300°F. Simultaneously it was necessary to place a heat gun on the prepreg entering the die to melt the resin. In 3 trials it was never possible to stabilize the run sufficiently to add the additional 2 ribbons before the prepreg stream would adhere to the die and stop the run. This prepreg system was abandoned at this point.

The second set of runs was made with the 5208 prepreg. It has a higher cure temperature and a slower cure time. The tapes were again cut into ribbons, and 6 ribbons were pulled through the die. The 5208 resin has a gel time of about 3 hours at 300°F. Therefore, the die temperature was brought to 350°F before the prepreg stream was started moving slowly. In this case a stabilized run was achieved at 8 inches per minute and a die temperature of 450°F. The product stream exiting the die was in a solid gel state. When attempts were made to introduce the final 2 ribbons of prepreg, the outer fibers commenced shearing off at the die entrance and the fiber-resin stream broke in the middle of the die. After 3 attempts, the use of prepreg was abandoned.

Actually, dry prepregs are a product form designed specifically for another production process: lay-up and autoclave cure. The Narmco 5208 prepreg can be pultruded by installing a temperature-controlled oven system before the die to preheat the resin to 300°F and maintain this temperature until the product stream enters the die. However, it would require a fairly extensive development of the prepreg guides, bushings and controls to achieve a production operation.

Bulk Prepreg Resins

The resins were shipped packed in dry ice and maintained at 0°F until used. The resins are tacky solids at room temperature and hard friable solids at 0°F; in the latter condition they may be easily broken into convenient sized pieces.

The initial testing was to establish the temperature at which the resins would have a viscosity of 1000 centipoise or less. Samples were heated in an oil bath until melted, and then the temperature was increased while measuring the viscosity with a Brooksfield Viscometer. The 5209 resin had a viscosity of about 900 centipoise at 200°F. However, the time required to heat the resin to this temperature was sufficient that it would gel shortly after. After several attempts to decrease the heat-up time, it was determined that there was not enough tank life, about 20 minutes, at 200°F to warrant making trial runs with this resin system.

The Rigidite 5208 resin was then melted and heated to determine its viscosity. At a temperature of 300°F the resin had a viscosity of about 900 centipoise. Checks on the tank life at this temperature showed almost no change in viscosity for 1 hour, and it required about 2 hours before gellation.

For the first pultrusion run,additional strip heaters were added to the side walls of the impregnation tank and insulation was added to facilitate maintaining a constant bath temperature. Cold resin would make wet-out difficult and excessively hot resin would shorten the tank life. The initial runs were made with Hercules AS graphite fiber and a 0.125-x 0.50-inch cross-section die using 53 tows of 10,000 filaments. The first run was made with the bath 15 inches from the die and with one squeeze-out bushing. The fiber-resin stream cooled so quickly on leaving the bath that at the squeeze-out bushing, the high viscosity of the resin began shearing off filaments. A second run with the bath 3 inches from the die was also unsuccessful. By keeping the impregnating bath exit with 0.50 to 0.75 inch of the die entrance, successful runs were made. The exit from the bath was used as the squeeze-out bushing. At a die temperature of 450°F the running speed was 15 inches per minute. The gelled parts were subsequently postcured in an oven for 1 hour at 275°F and then 2 hours at 350°F.

Interlaminar shear tests performed on the bars gave a strength of 18,500 psi and a coefficient of variation of 3.5%. This value agrees with the values reported for test specimens made from prepreg autoclave cured.

Discussion - Prepreg Resin Systems

Once the process parameters were established, the Narmco 5208 resin pultruded quite well. The short tank life of about 1 hour is satisfactory for a development program, but would preclude using the resin for a production process. In discussions with Narmco, they indicated that the resin system could be modified slightly so it would have a 900 centipoise viscosity at a lower temperature. The lower temperature would then extend the tank life. The change in the resin system would, however, result in a slight decrease in mechanical properties. Such a development may well be appropriate in further expanding the potential of epoxy resins in the pultrusion process.

FIBER SELECTION

The fiber reinforcement for pultrusion can be of any of the forms such as rovings, tows, cloth, mat, or tapes. The primary requirement of the various forms is that they be available in continuous lengths. The various forms can also be used in all combinations. Each form should have enough integrity to withstand any forces induced during pultrusion, though the more fragile types can be placed between stronger layers. In general, best results are obtained if the fibers in contact with the die surface are unidirectional rovings, tows or yarns. When cloth is against the die surface there will be a washing or displacement of the fill fibers. With some of the looser weaves the washing of the fibers can be sufficient to locally increase their density and cause jamming of the fiber stream in the die.

The unidirectional roving and tows are the most widely used reinforcements for pultruding. Yarns can also be used, but the twist makes impregnation more difficult. Also,they tend to stay as bundles of fibers with resin-rich areas between yarns. The size of the filament bundle can be very important. It requires 53 graphite tows with 10,000 filaments to fill a 0.10-x 0.50-inch cross-section die. For a part with one square inch cross section this translates into 1060 tows. While a high end or tow count can potentially offset this, too large a bundle can make adequate wet-out difficult.

As with filament winding, the filaments should have finishes applied to them to minimize the formation of "fuzz" and make handling easier. Additionally, such finishes generally promote resin wetting.

Catenaries should be absent if good fiber collimation is to be maintained and breakages from filament buildup obviated. The filamentary reinforcement should be supplied in the no-twist center-pull configuration to permit ease of splicing.

Woven cloths can be obtained woven or slit to given widths. These materials are convenient to enhance the transverse properties of pultrusions. In a continuous woven tape, it is only possible to get longitudinal and transverse reinforcement.

Tapes slit from mats offer in-plane isotropic reinforcement layers. With mats the fiber content is low in comparison to other forms of reinforcement.

By braiding instead of weaving,balanced angle ply tapes can be formed. The braided tapes can be obtained as either tubes or flat tape with fiber angles of $\pm 20°$ to $\pm 70°$. The inclusion of longitudinal yarns in the braid will prevent scissoring of the fibers during pulling.

Graphite Fibers Evaluated

During the program a number of graphite fiber tows were investigated and evaluated. In discussions with various airframe manufacturers and fiber suppliers,it became evident that the intermediate property grade of graphite was being used in the largest volume and, hence, was available at the lowest cost. Thornel 300, Hercules AS and Celanese GT30 are typical of this grade. Pultrusion runs with epoxy resin were made with all three fibers successfully. The Thornel 300 was a 3000-fiber tow and required 3-1/3 times as many packages to fill a die. The Celanese GT30 was new and not offered for sale. The Hercules AS is a 10,000-fiber tow and was supplied as four tows wound together on a bobbin. The results of short beam interlaminar shear tests carried out on samples produced using each filamentary type are shown in Table 5.

TABLE 5. INTERLAMINAR SHEAR STRENGTH OF VARIOUS INTERMEDIATE GRADE GRAPHITE FIBERS WITH SHELL 826/MPDA/DMF

Fiber	Interlaminar Shear Strengths PSI
Thornel 300	11,700
Celanese GT30	8,300
Hercules AS	14,300

On account of the results obtained above (Table 5), the conveniently available form of the tows, and the data base previously developed by other sources using other processes, the Hercules AS graphite fibers were chosen for this program.

Fiberglass Fibers Evaluated

Both E-glass and S-glass fibers were pultruded successfully during the program. The S-glass was Owens-Corning HTS-904 roving with 20 ends. The E-glass was Pittsburgh Plate Glass 764-NT-30 with 30 ends of K diameter fibers. This latter fiber is made specially for pultrusion. The 904 finish on the S-glass did, however, make the fiber stick in the die and as a result it was difficult to string the material prior to running. Also, the die force was higher than for the E-glass during runs. Nonetheless, since the S-glass is a higher strength and modulus fiber, it was chosen for the program.

Kevlar® Fibers Evaluated

The Kevlar® fibers manufactured by DuPont had no finish or size applied to them. As a result the adhesion of the epoxy resin to the fibers is poor. As a result the interlaminar and in-plane shear strengths, transverse tension strength, and compression strength are all lower than expected based on the fiber properties. (No temperature conditioning of the filaments was used, although this may enhance mechanical properties when using epoxy resins employing anhydride hardening agents. This fiber was included in the program because several airframe manufacturers are considering using it in hybrid Kevlar®-graphite laminates to improve resistance to low-velocity impacts.)

Braided Tape Material Used

The ability to add angle plied layers of reinforcing fibers to a pultruded product increases the flexibility of tailoring the mechanical properties of the material. For simplicity of operation and lower cost, the angle plied reinforcement should be in continuous lengths. The braiding process of weaving offers just such a capability.

To this end, Woven Structures Incorporated established the capability to braid graphite tows and fiberglass rovings into continuous flat tapes. Since the braiding process involves, of

necessity, sliding the tows (or yarns) over each other, a means had to be developed which prevented the graphite tow from pulling apart under the influence of these sliding forces. This was achieved by lagging the tow with a fine rayon yarn (4 turns per inch). The 904 finish on the S-glass roving produced sufficient cohesiveness to permit braiding without undue difficulty.

A ±45° braided tape was made with 10,000 fiber tows of Hercules AS graphite fiber. The tape was 2.25 inches wide and had a dry thickness of 0.055 inch. To prevent scissoring of the weave during pulling, Owens-Corning HTS-904 fiberglass 20 end roving was added to the tape. These rovings ran in the 0° direction and were uniformly spaced across the tape at five rovings per inch.

A similar tape was made with S-glass roving. However, on checking the tape after manufacture, the fiber pattern was ±20°. This tape was 2.25 inches wide and had a dry thickness of 0.040 inch. It also contained five S-glass rovings per inch in the 0° direction to prevent scissoring of the weave.

Both of these braided tapes were successfully pultruded with epoxy resin. Measurement of the fiber angle after pultrusion showed that in both cases the angles had only increased by 2°.

DETERMINATION OF DESIGN ALLOWABLES

The averages of the data obtained from testing the composite material produced during this program are given in the tables in this section. The material for the test specimens was fabricated by two processes:

(a) pultrusion and oven postcure

(b) hand lay-up, vacuum bag and oven cure

The pultruded material for test specimens included combinations of three types of fibers and two resin systems. Within each fiber-resin combination, the process conditions and fiber volume contents were held constant.

The graphite fiber was Hercules AS and it was maintained at 58 to 60 fiber volume content during all runs. The fiberglass was Owens-Corning HTS-904 roving and it was maintained at 67 to 69 fiber volume content during all runs. The third fiber was DuPont Kevlar® 49 roving and it was maintained at 67 to 69 fiber volume percent during all runs.

Process Conditions

The process conditions for the epoxy resins were maintained constant, independent of the fiber type. The Epon 826 resin system was 100 parts Epon 826, 14 phr MPDA and 5 phr DMF. The resin and MPDA were preheated to 150°F and the MPDA melted. Then the two were added together and mixed with an electric stirring motor for 5 minutes while adding the DMF. The impregnation tank was preheated to 100°F. Cooling of the resin during stirring and when added to the impregnation tank resulted in a final resin temperature of 115°F to 125°F. The bath temperature controller was reset to 130°F and the run started. The die temperature was 400°F during the runs. The fiber-resin stream speed was adjusted to just maintain solid material exiting the die. This speed was between 12 and 15 inches per minute. The pultruded material was cut on a bandsaw into 4-foot lengths and postcured in an oven for 2 hours at 175°F followed by 2 hours at 300°F.

The Narmco 5208 resin was preheated to 300°F in an oil bath which required about 1 hour. The impregnation bath was preheated to 300°F. Then the resin was added to the bath and the run started. The die temperature was maintained at 450°F during the runs. The fiber-resin stream speed was adjusted to just maintain a solid material exiting the die. This speed was between 8 and 12 inches per minute. The pultruded material was cut into 4-foot lengths on a bandsaw and postcured in an oven for 1 hour at 350°F followed by 3 hours at 450°F.

Process Conditions - Vacuum Bagging

The test specimen produced by vacuum bagging involved two types of fibers and two resin systems. The fibers were Hercules AS graphite 10,000 filament tows and Owens-Corning HTS-904 fiberglass 20 end roving. The resin systems were the Shell 826/MPDA/DMF and Narmco 5208.

Two sets of specimens were made with the Epon 826 resin system; one set with graphite fiber and one set with fiberglass. The procedure was to use the impregnating bath and squeeze-out bushing with the resin at room temperature. Then the fibers were drawn through the bath to make an impregnated tape 2 inches wide. As the tape was drawn from the bath, polyethylene fiber was placed on both sides to facilitate handling and cutting. The tape was then cut and hand laid-up on a vacuum table. The lay-ups were covered with perforated PVA film and then dry fiberglass bleeder cloth. A PVA vacuum bag was sealed to the table, a vacuum drawn and the table placed in the oven. The cure cycle was 2 hours at 200°F followed by 2 hours at 300°F.

For the Narmco 5208 resin, both graphite and S-glass 3-inch-wide prepreg tape were secured from Narmco. The tape was cut and laid up on the vacuum table following the same procedure as above. The cure schedule was 1 hour at 265°F followed by 2 hours at 355°F. (It should be noted that this material was cured in an oven rather than an autoclave so the properties can be expected to be lower than those generally accepted.)

RESULTS OF MECHANICAL PROPERTY EVALUATIONS

The mechanical property tests were performed using standard test specimen configurations and testing procedures as far as possible. All tests were performed on a Baldwin-Lima-Hamilton Universal Test Machine, Mark "G".

Tensile Tests

The tensile test specimens were standard IITRI coupons and are shown in Figure 9 for the 0° and off-axis fiber orientation and in Figure 10 for the 90° fiber orientation. The coupons were cut out with a diamond saw to ensure good edge cuts. The 0° and off-axis coupons were tested with Tinius Olsen rotary-type grips with horizontal closing of the wedges. The 90° coupons present a problem in that a slight offset in the grip alignment can cause a bending moment in the coupon and induce premature failure.

A special transverse tensile test fixture was built that maintained the alignment of the load application within .001 inch as shown in Figure 11.

The results of the testing are presented in Table 6. The results for the pultruded specimen tests are averages for 5 coupons.

Compression Tests

The compression specimens were 0.125 x 0.50 inch in cross section coupons and are shown in Figure 12 for all fiber orientations. Compression tests always present a problem of supporting the specimen to prevent buckling and end brooming. The load was introduced into the test fixture through a 5/8-inch-diameter steel ball mounted in two conical seats as shown in Figure 13. The coupon was held between 2 massive steel blocks, top and bottom, that gripped the coupon and introduced part of the load as shear. In this way the end load was reduced and brooming was prevented. The results of the testing are presented in Table 7. The results for the pultruded specimen tests are averages for 6 coupons and for the vacuum bag specimen tests are averages for 5 coupons.

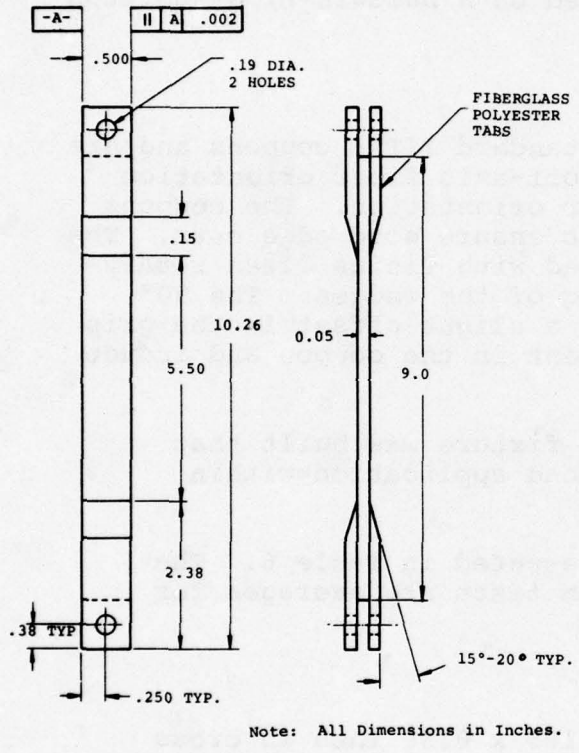


Figure 9. Tensile Test Specimens for 0° and Off-Axis Fiber Orientation.

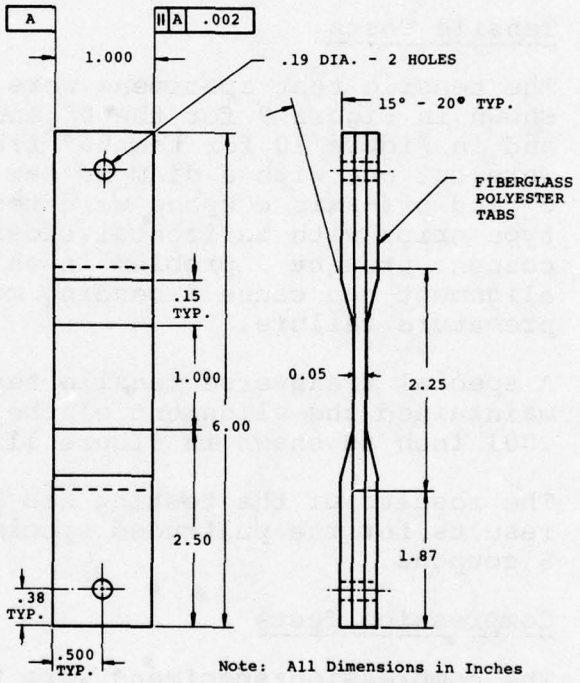


Figure 10. Tensile Test Specimens for 90° Fiber Orientation.

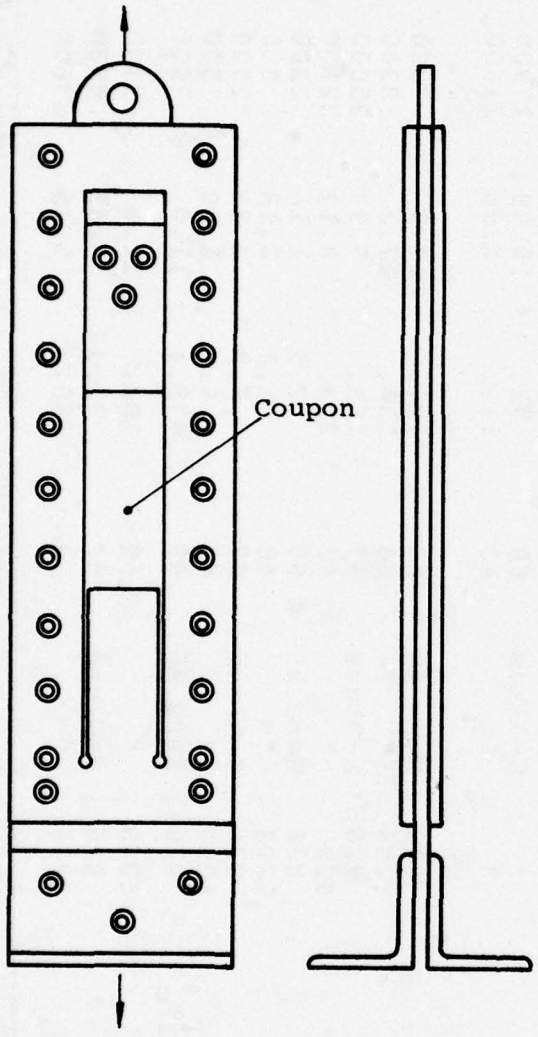


Figure 11. Loading Fixture to Maintain Alignment for 90° Tension Tests.

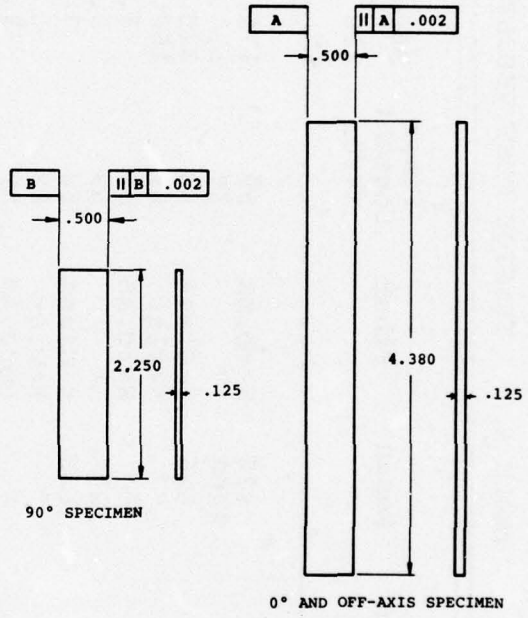


Figure 12. Compression Specimens.

TABLE 6. TENSION TEST RESULT AVERAGES

Test No.	Fiber Orientation to Load	Resin	Fiber	Fiber Content (V/O)	Strength (10^3PSI)	Young's Modulus (10^6PSI)	Ultimate Strain (10^{-6}in/in)	Poisson's Ratio
Pultruded								
1	$(0°)_c$	826	Herc.AS	59	175.	20.0	8500	.20
5	"	5208	"	59	154.	19.4	7500	.18
7	"	826	S-Glass	68	228.	7.23	32800	.34
11	"	"	Kevlar	68	160.	-	-	-
2	$(90°)_c$	"	Herc.AS	59	5.4	1.66	3700	.023
6	"	5208	"	59	2.9	2.06	1740	.029
8	"	826	S-Glass	68	7.0	1.81	2850	.094
12	"	"	Kevlar	68	1.6	-	-	-
3	$(\pm 45°)_c$	"	Herc.AS	59	59.	8.01	8470	.86
4	$(0°,\pm 45°)_s$	"	"	59	93.	12.5	7400	.98
9	$(\pm 20°)_c$	"	S-Glass	68	92.	5.89	17900	.49
10	$(0°,\pm 20°)_s$	"	"	68	118.	5.96	21600	.34
Vacuum Bagged								
1	$(0°)_c$	826	Herc.AS	60	124.	17.9	7800	.32
5	"	5208	"	60	134.	17.3	8300	.25
3	"	826	S-Glass	67	152.	7.97	25000	.20
7	"	5208	"	62	213.	8.19	32300	.28
2	$(90°)_c$	826	Herc.AS	60	2.5	1.16	2200	.097
6	"	5208	"	60	1.4	2.13	850	-
4	"	826	S-Glass	67	5.2	1.38	2500	.072
8	"	5208	"	62	4.7	1.90	1500	-
8A	$(0°_2,\pm 45,0°_2)_c$	826	Herc.AS	60	78.4	11.0	7900	.36
8B	"	5208	"	60	103.	12.0	9100	.48
8C	"	826	S-Glass	67	32.4	4.41	4930	.70
8D	"	5208	"	62	160.	5.45	33600	.47

TABLE 7. COMPRESSION TEST RESULT AVERAGES

Test No.	Fiber Orientation to Load	Resin	Fiber	Fiber Content (V/O)	Strength (10^3PSI)	Young's Modulus (10^6PSI)	Ultimate Strain (10^{-6} in/in)	Poisson's Ratio
Pultruded								
13	$(0°)_c$	826	Herc.AS	59	96.	20.5	4700	.15
17	"	5208	"	59	133.	18.9	6800	.17
19	"	826	S-Glass	68	82.	9.3	9000	.28
23	"	"	Kevlar	68	39.	-	-	-
14	$(90°)_c$	"	Herc.AS	59	6.4	1.4	7400	.023
18	"	5208	"	59	13.6	1.93	4400	.046
20	"	826	S-Glass	68	24.	1.64	7600	.037
24	"	"	Kevlar	68	5.1	-	-	-
16	$(\pm 45°)_c$	"	Herc.AS	59	25.	8.56	5700	.58
15	$(0°\pm 45°)_s$	"	"	59	51.	11.2	4500	.36
22	$(\pm 20°)_c$	"	S-Glass	68	58.	7.01	8500	.51
21	$(0°\pm 20)_s$	"	"	68	66.	7.35	9400	.49
Vacuum Bagged								
9	$(0°)_c$	826	Herc.AS	60	70.	17.2	3900	.48
13	"	5208	"	60	57.	13.1	4700	.46
11	"	826	S-Glass	67	72.	13.6	5600	.25
15	"	5208	"	62	98.	7.91	11900	.35
10	$(90°)_c$	826	Herc.AS	60	14.	1.17	13700	.011
14	"	5208	"	60	12.	1.44	8200	.0087
12	"	826	S-Glass	67	22.	1.19	32300	.34
16	"	5208	"	62	17.	2.43	9100	.060

Rail Shear Test

The rail shear test specimens were 6 inches long, and when mounted in the rails they had a gage section 0.50-inch wide. To prevent rotation of the rails during loading, the rounded nose of the rails was located in a vee grove. Each coupon had 2 strain gages mounted on it in the center of the coupon. The strain gages were oriented at $\pm$45° to the rails.

Originally, it was believed that the pultruded $\pm$45° laminates would require 0° layers on both surfaces to maintain alignment of the off-axis fibers. The final braid configuration with 0° rovings internal enabled the braided tapes to be pultruded alone. This capability allowed the off-axis properties to be measured directly, rather than being derived by separating the effects of the 0° and $\pm$45° layers by analysis.

The results of the tests are presented in Table 8. The averages for the pultruded specimens represent 6 coupons and for the vacuum bagged specimens (not shown on the table), they represent 5 coupons.

Four-Point Flexure Test Results

The flexure coupons were cut from bars 0.125 x 0.50 inch in cross section. The span-to-depth ratio was 32 and the load was applied at the quarter points, in accordance with ASTM Test Method D790. The test results are presented in Table 9.

Short Beam Interlaminar Shear Test

The interlaminar shear specimens were cut from bars with a 0.10- or 0.25-inch thickness and a 0.25-inch width. The testing procedure used was ASTM Method D-20345, with a span-to-depth ratio of 4. The test results are presented in Table 10.

Tensile Fatigue Test

The tension fatigue test was a tension-tension test conducted at constant load. The specimens were unnotched, giving a stress concentration factor of K=1. The stress ratio R during the test was maintained at .05. The test coupons are shown in Figure 14. The coupon is designed to be loaded primarily by a pin through the hole in end tabs and secondarily by friction from the grips. The 5.5-inch gage length was maintained the same as in the static tensile tests. During testing there was no failure of the end tabs; the majority of the failures occurred in the gage section. The cyclic rate of the testing

TABLE 8. IN-PLANE SHEAR TEST RESULT AVERAGES

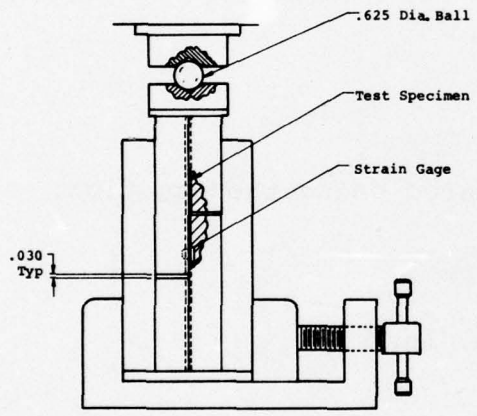
Test No.	Fiber Orientation to Load	Resin	Fiber	Fiber Content (V/O)	Strength (10^6PSI)	Flexural Modulus (10^6PSI)
Pultruded						
25	$(0°)_c$	826	Herc.AS	59	6.7	1.49
28	"	"	S-Glass	68	3.0	.80
27	$(\pm 45°)_c$	"	Herc.AS	59	13.	2.78
26	$(0° \pm 45)_c$	"	"	59	9.5	1.98
30	$(\pm 20°)_c$	"	S-Glass	68	12.	2.29
29	$(0° \pm 20°)_s$	"	"	68	10.	2.05

TABLE 9. FOUR-POINT FLEXURE TEST RESULT AVERAGES

Test No.	Fiber Orientation to Load	Resin	Fiber	Fiber Content (V/O)	Strength (10^3PSI)	Flexural Modulus (10^6PSI)
Pultruded						
31	$(0°)_c$	826	Herc.AS	59	180.	24.2
32	"	"	Cel.GT30	60	115.	17.2
33	"	"	Cel.GY50	60	207.	16.7
34	"	"	Cel.GY70	60	93.	33.3
35	"	"	S-Glass	67	184.	7.2
36	"	"	Kevlar	68	72.	9.8
37	"	"	Thornell 300	59	181.	17.0
37A	"	5208	Hercules AS	59	210	18.4

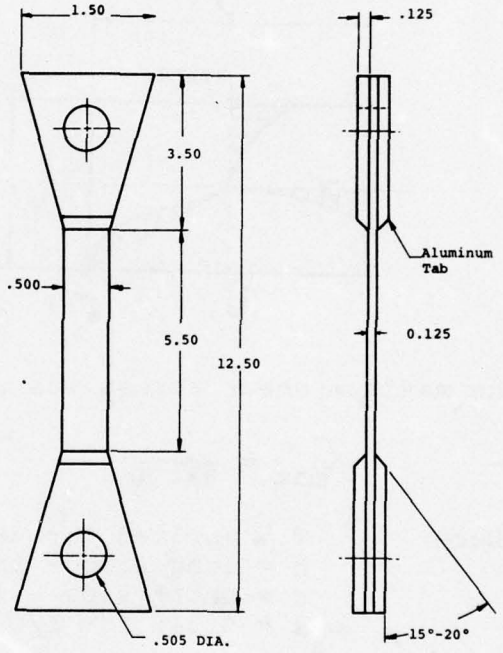
TABLE 10. SHORT BEAM INTERLAMINAR SHEAR TEST RESULT AVERAGES

Test No.	Fiber Orientation to Load	Resin	Fiber	Fiber Content (V/O)	Strength (10^3PSI)
Pultruded					
38	$(0°)_C$	826	Herc.AS	60	14.
39	"	"	Thornell 300	60	12.
40	"	"	Cel.GT-30	60	8.3
41	"	"	Cel.GY-50	60	9.5
42	"	"	Cel.GY-70	60	8.1
43	"	"	E-Glass	68	9.6
44	"	"	Kevlar	68	6.5
44A	"	5208	Hercules AS	60	11.4
44B	"	826	S-Glass	68	11.9
Vacuum Bagged					
17	$(0°)_C$	826	Herc.AS	60	8.9
18	"	5208	"	60	6.3
19	"	826	S-Glass	67	12.
20	"	5208	"	62	6.7



Note: All Dimensions in Inches

Figure 13. Compression Test Fixture Showing Load Introduction and Supports.



Note: All Dimensions in Inches

Figure 14. Tension Fatigue Specimens.

was 0.5 Hertz. The test results of the tension fatigue test are presented in Tables 11 and 12.

Torsional Fatigue Tests

The torsional fatigue specimens were rectangular bars with a cross section about .12 x .25 inch. The gage length between grips was 3.5 inches.

The shear stress distribution in a rectangular shaft is not uniform and therefore this coupon configuration is not normally considered for torsional testing. However, in applications such as helicopter tail rotors, a rectangular spar is a logical choice to transmit bending and torsion loads. Analytical solutions have been obtained for torsion of rectangular elastic shafts.[7] The shear stress distribution is shown in Figure 15.

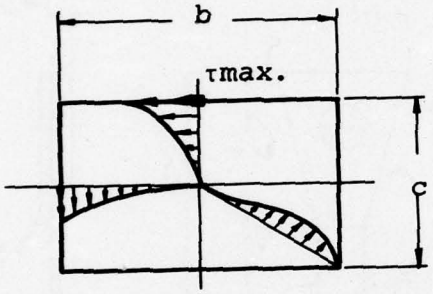


Figure 15. Shear Stress Distribution in a Rectangular Shaft.

The maximum shear stress was calculated using the equation:

$$\tau_{max} = \frac{T}{8kc^2b}$$

where T = applied torque - in. lb.
b = long side - in.
c = short side - in.
k = 0.246 for b/c = 21.

This equation is valid for a unidirectional composite since the properties will be isotropic in the plane of the shear stress.

The failure in a torsional test of this nature is not typically catastrophic as in the tensile fatigue test. At the high stress levels a visible crack actually appears; however, at the lower stress levels it is difficult to determine failure. For these tests, the slope of the load-deflection curve was monitored during cycling to detect a fairly definite change in

TABLE 11. TENSILE FATIGUE TEST RESULTS WITH HERCULES AS/826 RESIN, FIBER ORIENTED 0° TO LOAD - TENSILE STRENGTH σ MAX = 175,800 PSI
K = 1 R = .05

Specimen No.	Percent of Static (%)	Test Stress (10^3PSI)	Cycles to Failure
45-1	90	156.9	1
45-2	68	119.6	1
45-3	90	156.9	4
45-4	65	114.3	3.614×10^4
45-5	80	140.6	7.774×10^4
45-6	85	149.4	1.123×10^4
45-7	"	"	15
45-8	"	"	440
45-9	"	"	310
45-10	80	140.6	2.331×10^4
45-11	"	"	490
45-12	75	131.8	130
45-13	"	"	140
45-14	70	123.1	4
45-15	"	"	12
45-16	65	114.3	1.076×10^4
45-17	"	"	No Failure in 1.889×10^6

TABLE 12. TENSILE FATIGUE TEST RESULTS WITH OWENS-CORNING HTS-904 FIBERGLASS/826 RESIN, ORIENTED 0° TO LOAD - TENSILE STRENGTH
σ MAX = 205,600 PSI
K = 1 R = .05

Specimen No.	Percent of Static (%)	Test Stress (10^3PSI)	Cycles to Failure
48-1	65	133.6	1
48-2	65	133.6	390
48-3	"	"	140
48-4	"	"	270
48-5	55	113.1	530
48-6	45	92.5	1480
48-7	"	"	700
48-8	"	"	1.25×10^4
48-9	35	72.0	1.605×10^4
48-10	"	"	1.566×10^4
48-11	"	"	7.772×10^4
48-12	25	51.4	3.9712×10^5
48-13	"	"	No Failure in 1×10^6

modulus of the composite specimens. The point at which the modulus changed by 10% was taken as the failure point.

The tests were conducted at a stress concentration factor K = 1 and a stress ratio R = .10. The test results are presented in Tables 13 and 14.

DISCUSSION OF TEST RESULTS

The Shell 826/MPDA/DMF and Narmco 5208 resin systems used in the fabrication of the test specimens had a definite influence on the mechanical properties of the various composite materials. In general, the Shell 826 resin system that was formulated specifically for the pultrusion process performed best. The Narmco 5208 resin system was forced to conform to processing conditions required by the pultrusion process, and as a result, the mechanical properties reflect this condition. The Kevlar® fibers are still in development for use in advanced composites and exhibited low interlaminar shear, compression and flexural strengths indicative of a poor bond between the resin and the fiber.

Static Properties

The longitudinal tensile properties of a unidirectional composite are dominated by the fibers. Typical stress-strain curves for the Hercules AS graphite fiber are plotted in Figure 16. The modulus is quite similar for either the Shell 826 or Narmco 5208, whether pultruded (P) or vacuum bag fabricated (V). The strengths group more distinctly by type of process, with the pultruded specimens being significantly higher. This could possibly be due to inadequacies in the quality of the vacuum specimens.

The 90° tensile properties, however, are influenced strongly by the properties of the resin. As shown in Figure 17, there is a marked difference in the modulus, strength and elongation to failure. In this case the results from the pultruded Shell 826 show marked superiority.

The Owens-Corning HTS-904 fiberglass behaved in a different manner as shown in Figure 18. The 0° tensile strength of the pultruded 826 and vacuum bagged 5208 were essentially equal, as were the 90° tensile tests (Figure 19).

The compression properties basically show the same trends as indicated in Figures 20 through 23. The results obtained from pultrusion are higher than those obtained from vacuum bagged specimens. The Narmco 5208 resin tends to be better for properties dependent on the resin properties. The contrasts in interlaminar shear values are shown in Figure 24.

TABLE 13. TORSIONAL FATIGUE OF HERCULES AS/826 UNIDIRECTIONAL COMPOSITE - STATIC INTERLAMINAR SHEAR STRESS = 14,000 PSI, K = 1.0, R = .10

Specimen No.	Test Stress (10^3 PSI)	Cycles to Failure
51-1	6.74	2150
51-2	7.31	870
51-3	6.43	150
51-4	5.35	1650
51-5	4.59	4000
51-6	4.20	4800
51-7	5.35	2800
51-8	3.82	8000
51-9	10.30	10
51-10	8.20	18
51-11	7.50	96
51-12	6.10	450

TABLE 14. TORSIONAL FATIGUE OF S-GLASS/826 UNIDIRECTIONAL COMPOSITE - STATIC INTERLAMINAR SHEAR STRESS = 11,900 PSI, K = 1.0, R = .10

Specimen No.	Test Stress (10^3 PSI)	Cycles to Failure
52-1	12.66	45
52-2	13.14	30
52-3	7.90	1500
52-4	11.99	50
52-5	8.25	1200
52-6	7.58	1200
52-7	7.14	2700
52-8	6.37	5800
52-9	6.18	6500
52-10	11.85	96
52-11	10.20	303
52-12	14.80	11
52-13	5.10	10,000 *

(* run out)

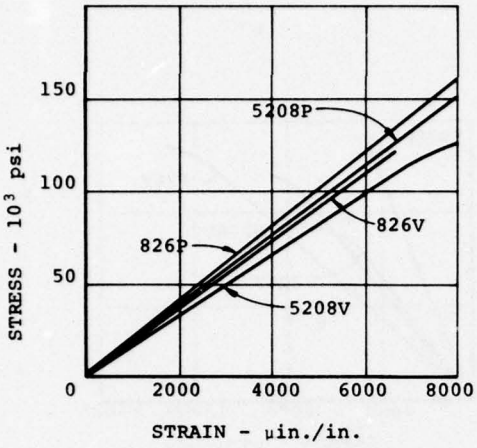


Figure 16. 0° Tensile Stress-Strain Relationships of Hercules AS With Various Resins.

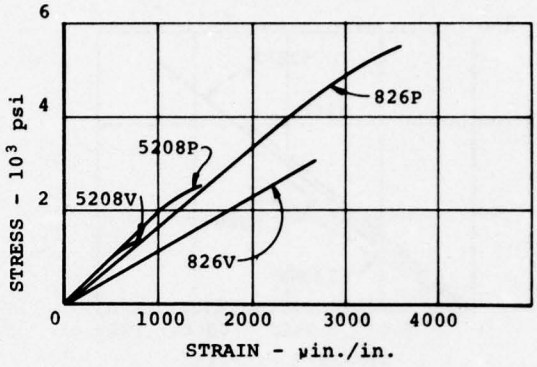


Figure 17. 90° Tensile Stress-Strain Relationships of Hercules AS With Various Resins.

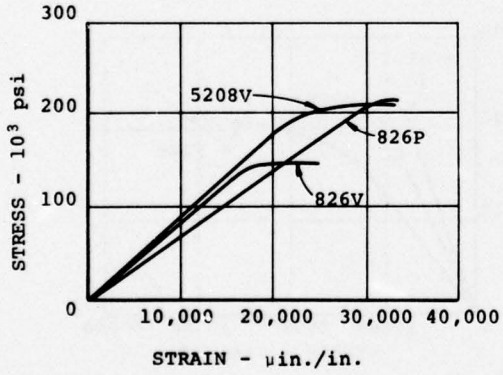


Figure 18. 0° Tensile Stress-Strain Relationships of OC HTS-904 Fiberglass With Various Resins.

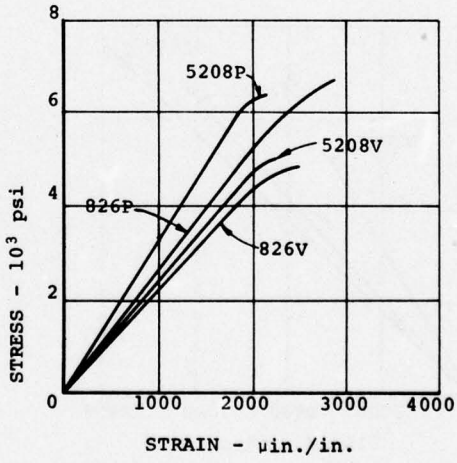


Figure 19. 90° Tensile Stress-Strain Relationships of OC HTS-904 Fiberglass With Various Resins.

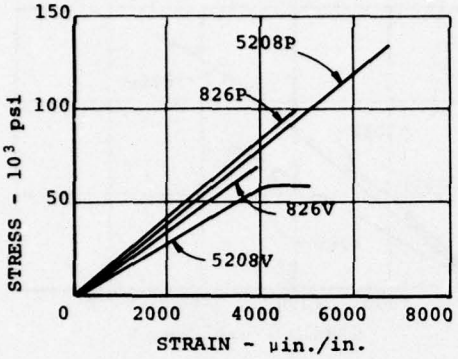


Figure 20. 0° Compression Stress-Strain Relationships of Hercules AS With Various Resins.

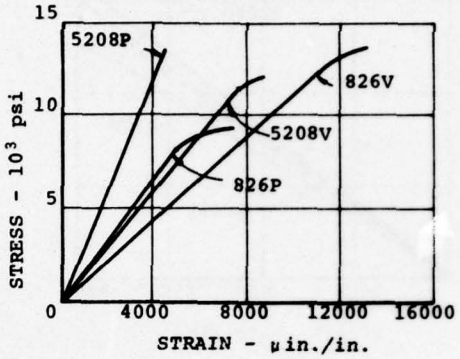


Figure 21. 90° Compression Stress-Strain Relationships of Hercules AS With Various Resins.

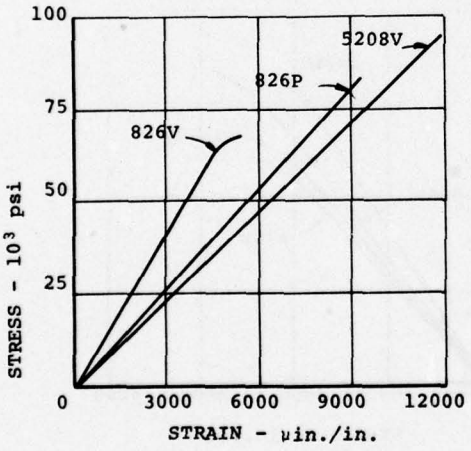


Figure 22. 0° Compression Stress-Strain Relationships of OC HTS-904 Fiberglass With Various Resins.

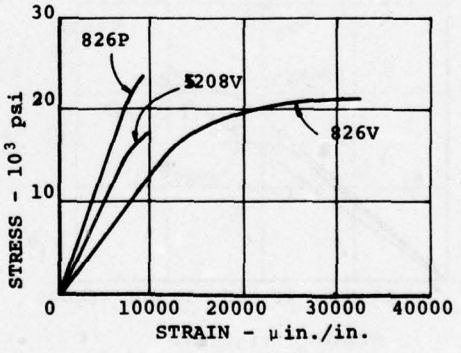


Figure 23. 90° Compression Stress-Strain Relationships of OC HTS-904 Fiberglass With Various Resins.

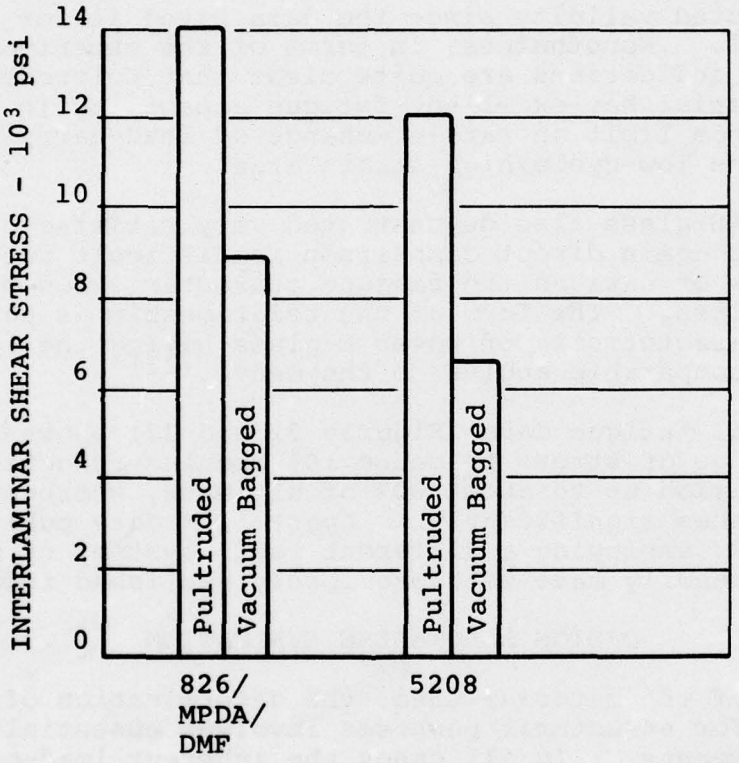


Figure 24. Short Beam Interlaminar Shear Strength Comparison.

Fatigue Properties

The S - N curves for the tensile fatigue data are shown in Figures 25 through 30. The Hercules AS/Shell 828/MPDA/DMF unidirectional laminates tested in the 0° direction had an endurance limit of 65% of the static tensile strength. This is in agreement with other published data.[8] The endurance limit for the S-glass/826 composite was 25% of the static tensile strength, which is again typical of that generally accepted.[9]

For the braided graphite materials, the data (Figures 27 and 28) compare favorably with that published in Reference 10. It must be pointed out, however, that such a comparison has only restricted validity since the data cited is for ply-on-ply material. Nonetheless, in terms of the experiments performed, the indications are quite clear that pultruded, braided material has excellent fatigue capability in terms of both endurance limit on rate-of-change of load-carrying capability in the low-cycle/high-strain area.

The braided S-glass also demonstrated very satisfactory performance but again direct comparison is difficult due to the general lack of data on the fatigue characteristics of woven, biased, S-glass. The form of the relationship is consistent with the characteristic of woven E-glass having the load applied at comparable angles to the weave.[11]

The torsional fatigue data (Figures 31 and 32) shows a high rate of change of stress to cause 10% modulus reduction with load application up to about 30% of ultimate, whereupon the rate diminishes significantly. Apart from data published in Reference 12, employing a different resin system, no comparisons can be readily made with previously published information.

DESIGN ALLOWABLES EVALUATION

Regardless of the material used, the determination of design allowables for structural purposes involves essentially the same requirements. In all cases the inherent load-carrying ability of a structure must be such that the limit load can be sustained without excessive deformation and without a significant amount of permanent set. Of equal importance is the need to ensure that the structure is capable of withstanding the operational spectrum of loading and environment for a period considerably in excess of the specified service life. These requirements do not refer to the characteristics of the material being employed; nevertheless, they are the foundations upon which the design allowables must be established. It is the unique phenomenological behavior of laminated com-

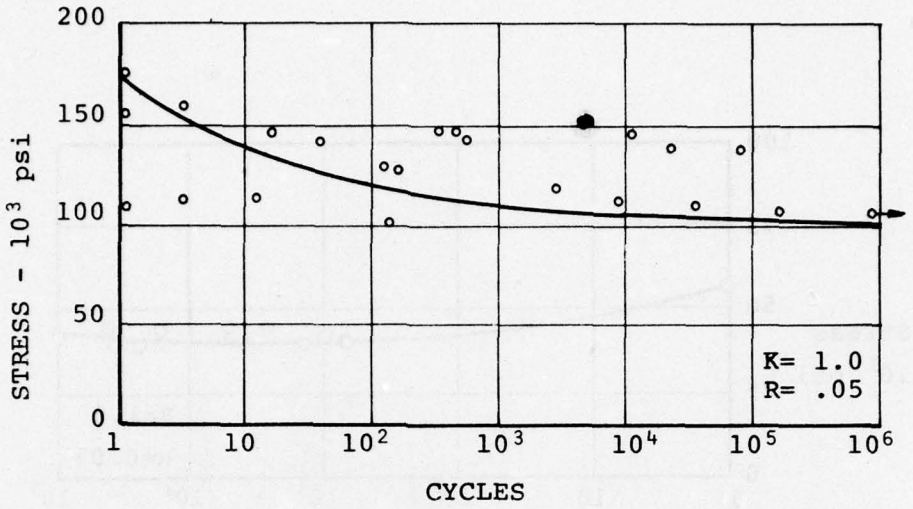


Figure 25. S-N Curve For Hercules AS/Shell 826 Unidirectional Laminate Tested in 0° Direction in Tensile Fatigue.

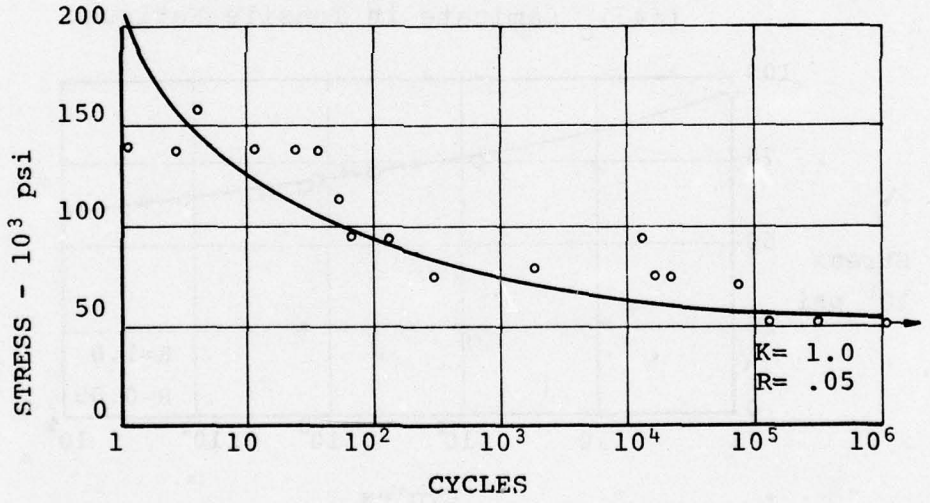


Figure 26. S-N Curve For OC HTS-904/Shell 826 Unidirectional Laminate Tested in 0° Direction in Tensile Fatigue.

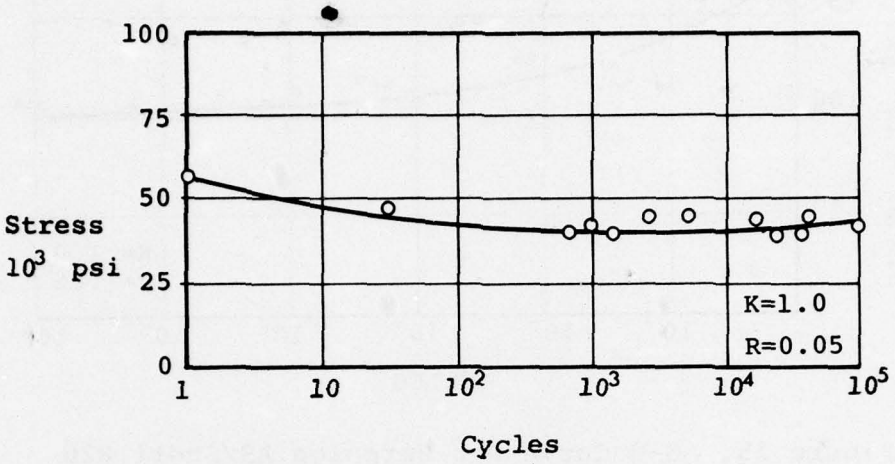


Figure 27. S-N Curve For Hercules AS/Shell 826 $(\pm 45)_c$ Laminate in Tensile Fatigue.

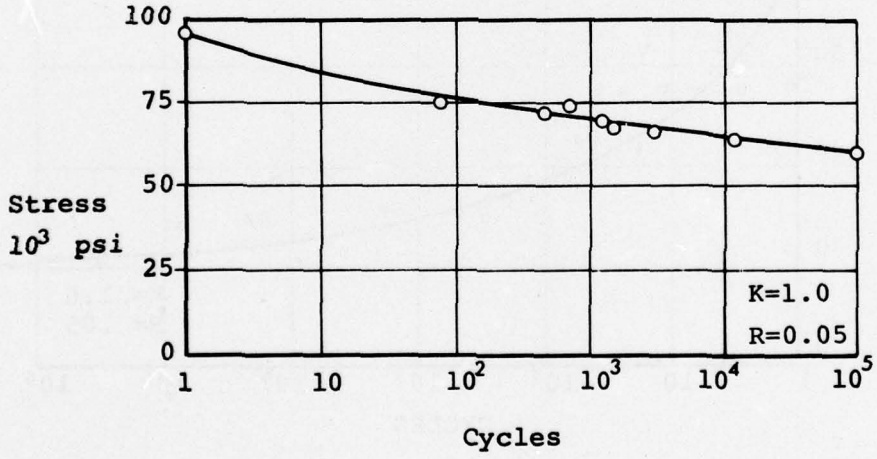


Figure 28. S-N Curve For Hercules AS/Shell 826 $(0,\pm 45)_s$ Laminate in Tensile Fatigue.

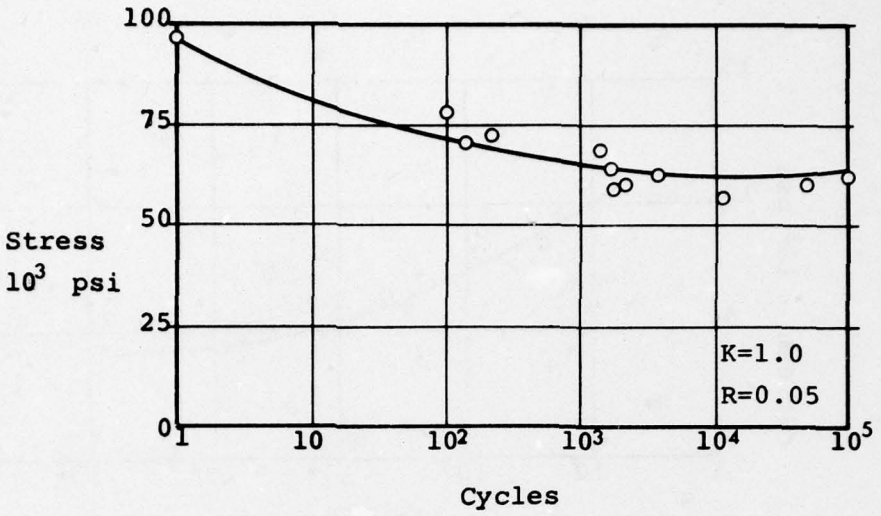


Figure 29. S-N Curve for OC HTS-904/Shell 826 $(\pm 20)_c$ Laminate in Tensile Fatigue.

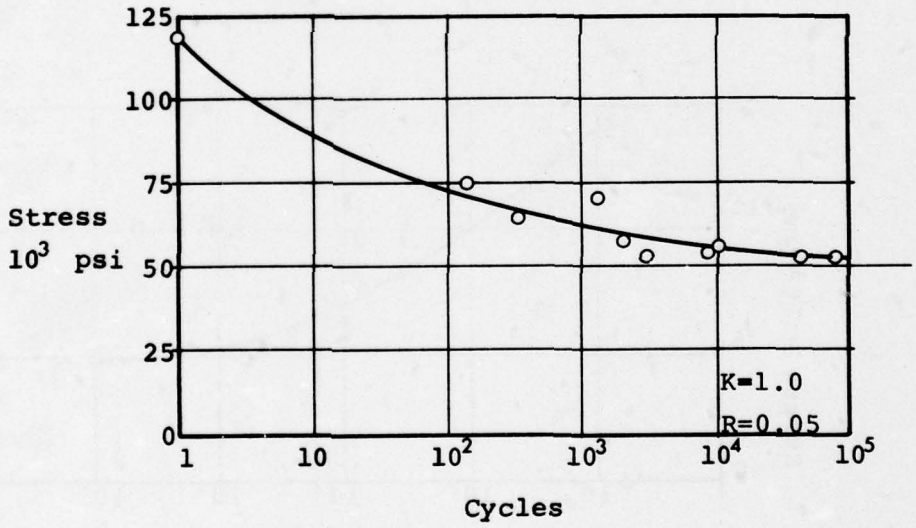


Figure 30. S-N Curve for OC HTS/Shell 826 $(0, \pm 20)_s$ Laminate in Tensile Fatigue.

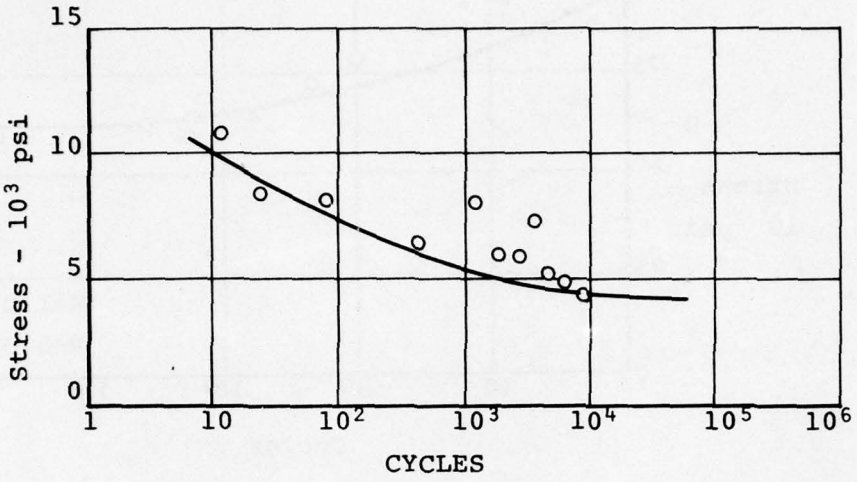


Figure 31. S-N Curve for Hercules AS/Shell 826 Unidirectional Laminate in Torsional Fatigue.

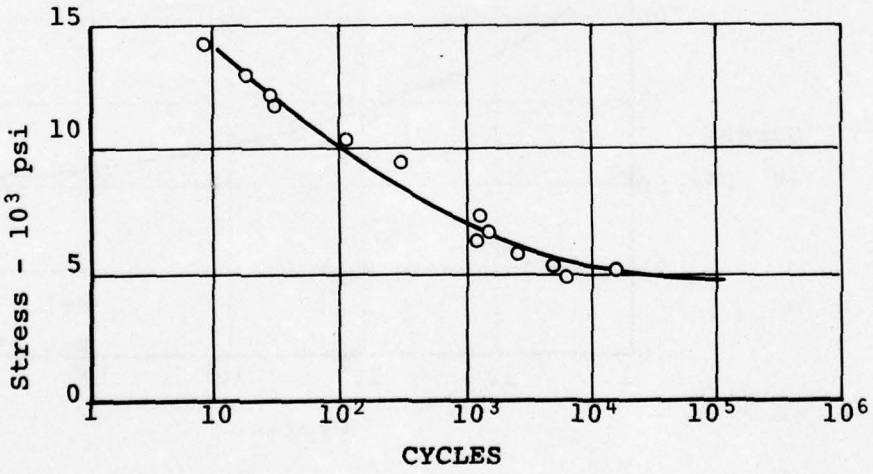


Figure 32. S-N Curve for OC HTS-904/Shell 826 Unidirectional Laminate in Torsional Fatigue.

posite materials that make the determination of allowables for optimum design a challenge.

Because data are obtained from samples of finite size, it is necessary to account for variations in sample standard deviations and means for their relation to the true population by specifying confidence levels. Current aerospace practice [13] for metallic materials generally is to define a value above which at least 99 percent of the population is expected to fall with a confidence level of 95 percent (A-value). For composite materials, more realistic figures are 90 and 95 percent respectively (B-value). If the design allowable is X_{AQ} and the mean and standard deviations for the sample are $\overline{X}_s$ and σ_s respectively, then,

$$X_{AQ} = \overline{X}_s - k\sigma_s$$

where k is the one-sided tolerance factor for the normal distribution at some particular confidence level and probability as shown in Figure 33. (The significance of using data derived from small samples rather than the population is discussed in Reference 11.)

Design allowables for the Hercules AS/ Shell 826/MPDA/DMF and OC HTS-904 fiberglass/Shell 826/MPDA/DMF composite are shown in Table 15 reduced to a B basis by use of the relationship given in Figure 33. Variances are summarized in Table 15.

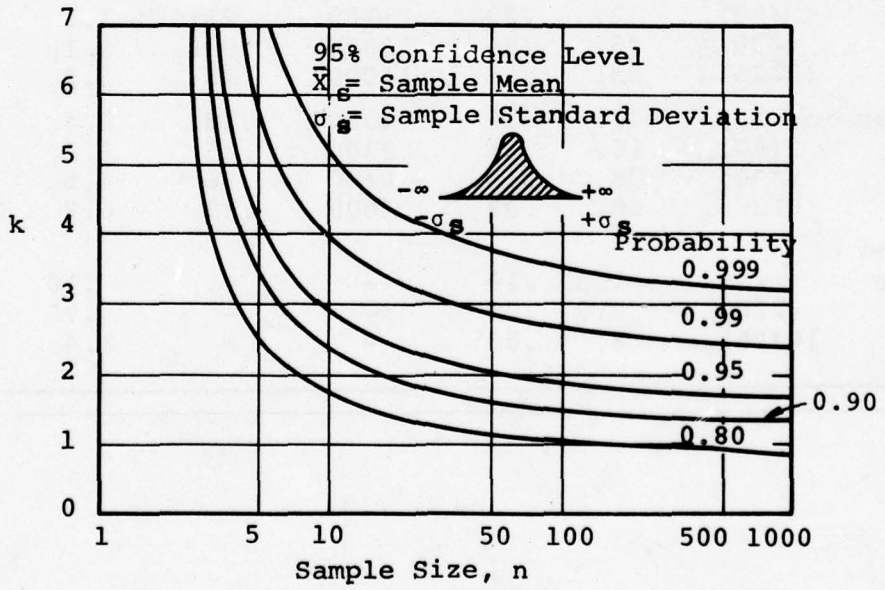


Figure 33. One-Sided Tolerance Limits and Sample Size for the Normal Distribution.

TABLE 15. DESIGN ALLOWABLES (B-VALUE) FOR PULTRUDED COMPOSITE - SHELL 826/ MPDA/DMF RESIN

Load Direction to Fibers		Mechanical Property: Ultimate Strength Ksi	C.V.	Ultimate Strain μin/in	C.V.	Modulus 10^6 PSI	C.V.
Hercules AS - 60 V/O							
Tension	$(0)_c$	99.	.14	5500	.13	19.	.009
	$(90)_c$	1.4	.32	1500	.23	.4	.29
	$(\pm 45)_c$	43.	.08	2500	.28	4.4	.15
	$(0 \pm 45)_s$	63.	.11	4800	.11	10.9	.04
Compression	$(0)_c$	65.	.10	2600	.15	17.	.05
	$(90)_c$	3.2	.16	1900	.36	.9	.11
	$(\pm 45)_c$	15.	.12	1100	.35	3.4	.20
	$(0 \pm 45)_s$	28.	.16	2200	.24	8.4	.09
Inplane Shear	$(0)_c$	35.	.16	-	-	.6	.21
	$(\pm 45)_c$	10.	.07	-	-	2.	.10
	$(0 \pm 45)_s$	7.9	.05	-	-	.8	.22
OC HTS-904 Fiberglass 68 V/O							
Tension	$(0)_c$	160.	.10	-	-	.5	.10
	$(90)_c$	2.	.29	1100	.21	1.9	.10
	$(\pm 20)_c$	76.	.05	13000	.086	5.1	.04
	$(0 \pm 20)_s$	92.	.07	14000	.12	3.9	.12
Compression	$(0)_c$	42.	.16	4000	.18	8.4	.04
	$(90)_c$	16.	.11	2300	.25	2.1	.12
	$(\pm 20)_c$	38.	.11	6400	.08	4.5	.12
	$(0 \pm 20)_s$	48.	.08	4000	.19	6.2	.05
Inplane Shear	$(0)_c$	1.3	.19	-	-	.16	.41
	$(\pm 20)_c$	8.7	.08	-	-	.75	.24
	$(0 \pm 20)_s$	8.	.06	-	-	1.4	.0

PRODUCTION AND TEST OF DEMONSTRATION ARTICLE

In order to convincingly demonstrate application of the pultrusion technology established under this program, a structural component was designed and manufactured which utilized all aspects of the results obtained. The design chosen was an integrally stiffened hybrid composite having the layup configuration and general dimensions shown in Figure 34. The panel consisted of 0° Hercules AS graphite fiber on the exterior surface and a ±45° braided inner ply of Owens-Corning HTS-904 fiberglass.

The arrangement of material used during the pultrusion operation is shown in Figure 35. To maintain precise filament placement, the ends of the impregnation tank were constructed from Teflon sheets into which a series of guidance slots were machined. These slots also served to separate the filament tows, thus aiding impregnation. The exit plate had an opening area established to control resin squeeze-out. The entrance end of the impregnation tank may be seen in Figure 36. In Figure 37 the filament resin stream entering the heated die is shown.

The pultrusion conditions were

(a) Resin temperature, 125°F

(b) Resin viscosity, 500 centipoise

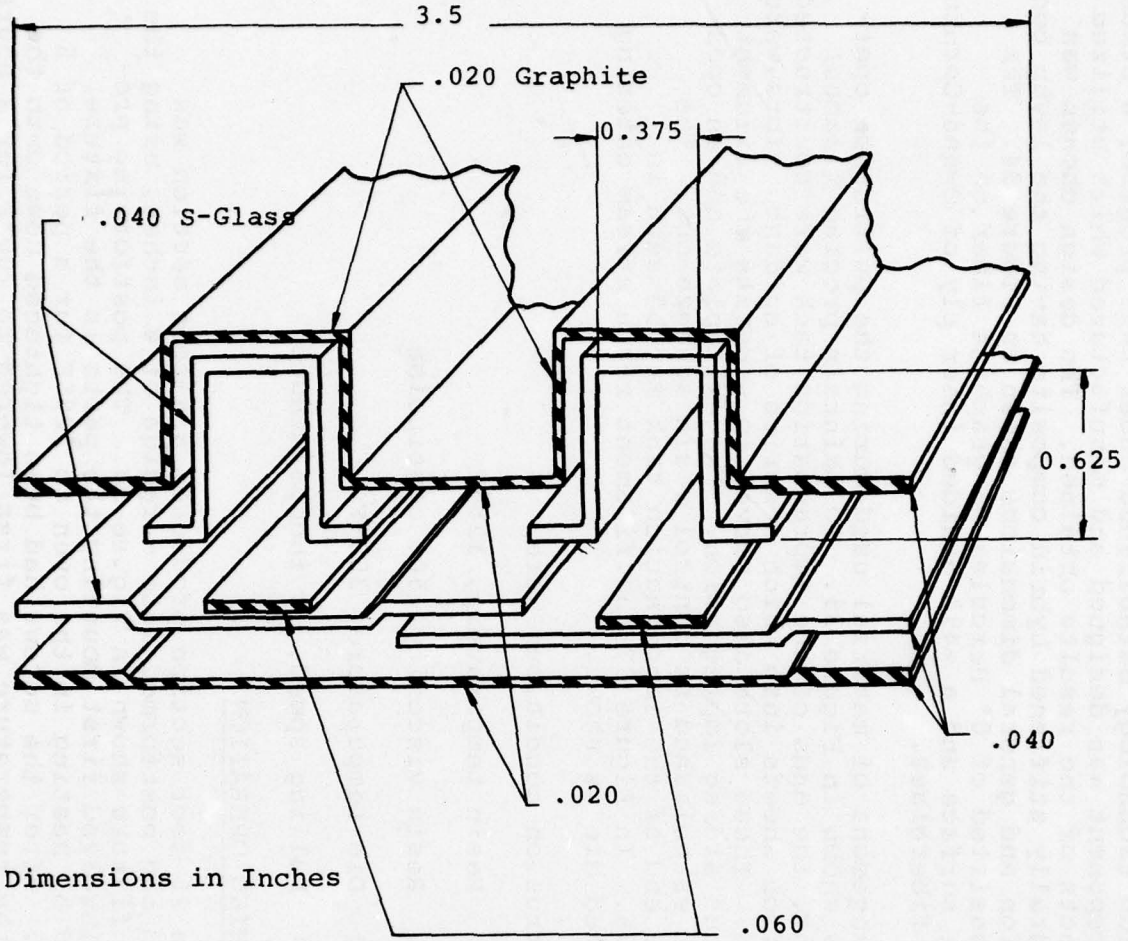
(c) Die temperature, 350°F

(d) Pulling speed, 12 inches/minute

POSTFORMING OPERATION

From the 25-foot section produced, a 6-foot section was selected and postformed into a radius of 6 inches, using the forming fixture shown in Figure 38. The postforming procedure involved first mounting the parts in the fixture, followed by heating in the oven to 325°F for a period of 5 minutes. After the screws had been tightened down onto the shims, the temperature was first lowered to 200°F for 2 hours and then raised to 300°F for 2 hours for the purpose of affecting the postcure.

A section of the postformed article is shown in Figure 39.



Note: All Dimensions in Inches

Figure 34. Demonstration Article - Integrally Stiffened Panel.

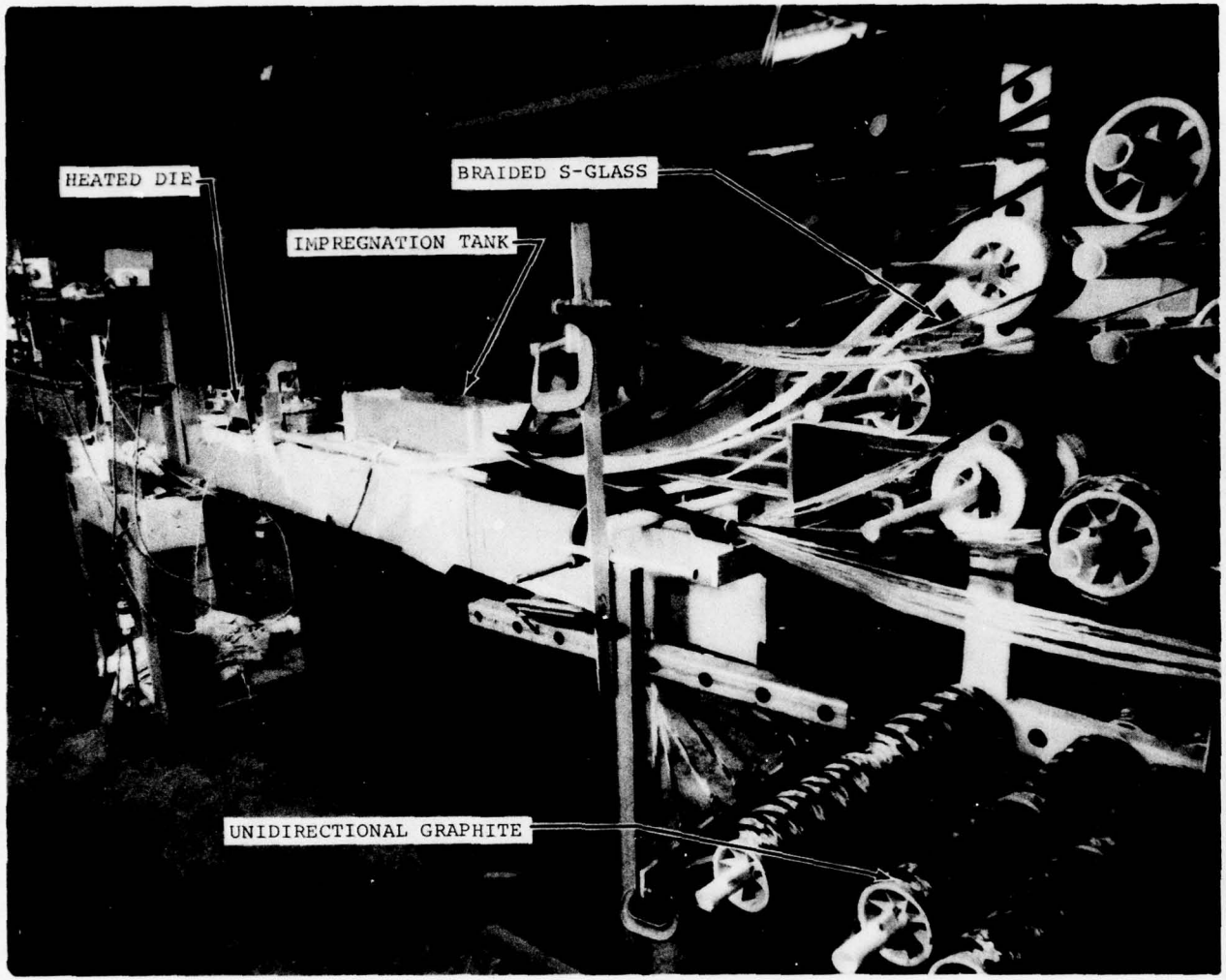


Figure 35. Pultrusion of Demonstration Article

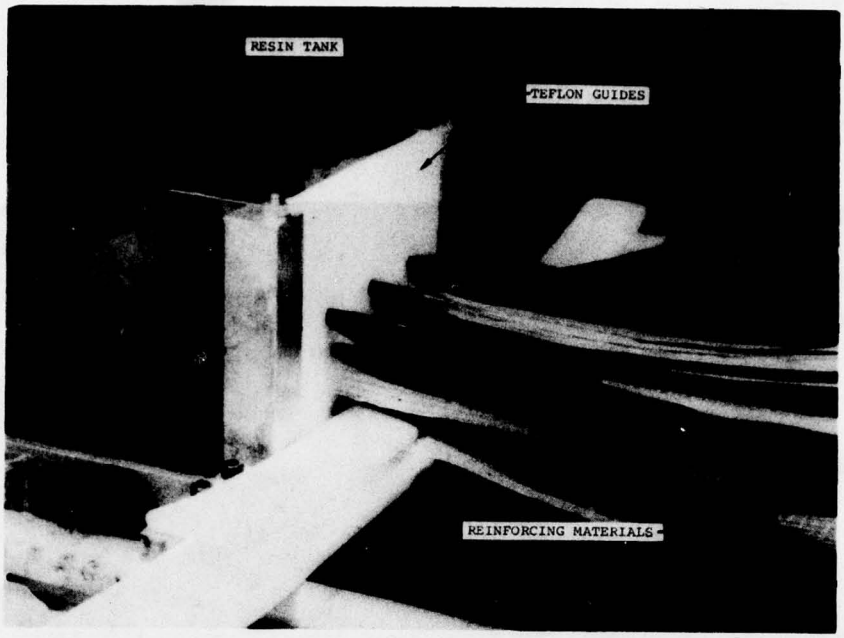


Figure 36. Entrance to Resin Tank.

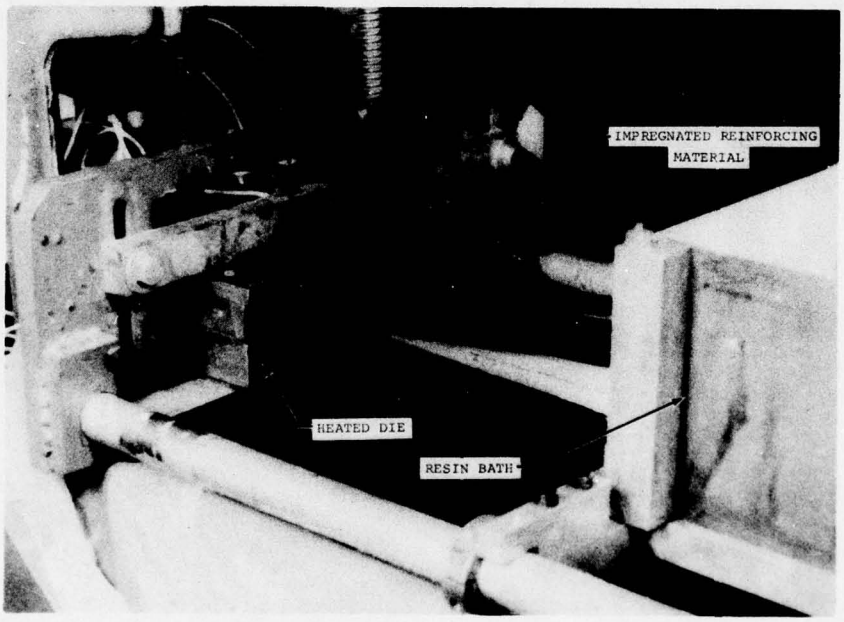


Figure 37. Entrance to Pultrusion Die.

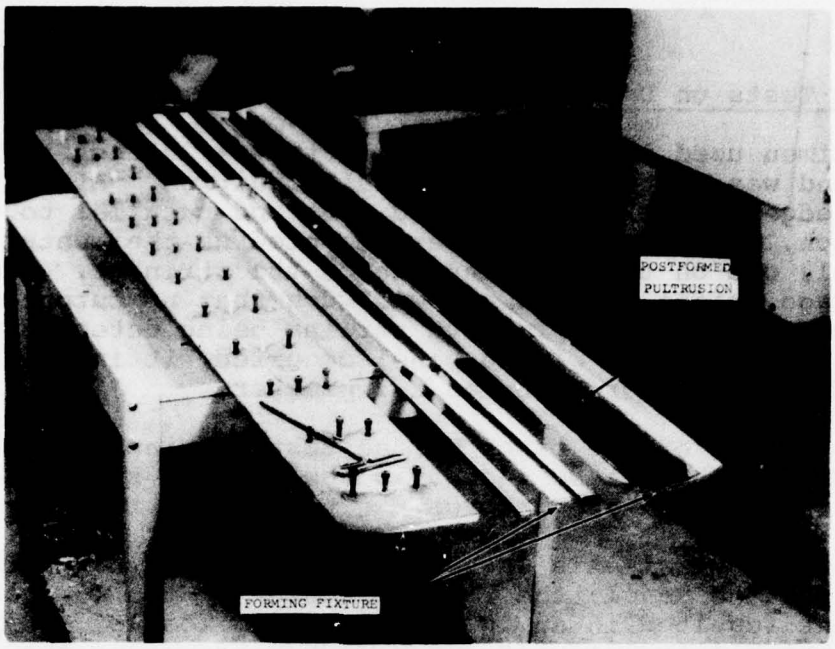


Figure 38. Postforming Tool.

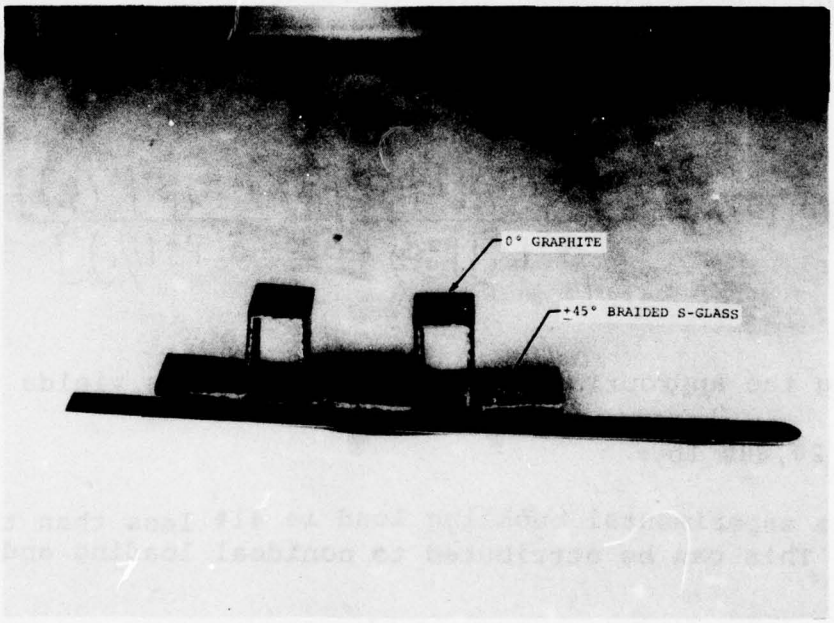


Figure 39. Section of Postformed Material.

Buckling Tests on Demonstration Article

The specimen used in the buckling tests was 20 inches in length and was postcured in the flat condition. After grinding the edges (short) to be loaded flat and parallel to within 0.005-inch, two strain gages were mounted on the center of the panel, one on the skin and one on the stringer. The strain gage bridge arrangement was such that no output occurred provided the compressive strains being detected were equal. When buckling of the panel occurred, it induced a signal that was recorded on an X-Y plotter.

The arrangement of the panel in the test machine may be seen in Figure 40, which also indicates the loading system (based upon pins acting on vee grooves).

The elastic neutral axis was calculated to be 0.239-inch from the face of the panel; the line of action of the load through this point resulted in an initial buckling load of 700 pounds and an instability load of 9950 pounds. Adjusting the load application points to a distance of 0.225-inch from the panel face resulted in the buckling load occurring at 4100 pounds and the instability load at 12,340 pounds. These results are shown in the load-deflection trace of Figure 41. P critical can also be calculated from Equation (C-30) presented in Appendix C:

$$P_{cr} = \sqrt{D_{11}D_{22}}\,\frac{\int_0^b \phi\,dy + b\sum_{i=1}^{N}\left[f_i\beta^4 f^2(\eta_i) + x_i\beta^2 f'^2(\eta_i)\right]}{\beta^2\left[\int_0^b f^2\,dy + b\sum_{i=1}^{N}\delta_i f^2(\eta_i)\right]}$$

Inserting the appropriate structural properties yields the result,

P_{cr} = 20,880 lb.

Thus, the experimental buckling load is 41% less than that predicted. This can be attributed to nonideal loading and efge effects.

Crippling Tests on Demonstration Article

Small angle and channel coupons were cut from the final part and tested in compression for crippling strength; the results are presented in Table 16 and plotted as dimensionless ratios

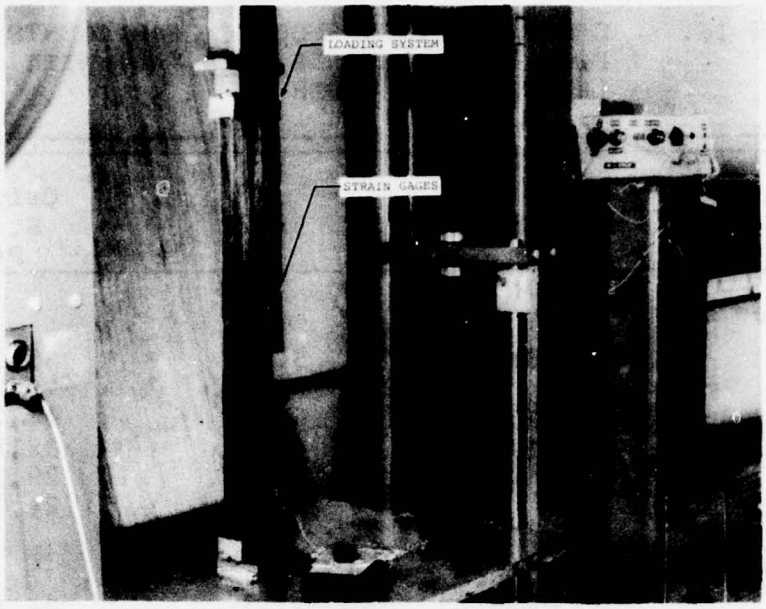


Figure 40. Panel Undergoing Buckling Tests.

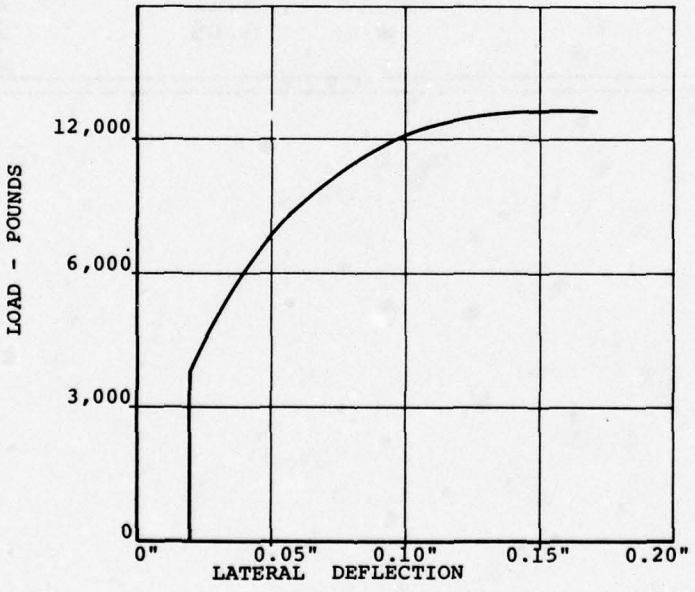


Figure 41. Load Deflection Relationships Obtained During Buckling Tests.

TABLE 16. CRIPPLING TEST RESULTS OF ELEMENTS FROM FINAL ARTICLE - (0,±45) WITH LENGTH = 4 x WIDTH

Test No.	Shape	b/t	Crippling Stress Psi
One Edge Free			
155-1	Angle	6.66	35,390
155-2	"	6.94	28,710
155-3	"	6.54	44,210
155-4	"	4.16	32,160
155-5	"	3.84	29,180
155-6	"	4.31	24,330
No Edge Free			
155-7	Channel	7.34	21,120
155-8	"	7.08	32,200
155-9	"	7.46	22,620
155-10	"	9.13	27,000
155-11	"	9.11	26,770
155-12	"	9.11	26,200
155-13	"	9.05	24,100

TABLE 17. UNIDIRECTIONAL PROPERTIES OF COMPOSITE MATERIALS USED IN EFFICIENCY ANALYSIS

Material	E_o^c (10^6 psi)	E_{90}^c (10^6 psi)	G (10^6 psi)	ν_{12}	ε_o^{cu} (μin/in)	ρ (lb/in^3)
Modmar II/5206	23	1.4	.7	.24	11,900	.055
Hercules AS/3002	16	3.7	.8	.25	13,500	.055
Celanese GY-70/904	42	.9	.6	.25	2,100	.061
120 Fiber-glass cloth/ MIL-R-9300 Epoxy	2.2	2.2	.6	.11	20,000	.065

in Figure 42. Due to the limitations imposed by the available specimen size, the b/t ratios are considered to be too low to demonstrate any significant changes in the relationship between the two parameters. The results are generally somewhat lower than that expected.

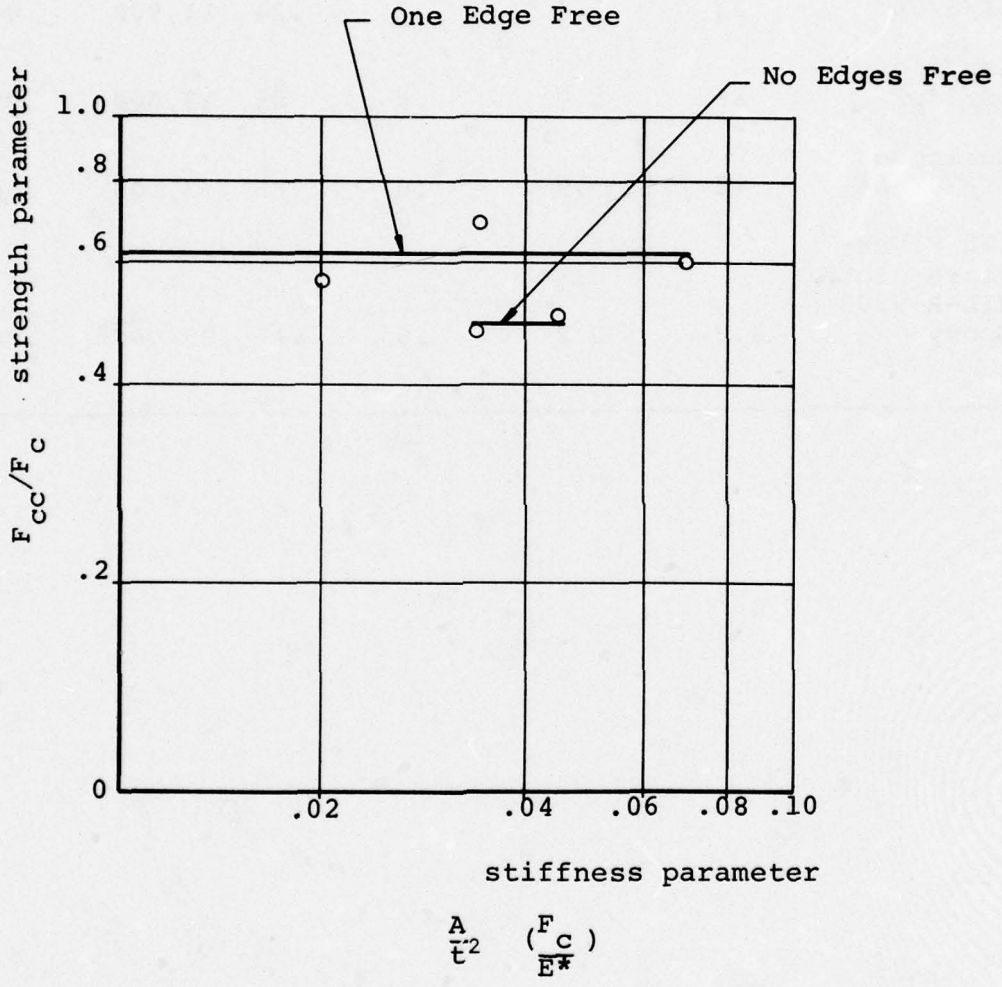


Figure 42. Crippling Stress of (0, ±45) Hybrid Composite.

APPLICATION STUDIES

The application study established the potential performance and cost advantages that the pultrusion process would offer in manufacturing high-performance aircraft structural components. The approach was to parametrically evaluate composites for specific structural applications and then to develop conceptual designs based on the parametric studies and manufacturing limitations of pultrusion.

PARAMETRIC STUDY

To assess the potential of various fibers, matrices and structural proportions, a structural efficiency analysis approach was used. The low density and high strength and stiffness of composites, relative to conventional aerospace metals, indicates that they should be highly efficient as structural members. For a unidirectional intermediate strength graphite/epoxy, the strength-to-density ratio in the direction of the fibers is in the order of 3.6×10^6 inches. This value compares to 0.7×10^6 inches for 7075-T6 aluminum alloy. The conclusion drawn from the values that a graphite/epoxy tension member would be 1/7 the weight of an aluminum member would most likely be invalid since other design considerations such as secondary loads, minimum gage, eccentricity of load, etc., would completely change the relationships.

Various techniques have been used to determine optimum designs for structural elements constructed from conventional isotropic metals. These techniques, for many reasons, are insufficient for the optimum design of composite structural elements. Unlike conventional metals, filamentary reinforced composite materials are orthotropic, or even anisotropic. The full determination of the appropriate form and optimum proportions of structural elements using these materials requires consideration of significantly larger numbers of design variables than do isotropic designs. Imposing undue restrictions on the design process just to effect a simpler solution to the optimization problem excludes many of the advantages offered by using composite materials.

Integrally Stiffened Panels

The structural efficiency analysis used involved the determination of generalized weights of the integrally stiffened panels required to carry given axial loading intensities.

The appropriate parameters for this generalization have been found to be weight per unit surface area divided by panel width as a function of axial running load per unit width. Evaluation of the minimum weight form and proportions in each case required the application of appropriate failure criteria. Overall panel stability was described by orthotropic stiffened plate theory; local stability of the panel elements was described by orthotropic plate theory.[15] A maximum strain criterion was used to describe strength limitations of the composite materials.

The optimum minimum weight configuration is obtained when two failure modes occur simultaneously for a given load. An example would be the panel elements failing by local instability at the same stress level that overall buckling occurs. The solutions are obtained graphically by cross plotting the weight parameter and the load parameter in terms of panel dimension ratios.

Two panel configurations were studied, a webcore panel and a single-face corrugated panel, as defined in Figures 43 and 44.

To reduce the number of variables, certain of the panel dimensions were either held constant or related to another variable. For the webcore panel, the skin and webs were the same thickness. The height of the web was related to the web spacing such that the web and skin elements had the same resistance to local buckling. The panel width-to-height ratio was maintained at b/a = 2, representative of a panel element between frames in a fuselage. For the single-face corrugated panel, the height and width of the stiffener were maintained equal. The space between stiffeners was related to the stiffener height such that both elements had the same resistance to local buckling. These restrictions on dimensions minimize the weight as regards local buckling by ensuring that all material fails at the same time.

The load parameter for overall stability of the webcore panel is

$$\frac{N_x}{b} = \frac{\pi^2 E_x}{2 m^2}\left(\frac{1 + t/d}{1 - \nu_{xy}\nu_{yx}}\right)\left(\frac{t}{d}\right)\left(\frac{d}{a}\right)^3\left(\frac{a}{b}\right)^5 (A+B) \qquad (1)$$

where

A and B are defined in Appendix C.

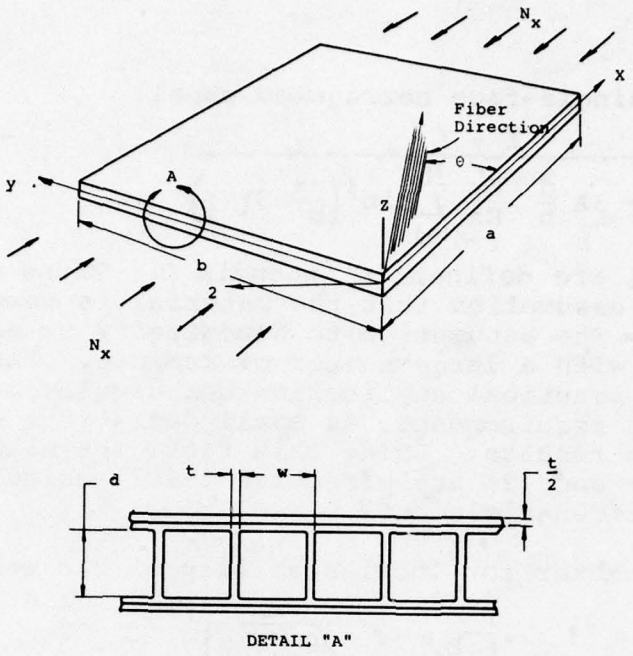


Figure 43. Webcore Panel - Dimensions and Coordinate System.

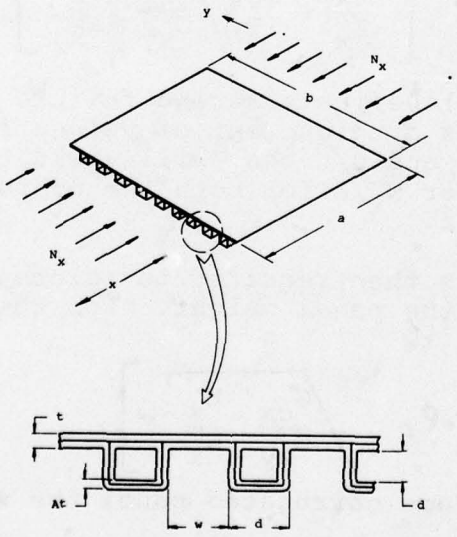


Figure 44. Single-Face Corrugated Skin Panel - Dimensions and Coordinate System.

and for the single-face corrugated panel:

$$\frac{Nx}{b} = \frac{K + L}{\frac{1}{2} + 3A \frac{d}{b} \frac{E'x}{Ex} \sum_{i=1}^{N} \sin^2\left(\frac{\eta\pi}{b} \eta_i\right)} \qquad (2)$$

where K and L are defined in Appendix C. These equations are based on the assumption that the material is homogeneous and orthotropic. The assumption to homogeneity is met for a balanced lay-up with a large number of laminae. The sequence of laminae in a practical application can usually be arranged to satisfy these requirements, as small deviations will not grossly affect the results. Using this fact, the elastic moduli in equations (1) and (2) are effective moduli calculated for the plate and stiffener elements.

The load parameter for local stability of the webcore panel is

$$\frac{N_x}{b} = \left(\frac{t}{d}\right)^3 \left(\frac{d}{b}\right) G'_{cx} \left[2\frac{E_x}{E'_x} + \sqrt{\frac{G'_{cx} E_x}{G_{xy} E'_x}}\right] \qquad (3)$$

and for the single face corrugated panel is

$$\frac{N_x}{b} = \left(\frac{t}{d}\right)^3 \frac{d}{b} G'_{xy} \left[A^2 \frac{E_x}{E'_x} + 3A^4 \sqrt{\frac{G'_{xy}}{G_{xy}} \frac{E_x}{E'_x}}\right] \qquad (4)$$

Equations (3) and (4) define a second failure criterion for the panels. There is a unique set of values for the panel dimension ratios b/d and d/t that will yield the same value for the load parameter N_x/b for both the overall and local instability condition.

A weight parameter is then required to relate the panel dimension ratios to the panel weight. For the webcore panel the weight parameter is

$$\frac{W}{ab^2} = \frac{t}{d} \frac{d}{b} \left[2\rho_f + \rho_r \sqrt{\frac{G'_{cx}}{G_{xy}} \frac{E_x}{E'_x}}\right] \qquad (5)$$

and for the single-face corrugated panel the weight parameter is

$$\frac{W}{ab^2} = \frac{t}{d}\,\frac{d}{b}\left[\rho_p + 3A^2\rho_s\sqrt{\frac{G'_{xy}}{G_{xy}}\,\frac{E_x}{E'_x}}\right] \tag{6}$$

By solving Equations (2), (4) and (6) for various b/d and d/t ratios and substituting in the elastic properties of the composite, a family of curves is obtained that relates panel weight and dimensions to the ability to transmit an axial compressive load. In Figure 45 the results are plotted for a single-face corrugated panel based on the properties of Hercules AS graphite fiber and epoxy resin. Half the fibers in the plate and stringers are oriented 0° to the load and the remaining half are oriented ± 45° to the load. For clarity, only the pertinent curves are plotted. Three points of common intersection can be noted for different sets of dimension ratios and parameters, as follows:

1. $\frac{N_x}{b^2} = 280$ for $\frac{b}{d} = 20$, $\frac{d}{t} = 3$

2. $\frac{N_x}{b^2} = 24$ for $\frac{b}{d} = 40$, $\frac{d}{t} = 6$

3. $\frac{N_x}{b^2} = 5.7$ for $\frac{b}{d} = 60$, $\frac{d}{t} = 9$

A line drawn through these points defines the minimum weight panel that will carry any given load.

A third failure criterion of ultimate compressive strength can also be applied. The load parameter for a webcore panel is

$$\frac{N_x}{b} = \varepsilon_{0^\circ}^{cu}\left(\frac{t}{d}\right)\left(\frac{d}{b}\right)\left[2E_x + E'_x\sqrt{\frac{G'_{cx}}{G_{xy}}\,\frac{E_x}{E'_x}}\right] \tag{7}$$

and for a single-face corrugated panel it is

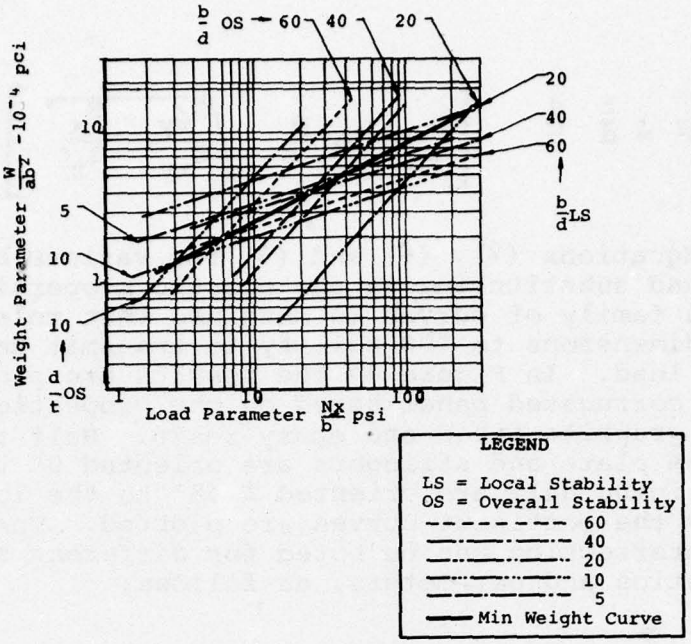


Figure 45. Minimum Weight Curves for Structural Efficiency Analysis.

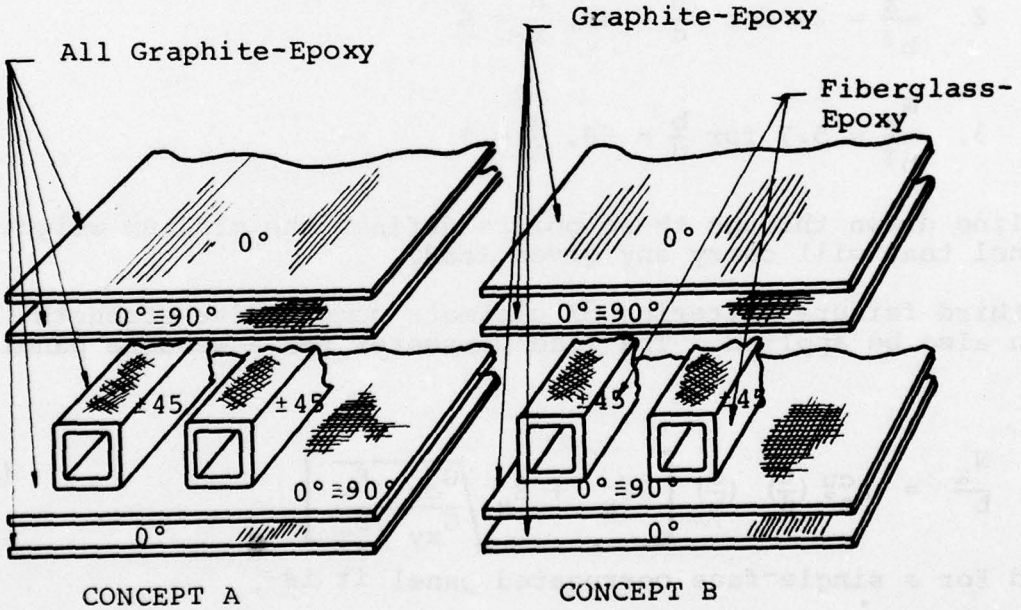


Figure 46. Webcore Designs Analyzed.

$$\frac{N_x}{b} = \frac{t}{d}\frac{d}{b}\varepsilon_{0^\circ}^{cu}\left[E_x + 3E'_x A^2\sqrt{\frac{G'_{xy}}{G_{xy}}\frac{E_x}{E'_x}}\right] \quad (8)$$

The ultimate strength criterion interacts with the overall stability to set the minimum weight curve since, as the elements thicken, it precludes local instability.

Practical designs must also consider the minimum gage that can be used for a material in a particular application. The minimum gage is set by secondary factors such as manufacturing requirements, ballistic damage tolerance, foreign object impacts and resistance to environment to name a few. Since minimum gage cannot be considered in the context of the loads, it is included in the structural efficiency analysis when considering a specific application. The effect of minimum gage was included by considering a helicopter fuselage application. In studies of the application of composite materials to helicopter fuselages by Sikorsky Aircraft[16] and Boeing Vertol,[17] the frame spacing in both cases was 20 inches. By assuming a = 20 inches and considering two minimum gages as t = .020 inch and t = .040 inch, a lower bound is defined for the minimum weight curve.

The mechanical properties used in this study are shown in Table 17. Using laminated plate theory, the elastic constants for the composite material were calculated. Then, by assuming the plate to be orthotropic and homogeneous, the equivalent elastic modulii were calculated.

For a webcore panel, two concepts were studied as shown in Figure 46. The graphite-epoxy properties used were for Modmar II/5206 and the fiberglass-epoxy was with E-glass 120 cloth. The results of the calculations are presented in Figure 47. The effects due to local stability are cut off by the minimum gage lines, and the sloped portion for $N_x/b > 80$ is set by ultimate compressive strength and overall stability. Superimposed are the load and weight ranges reported[16] for the CH-53D helicopter fuselage converted to efficiency parameters. For this application, the composite webcore skin at 0.020-inch thick would show a 19% weight savings over the areas with 0.032-inch aluminum skin and be equal for the areas with 0.025-inch skin. However, a minimum gage of 0.020-inch would

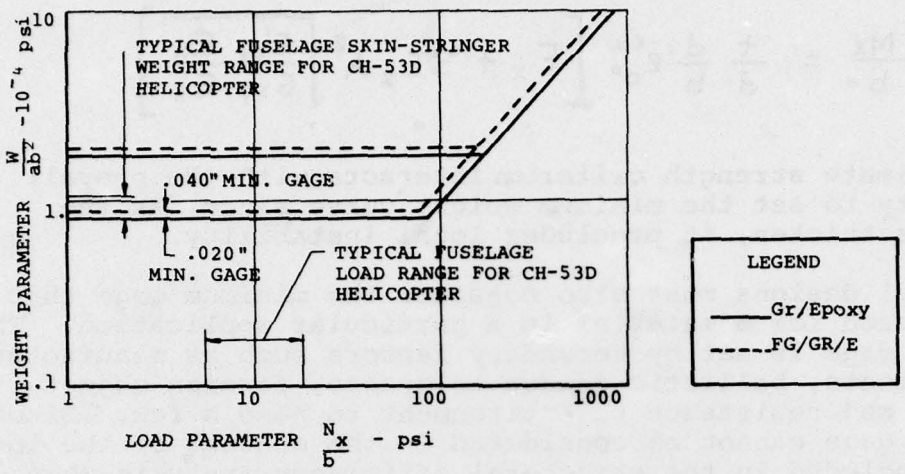


Figure 47. Structural Weight Relation for Webcore Panel.

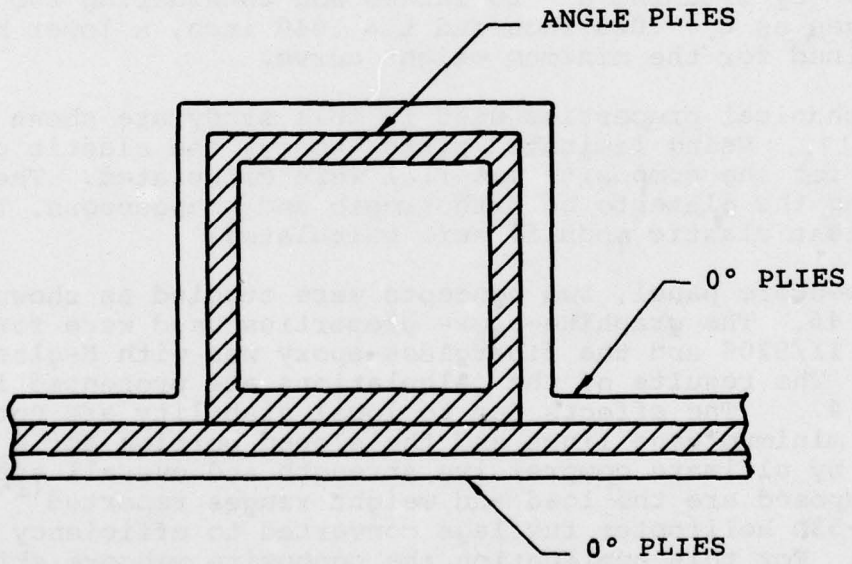


Figure 48. Distribution of Plies in Single-Face Corrugated Panels.

probably not be satisfactory when all the design considerations were included. It is of interest to note the small weight penalty incurred by using fiberglass for the webs and part of the skin thickness, pointing out the viability of the hybrid fiber approach.

The webcore panels will be effective at higher loadings than would be found on wing and tail surface skins.

The number of cases were run for single-face corrugated panels to explore their weight sensitivity to various parameters. The ply distribution within the laminate is shown in Figure 48. The actual ratio of 0° plies to angle plies was varied. In the first case, the stringer thickness to plate thickness ratio was 0.5 and the angle plies represented 50 percent of the respective thicknesses. The results are plotted in Figure 49. The use of fiberglass for the angle plies in this case causes a 50-percent increase in structural weight over the all graphite panel. The graphite panel is 40 percent heavier than the aluminum skin-stringer panel.

Next, the ratio of 0°:± 45° plies was changed from 1:1 to 2:1, thereby increasing the modulus in the load direction. The results are plotted in Figure 50. The solid line is the same as that in Figure 49. In this case the weight of the graphite-epoxy composite panel has been reduced and now is only 15 percent heavier than the aluminum skin-stringer panel. In the balance of the cases studied, the thickness ratio for 0°:± 45° was maintained at 2:1.

The modulus of the fiber should have a marked effect on the response of structures to buckling. Therefore, the efficiency was calculated for a low, medium and high modulus graphite. The material properties used were for Hercules AS/3002, Modmar II/5206 and Celanese GY-70/904 epoxy systems. The results are plotted in Figure 51. The graphite-epoxy composite panels based on Modmar II and Hercules AS fibers had essentially the same efficiency. However, the Celanese GY-70 fiber-based composite showed a marked reduction in weight of 35 percent. This panel would average about 10 percent lighter than the aluminum skin-stringer panels for the CH-53D helicopter.

The orientation of the angle plies has a marked effect on buckling. Four different fiber orientations were compared to evaluate this effect. The orientations chosen were ±45°, ±60°, ±30° and 0;90°. The results of the calculations are shown in Figure 52 for a Hercules AS/904 composite. The ±45° orientation for the angle plies results in the lowest weight for a given load. This result is primarily influenced by the

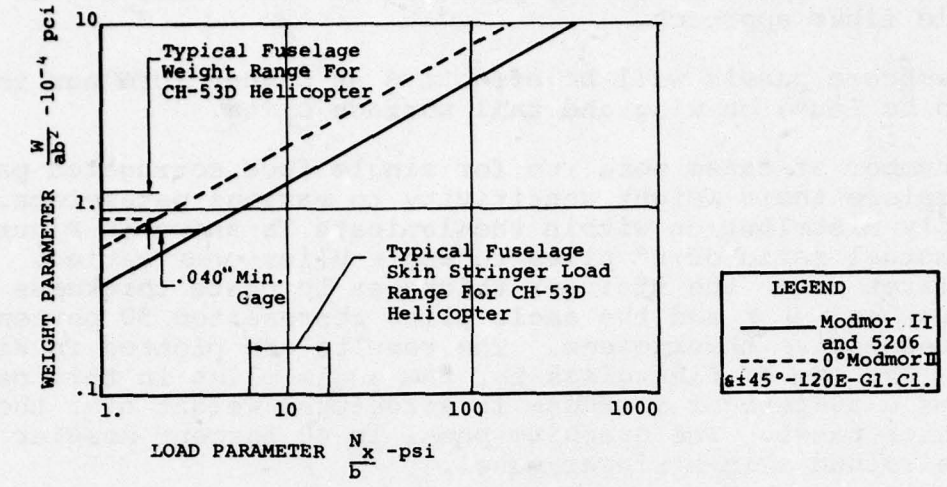


Figure 49. Fiberglass Vs. Graphite for Angle Ply Layers With Single-Face Corrugated Panels.

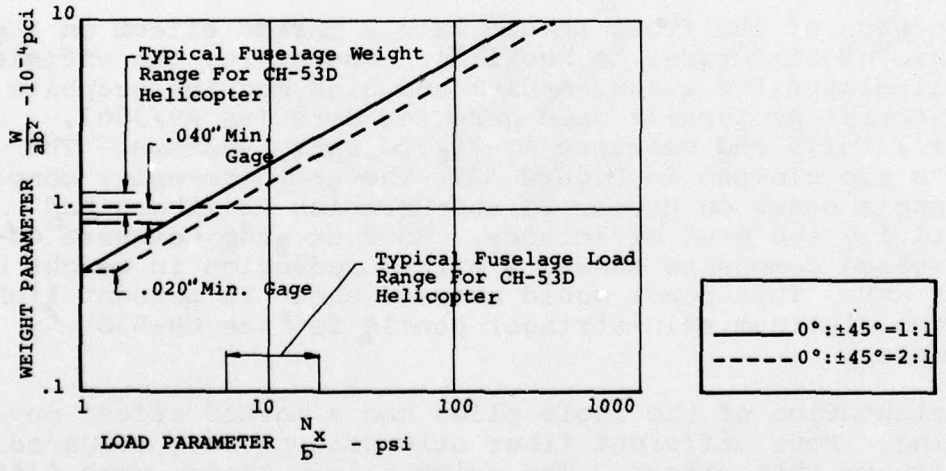


Figure 50. Thickness Effect in Single-Face Corrugated Panels.

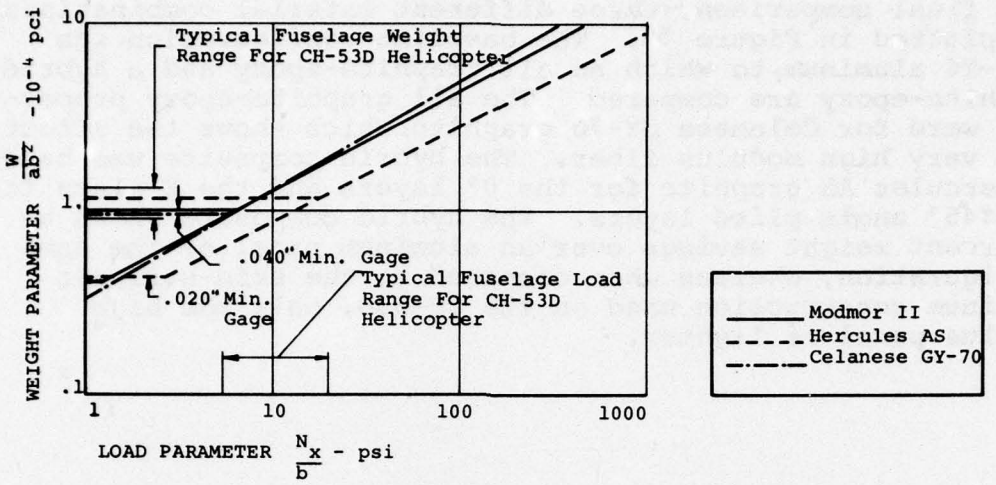


Figure 51. Modulus Effect in Single-Face Corrugated Panels.

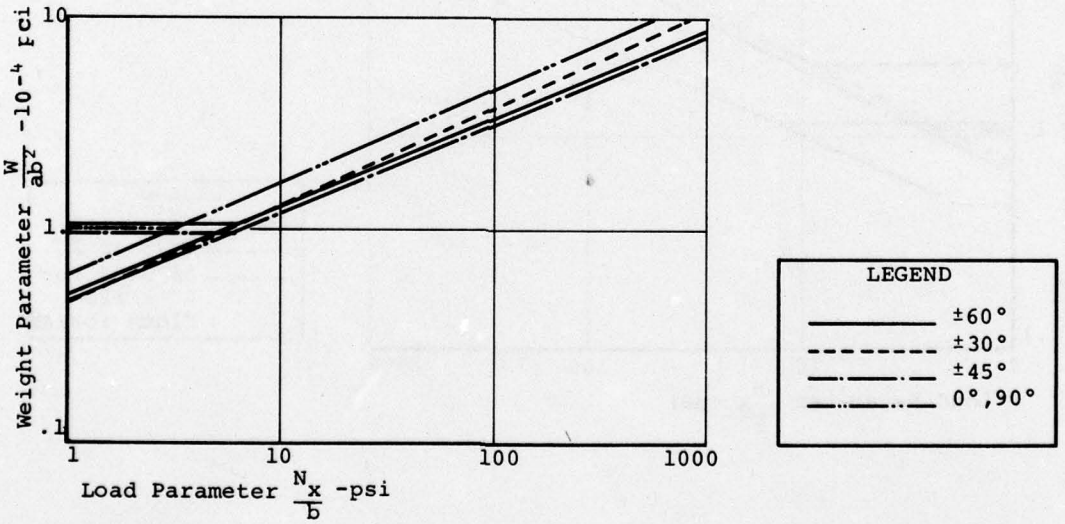


Figure 52. Orientation Effect of Fibers for Single-Face Corrugated Panels.

Load Parameter for local buckling, which is directly dependent on the shear modulus of the material.

As a final comparison, three different material combinations are plotted in Figure 53. The baseline configuration was 7075-T6 aluminum, to which an all graphite-epoxy and a hybrid graphite-epoxy are compared. The all graphite-epoxy properties were for Celanese GY-70 graphite, which shows the effect of a very high modulus fiber. The hybrid composite was based on Hercules AS graphite for the 0° layers and the E-glass for the ±45° angle plied layers. The hybrid composite shows an 8-percent weight savings over an aluminum panel of the same configuration, whereas when compared to the skin-stringer aluminum construction used on the CH-53D, only the high modulus panel is lighter.

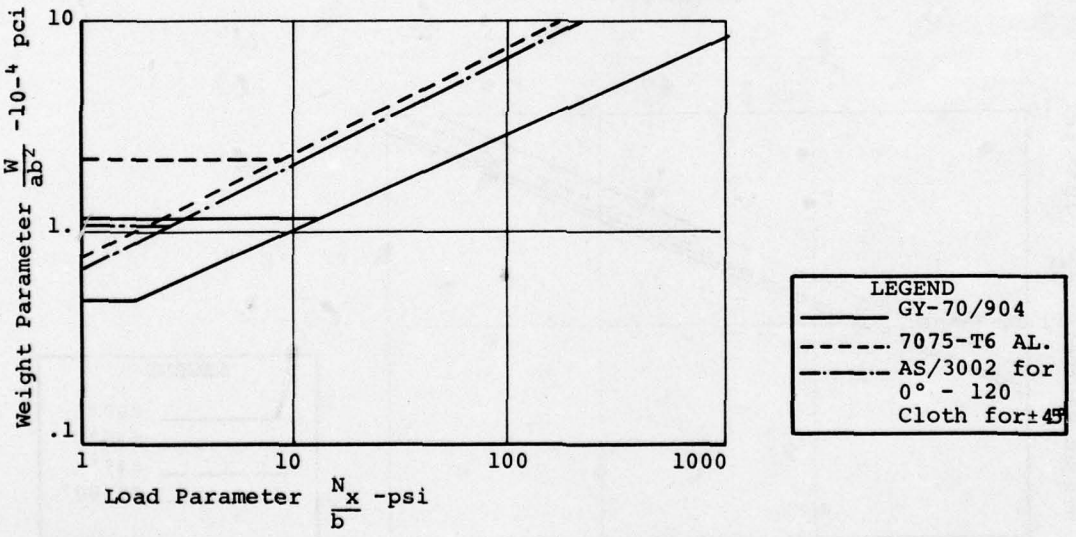
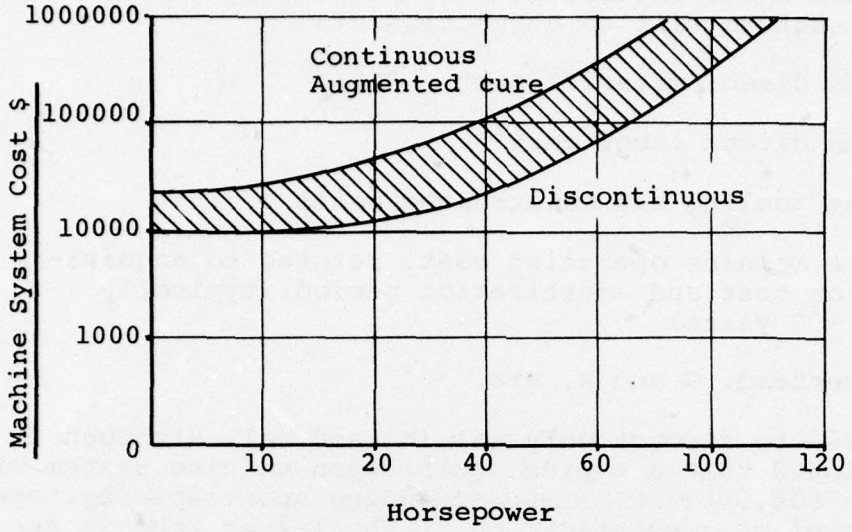


Figure 53. Material Comparison for Single-Face Corrugated Panels.



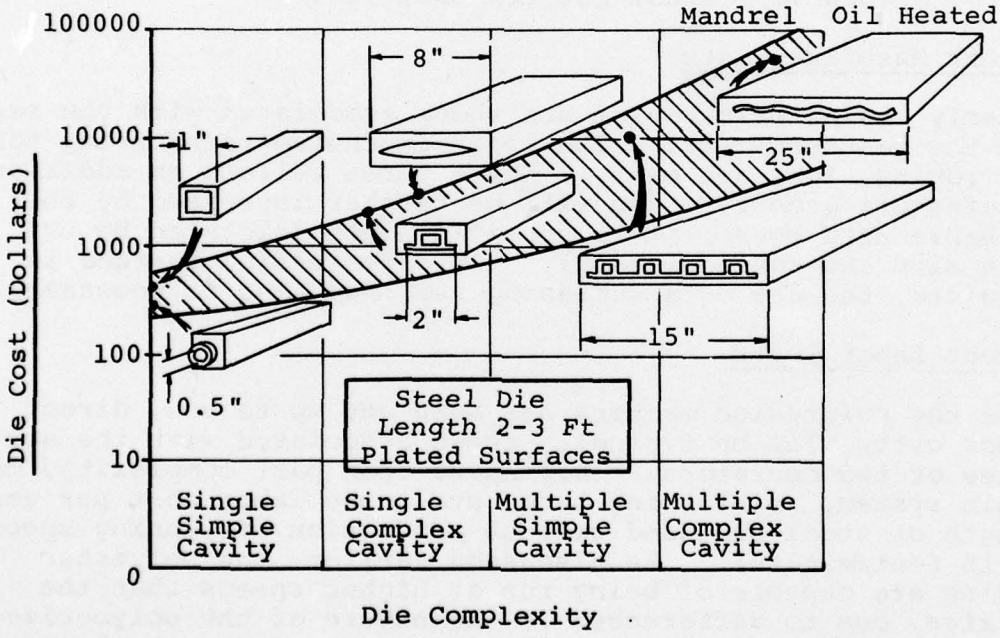


Figure 54. Characteristic Die Costs.

MANUFACTURING COST STUDIES

The production costs associated with pultruding a specii length of structure will be a function of:

(a) the direct material cost

(b) the direct labor cost

(c) the tooling and maintenance costs

(d) the machine operating cost, related to acquisition cost and amortization period (typically 5 - 7 years)

(e) overhead, G and A, etc.

It is proposed to discuss only (a), (b) and (c), although it may be mentioned that a typical pultrusion machine system will cost between $30,000 and $150,000, depending upon capacity, speed, power and level of sophistication. The latter item is related to the use of continuous or discontinuous pullers, use of a preheating system (dielectric, inductive, infrared, etc.), use of automatic product cut-off saw, etc.

Direct Material Costs

Clearly the material costs are those associated with the resin and the reinforcement. The least expensive reinforcing forms are roving, tows and mats. Woven forms reflect an additional manufacturing cost, which will be further increased by the probable need to slit to a specific width (dictated by the part size and configuration). If a resin-rich surface is required, the use of a surfacing veil may also be necessary.

Direct Labor Costs

Once the pultrusion machine has been set up to run, direct labor costs will be typically those associated with the services of two operators. Dependent upon part complexity, mass, resin system, reinforcing form, etc., the labor cost per unit length of stock produced will be a function of running speed (1-15 feet/minute). As discussed earlier, the polyester resins are capable of being run at higher speeds than the epoxies, due to differences in the nature of the polymerization chemistry for these materials. Products involving woven forms generally are run at lower speeds, due to constraints on material feed-in and the need for adequate resin impregnation.

Tooling and Maintenance Costs

The costs of tooling are those due to dies, special heaters, mandrels (for hollow products), creels, in-feed devices (for reinforcing materials), special resin impregnation systems (tanks, pressurizing units), shaped gripper faces, etc.

With the exception of the die, most production requirements can be met with standard equipment readily adapted to meet changing needs. Die costs are highly variable, depending upon complexity and size. As a generality, such costs may vary from $1,000 to $50,000. To illustrate this concept, Figure 54 shows the acquisition costs of typical dies purchased recently, related to geometric and size factors.

The maintenance costs of dies are generally related to such needs as cleaning and replating and will not normally exceed 10% of acquisition cost per 100,000 feet of stock produced.

AD-A035 217 GOLDSWORTHY ENGINEERING INC TORRANCE CALIF F/G 11/4
MM AND T-PULTRUDED COMPOSITE STRUCTURAL ELEMENTS.(U)
DEC 76 B H JONES, W JAKWAY DAAJ02-74-C-0053
UNCLASSIFIED USAAMRDL-TR-76-5 NL

2 OF 2
ADA035217



END

DATE
FILMED
3-77

CONCLUSIONS

This program enables the following conclusions to be reached:

1. The use of existing epoxy resin systems, of the epichlorohydrin bisphenol A type, are suitable for use in the pultrusion process. In order to minimize die adherence, the use of diamine hardeners appears beneficial.

2. From the experience obtained during this program, the use of internal mold releases is not effective and will degrade mechanical properties.

3. The use of polyester resins with graphite reinforcements should include pretreatment of the graphite to enhance filament-matrix bonding.

4. The viscosity of the resin system for optimum processing should be in the range of 300-1000 cps, depending upon product size and form of reinforcing.

5. When pultruding with the epoxy resin systems investigated during this contract, stock speeds of 1 to 2 ft/min would produce a level of cure such that the material would be totally solid and tack-free. Fully-cured conditions could be attained by simply subjecting the product to a normal post-curing cycle.

6. The mechanical properties exhibited by the specimens produced by pultrusion were generally superior or equal to those exhibited by equivalent specimens produced by vacuum bagging.

7. While experience with the resin systems intended for prepregging demonstrated some difficulties in processing, the mechanical properties exhibited by these materials were very satisfactory. This suggests that reformulation of such a resin system for use in pultrusion may be advantageous.

8. For the epoxy resin systems investigated, post-forming could easily be carried out during the final curing cycle, provided no curvature was induced along the axes of the filaments.

9. The static and fatigue properties demonstrated by the specimens pultruded were consistent with those

characteristic of other processing techniques. It may, therefore, be asserted that pultrusion does not intrinsically degrade the short- or long-term behavior of a composite material.

10. In the absence of ply-on-ply biased reinforcement, the use of braiding to provide a convenient form for pultrusion is viewed as acceptable.

11. Complex, hybrid structures may be produced by pultrusion, which is both cost-effective and efficient. Any limitations inherent in the process, from a material orientation standpoint, are offset by the cost and repeatability of the technique. Good translation of coupon properties into larger scale structures appears readily attainable.

RECOMMENDATIONS

Based on the information derived from this program, it is recommended that:

1. Effort be directed toward the formulation of high-performance resins specifically suited to pultrusion processing requirements, which possess good processability and mechanical properties at low and elevated temperatures.

2. Advanced design studies be initiated to enable pultruded substructures to be incorporated into major assemblies.

3. Programs be instituted to develop methods for producing and in-feeding multi-oriented reinforcements to remove the existing limitation on available reinforcing forms.

REFERENCES CITED

1. Dhonau, O.E., CONCEPTUAL DESIGN OF COMPOSITE V/STOL TACTICAL FIGHTER, LTV Corporation, AFML TR 73-3, Air Force Material Laboratory, Wright-Patterson Air Force Base, Ohio, July 1973.

2. Ewald, G.W., PULTRUSION, MODERN PLASTICS ENCYCLOPEDIA 75-76, Vol. 52, October 1975.

3. Goldsworthy, W.B., PULTRUSION - A GROWING TONNAGE MARKET FOR REINFORCED PLASTICS END PRODUCTS, Reinforced Plastics (London), June 1971.

4. Jones, B.H., PULTRUDING FILAMENTARY COMPOSITES, AN EXPERIMENTAL AND ANALYTICAL DETERMINATION OF PROCESS PARAMETERS, SPI 29th Annual Technical Conference, Reinforced Plastics Composites Institute, February 1974.

5. Maximovich, M.G., Hollingsworth, C.D., Neff, R.M., DEVELOPMENT OF IMPROVED ENVIRONMENTAL RESISTANT ORGANIC-REINFORCED MATRIX SYSTEMS, SPE Pactec 75, Las Vegas, 1975.

6. Oleesky, S., and Mohr, G., HANDBOOK OF REINFORCED PLASTICS OF THE SPI, Reinhold Publishing Co., 1964.

7. Timoshenko, S., and Goodier, J.N., *THEORY OF ELASTICITY*, McGraw Hill Book Company, 1951.

8. Anon., ADVANCED COMPOSITES DESIGN GUIDE (3rd Ed.), Air Force Materials Laboratory, Vol. IV, 1973.

9. Boller, K.H., SOME FATIGUE CHARACTERISTICS OF GLASS REINFORCED COMPOSITE LAMINATES, ASME Design Engineering Conference, Pages 70-DE-6, 1970.

10. Rao, N. and Hofer, K.E., FATIGUE BEHAVIOR OF GRAPHITE/GLASS/EPOXY COMPOSITES, Final Report on Contract No. N00019-72-C-0294, Naval Air Systems Command, April 1973.

11. Anon., PLASTICS FOR FLIGHT VEHICLES PART I REINFORCED PLASTICS, MIL-HDBK-17, 1959.

12. Novak, R.C., TORSIONAL FATIGUE BEHAVIOR OF UNIDIRECTIONAL RESIN MATRIX COMPOSITES, Composite Materials Testing and Design, ASTM, STP 546, 1974.

13. Anon., METALLIC MATERIALS AND ELEMENTS FOR AEROSPACE VEHICLE STRUCTURE, MIL-HDBK-5B, 1972,

14. Jones, B.H., PROBABILISTIC DESIGN AND RELIABILITY, in Composite Materials, Vol. 8, Structural Design and Analysis Part II, Academic Press, New York, 1975.

15. Lekhnitskii, S.C., Anisotropic Plates, Gordon and Breach, 1968.

16. Rich, M.J., et al, APPLICATION OF COMPOSITES TO HELICOPTER AIRFRAMES AND LANDING GEAR STRUCTURES, Sikorsky Aircraft, NASA CR-112333, National Aeronautical and Space Administration, Langley, Virginia, June 1973.

17. Swatton, S., STUDY OF ADVANCED STRUCTURAL CONCEPTS FOR FUSELAGE, Final Report on Contract DAA-JO2-72-C-0056, U.S. Army Air Mobility Research and Development Laboratory, October 1973.

18. Cagle, C.V.(Ed.), HANDBOOK OF ADHESIVE BONDING, McGraw Hill Book Co., 1973.

19. Timoshenko, S.P., and Gere, J.M., Theory of Elastic Stability, McGraw Hill Book Co., 1961.

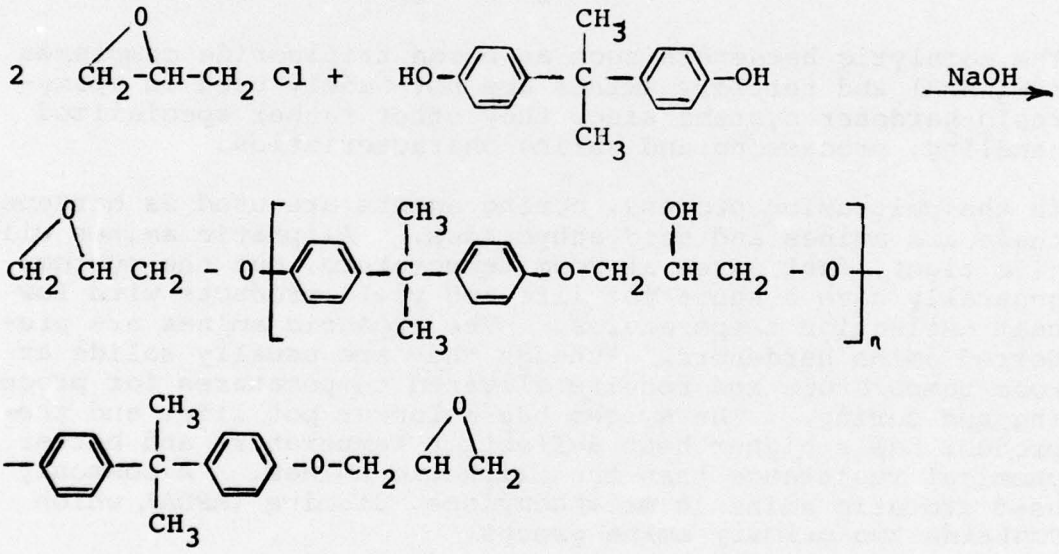
20. Roark, R.J., Formulas for Stress and Strain, McGraw-Hill Book Co., 1954.

APPENDIX A

CHEMICAL CONSIDERATIONS FOR EPOXY RESINS WHEN BEING USED IN PULTRUSION

Since 1950, the epoxy resins have become increasingly important to the reinforced plastics industry. Although many different types of epoxy resins can be produced, three are of major commercial importance: (1) conventional epoxy resins, based on epichlorohydrin and bisphenol A; (2) epoxy novolac resins; and (3) cycloaliphatic epoxy resins. The conventional resins are generally the most commonly used, and are now the least expensive to manufacture. This is presently the most suitable epoxy system for use in pultrusion; some of its properties in relation to the process are examined below:

The conventional epoxy resin is synthesized by adding epichlorohydrin to bisphenol A in the presence of sodium hydroxide to remove the hydrochloric acid given off.

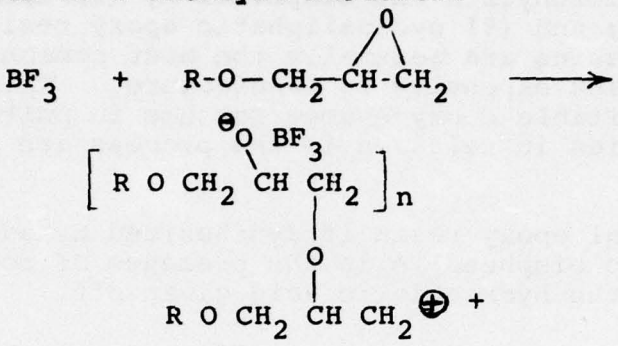


In the above, n determines the molecular weight and the viscosity of the resin. The lower molecular weight products are liquids with an n value of zero. This resin is used in the pultrusion process, since room temperature handling is generally desired. When n is equal to or greater than one, the resins are thermoplastic solids.

An epoxide resin must be converted from a liquid (thermoplastic) state to a tough, hard, solid (thermoset) state by the

addition of hardeners, which are chemically reactive toward the epoxide group of the resin.

The hardener may either be a catalyst or a curing agent. A catalyst initiates self-polymerization of the resin, forming direct linkages between the epoxide groups. A curing agent acts as a cross-linking compound, becoming an integral part of the three-dimensional polymer network. The Lewis acid boron trifluoride acts as a catalyst hardener.

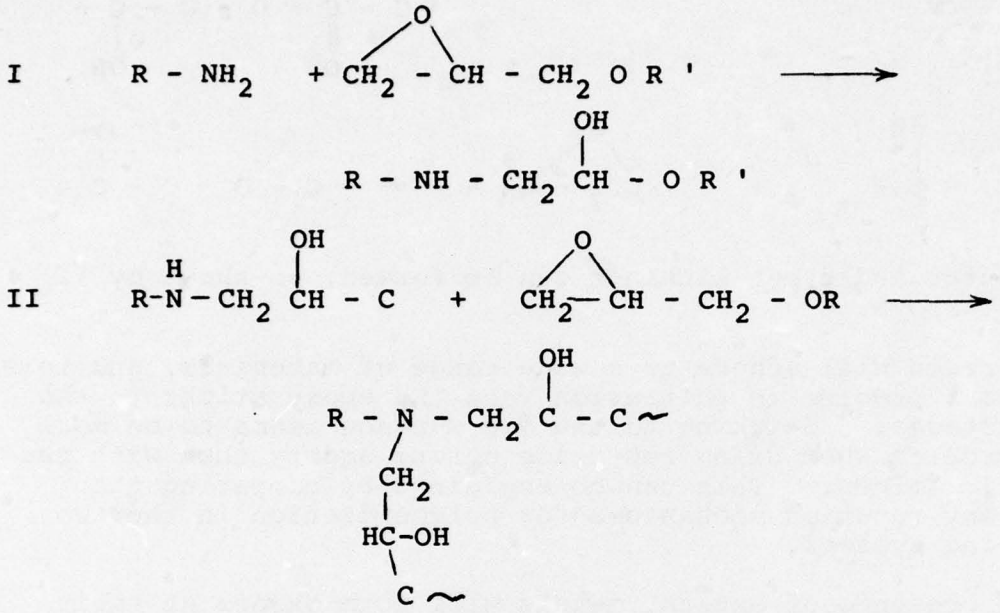


The catalytic hardeners such as boron trifluoride complexes (BF_3 MEA) and tertiary amines are not widely used in epoxy-resin-hardener systems since they offer rather specialized handling, processing and curing characteristics.

In the pultrusion process, curing agents are used as hardeners; these are amines and acid anhydrides. Aliphatic amines will give tight, fast cures at room temperature, but the systems generally have a short pot life and yield products with low heat deflection temperatures. The aromatic amines are preferred amine hardeners, although they are usually solids at room temperature and require elevated temperatures for processing and curing. The system has a longer pot life, and the product has a higher heat deflection temperature and better chemical resistance than the aliphatic amines. A commonly used aromatic amine is metaphenylene diamine (MPDA), which contains two primary amine groups.

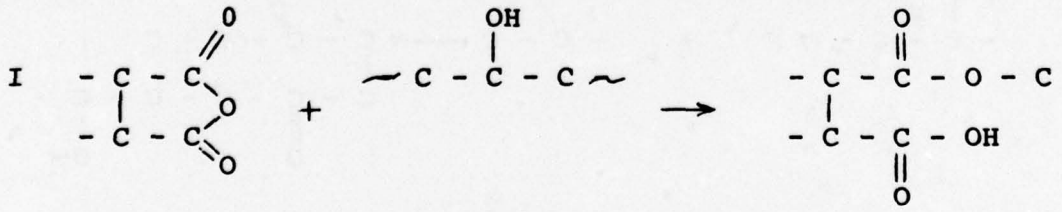
Anhydrides are also used as curing agents. Like aromatic amines, anhydrides require elevated temperature curing; they also yield products with high heat deflection temperatures and good chemical resistance. They provide long pot lives and low exotherms, and anhydrides are available which are low viscosity liquids at room temperature, thus providing low viscosity systems with excellent wetting and processing properties. However, the aromatic amines are preferred since they cause less problems with sticking to die surfaces than the anhyrides.

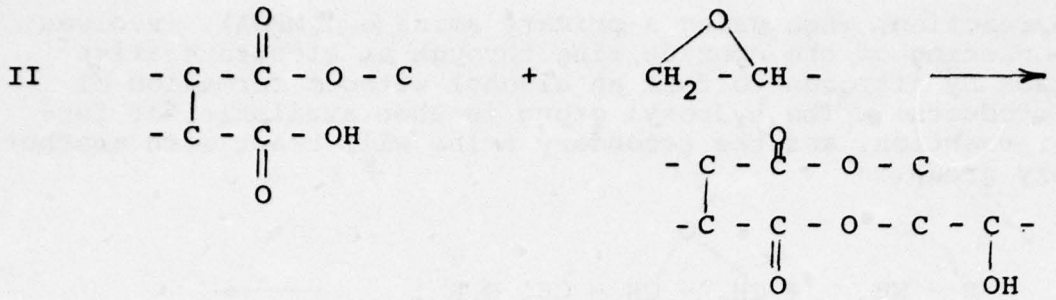
The reaction, when using a primary amine (e.g., MPDA), involves the opening of the epoxide ring through an electronegative attack by nitrogen to form an alcohol without formation of by-products. The hydroxyl group is then available for further reaction, and the secondary amine will react with another epoxy group.

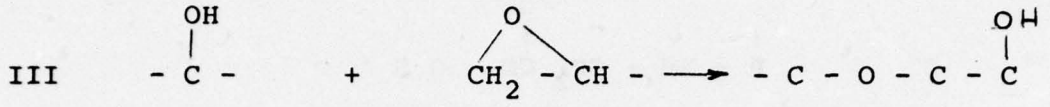


During the reaction, no rearrangement occurs in the backbone of the resin molecule, the reactive epoxide groups being held on the uncured molecule as appendages.

The anhydride (e.g., nodic ethyl anhydride) reaction is initiated by the formation of an ester through the anhydride and a hydroxyl group present on the resin. Water, alcohol, or a tertiary amine can also be used for initiation. Then, the remaining acid group will react with an epoxy group. In addition, self-polymerization of the epoxy group through the epoxy hydroxyl reaction:



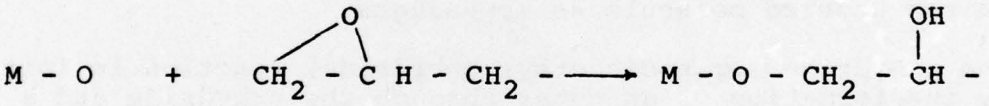
II 

III 

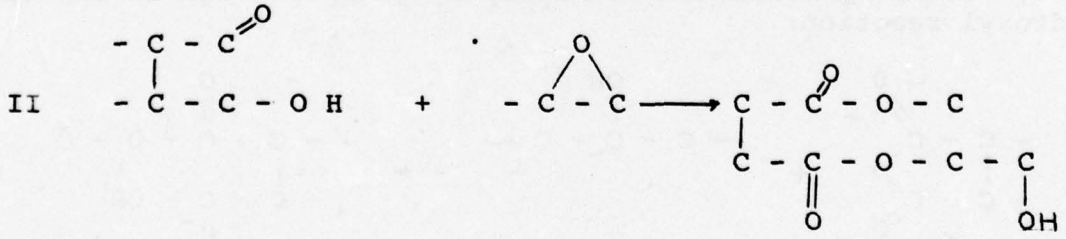
Both ester and ether linkages can be formed, as shown by II and III above.

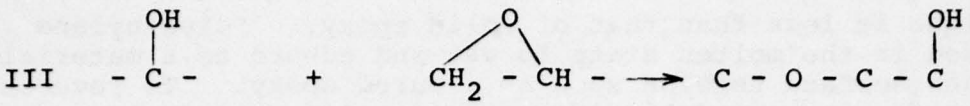
Epoxy resin will adhere to a wide range of materials, and this becomes a problem in pultrusion when the epoxy sticks to the die surfaces. Sticking to the die surface seems to be more of a problem when using anhydride curing agents than with the aromatic amines. This can be explained by comparing the different reaction mechanisms for polymerization in the two hardening systems.

In the presence of oxygen, metals will form oxides at their surface. The metal oxides will electronegatively attack epoxide groups, creating adhesion at the die surface.

I 

This is similar to the mode of reaction in an acid anhydride, in which acidic hydroxyl groups and secondary alcohols open the epoxy ring through electronegative attack by oxygen:

II 



Thus, the metal oxide or metal hydroxyl (M -O-H) group may attack an epoxide ring in a manner similar to the secondary alcohol in the anhydride case.

The same metal oxides are present in the amine hardened system, but the mode of polymerization is opening the epoxide ring. This involves electronegative attack by a nitrogen upon the epoxy ring. Electronegative attack is favored with nitrogen since the lone pair of electrons is more electronegative, and thus more reactive, than the two lone pairs on oxygen. This leads to a greater free energy drop when an epoxide reacts with a nitrogen than with a hydroxyl group, making attack by nitrogen the favored reaction. No chemical reaction is absolute when more than one pathway is possible, but the reaction with the amine group will predominate. Since the anhydride proceeds with electronegative attack by oxygen, side reactions with metal oxides will be more apparent here.

Epoxy resins have adhesion superior to that for polyesters[16]. They will bond to a wide range of materials such as metal, glass, concrete, and plastics. This is due to their wetting and penetrating ability, low viscosity, and the presence of both polar (hydroxyl) and nonpolar (ether) groups within the molecule, and low degree of volume shrinkage during polymerization (1-6% for epoxy compared with 7-10% for polyester)[17]. The presence of both polar and nonpolar groups provides outstanding adhesion between dissimilar materials, such as metal and plastic. Wetting allows the epoxy to come into close contact with the surface, and van der Waals[18] law of interaction between molecules comes into action.

Surface energetics in adhesion states that for a liquid to wet and spread on a solid surface, the critical surface tension γ_s of the solids must be greater than the surface tension of the liquid, γ_L, thus

$$\gamma_s > \gamma_L .$$

Metals and metal oxides have surface free energies ranging from 100 to 3,000 ergs/cm^2, and organic liquids, such as epoxy, and water have free energies of less than 100. Whenever oxygen becomes a part of the chemical structure of the surface, polarity and thus surface energy is increased, making wetting by an adhesive such as epoxy easier. The role surface oxidation plays in adhesion may be illustrated by the bonding of liquid epoxy to solid polyethylene. The surface tension of molten

polyethylene is less than that of solid epoxy. Polyethylene may be used in the molten state to wet and adhere to a material with higher surface tension such as a cured epoxy. To reverse the situation, i.e., bond liquid epoxy to solid polyethylene, the surface energy of polyethylene must be made greater than the surface tension of liquid epoxy. This can be accomplished by oxidation of the polyethylene surface. This same surface oxidation occurs in the metal dies used in the pultrusion process. Inherent roughness of a surface is also contributory to adhesion since more surface area is present for molecular attraction due to van der Waal's forces. Metal dies for pultrusion should have highly polished surfaces, and either be fabricated from or plated with a metal which undergoes minimal surface oxidation in the presence of air.

APPENDIX B

POLYESTER RESINS - THEIR CHEMISTRY AND APPLICATION TO THE PULTRUSION PROCESS

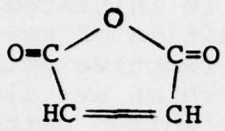
In the pultrusion process, polyester resin systems give fewer problems with sticking to metal die surfaces than the epoxy resins. This may be attributed to radical chain polymerization in epoxies and the absence in polyesters of reactive terminal groups which can form chemical bonds to metal substrates. Polymerization in polyesters is initiated through free radicals formed during the decomposition of peroxide catalysts. These free radicals attack reactive points of unsaturation within the polyester system, which are aliphatic carbon-carbon double bonds, to form an electron paired bond and another free radical. The carbon radicals formed propagate a chain reaction, and all available points of unsaturation are quickly cross-linked. These points of unsaturation, being preferentially attacked by free radicals, are less susceptible to chemical bond formation with an oxide or hydroxide group on the metal die surface. This is due to thermodynamic differences between free radical and substitution reacting. Secondly, polyester resins contain no terminal groups reactive toward chemical groups on metal surfaces.

Chemical Characteristics of Polyesters

The properties of polyester resins may be varied over a wide range by adjusting the starting materials used for formulation of the resin. A vinyl - unsaturated monomer, such as styrene, is added to the polyester. This becomes a cross link between the resin molecules during polymerization and also serves to lower the viscosity of the system. The points of unsaturation in the polyester molecules and monomer act as the points of reactivity by combining together. Polymerization is initiated by free radicals formed in peroxide decomposition which attack reactive carbon-carbon double bonds with formation of another free radical. The free radicals formed on polyester molecules and monomer molecules will attack all other available points of unsaturation in a chain reaction (propagation). Free radicals will then combine to end the polymerization reaction (termination). Initiation of polymerization propagation can be accomplished at high temperatures with catalyst alone, or at room temperature with catalyst and promoter. The elevated temperature system, which gives a longer pot life, is better suited to the pultrusion process.

Polyesters used as a matrix for reinforcement with glass fiber are condensation products of unsaturated dibasic acids, such as maleic acid anhydride, and dihydric or polyhydric alcohols,

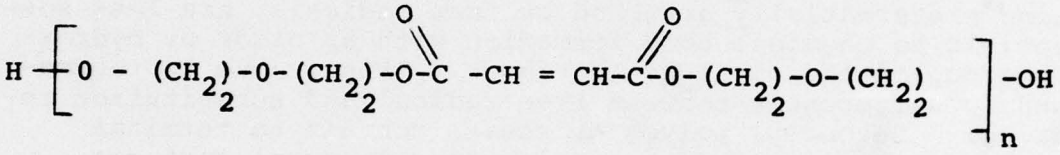
such as diethylene glycol. A combination of maleic anhydride and diethylene glycol will give a rigid resin when cured with many points of cross-linking. Resilient and flexible resin systems are obtained by adding saturated aromatic or aliphatic dibasic acids and by changing the alcohol used. Fewer points of reactive unsaturation lead to fewer cross-links between resin and monomer, and this imparts greater flexibility to the resin. The polyester resin is formed by a condensation reaction between the dibasic acid and dihydric alcohol as shown below:



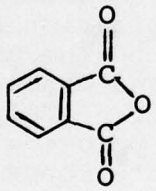
Maleic acid anhydride

+ $HOC\ H_2\ CH_2\text{-}O\text{-}CH_2\ CH_2\ OH$ ⟶

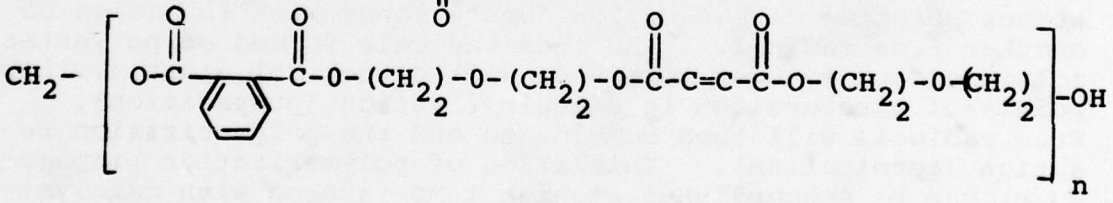
Diethylene Glycol



In the pultrusion process, a resilient polyester resin is preferred. This can be manufactured by adding phthalic anhydride to the above reaction mixture, in a ratio of 1:1 with maleic anhydride.



Phthalic Anhydride



Average polyester molecular weight is determined by the length of time the glycol and the acid anhydrides are allowed to react together, and this may be increased by reacting for a longer time at lower temperatures and by addition of an inhibitor such as hydroquinone during esterification. A general increase in molecular weight has a beneficial effect on most of the im-

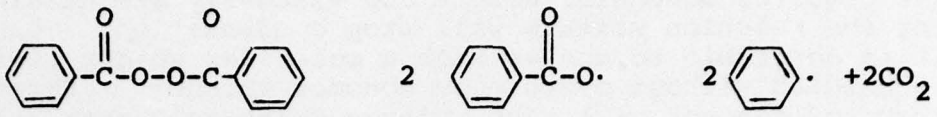
portant properties of the cured resin, such as higher tensile, flexural, and impact strength. The polyester monomer will also attain strength faster during the curing process. When the required molecular weight and viscosity are attained, cooling the reaction mixture will stop condensation. Generally, it is desirable to use as high a molecular weight resin as can be handled without overuse of monomer thinner. Excessive addition of monomer will give a large exothermic heat release, and a composite which is hard, brittle, subject to crazing, and possessing low mechanical and weathering characteristics.

Styrene was originally used as a monomer, and due to economics it has become the most generally used monomeric material. Actually, almost any of the common vinyl unsaturated compounds, which are compatible with the resin and will either homopolymerize or copolymerize with other reactive materials, may be used as a monomer. Between one and two moles of styrene are required for each mole of unsaturated acid in the original ester. Diallyl phthalate may also be added to slow down the cure rate. If a polyester is made from an unsaturated dibasic acid and propylene or diethylene glycol, a highly reactive resin results which forms a rigid thermoset upon curing due to a highly cross-linked structure. This resin is shown above. The addition of a saturated aromatic dibasic acid, such as phthalic anhydride or isophthalic acid, will give the cured polyester more resiliency than the resin with the unsaturated dibasic acid alone. The unsaturation contained within the aromatic ring is not subject to free radical attack, due to the inert nature of the benzene ring, so it does not enter into polymerization. Since there are no points of unsaturation outside the ring for cross-linking, more flexibility of the cured resin is allowed. However, the degree of flexibility allowed by aliphatic chain is not present due to the rigid aromatic ring structure. A flexible resin is manufactured by adding saturated dibasic acids, such as adipic and pimelic acids. Flexibility is imparted by the flexible aliphatic structure between the carboxylic acid groups. The increase in saturation reduces cross-linking, introducing longer chain lengths between cross-linking points. On a molecular level, more bending of the cured resin network is allowed, leading to a more flexible thermoset. Flexibilizers are frequently used in the pultrusion process to minimize thermally induced cracks.

Catalysts for Pultrusion

For pultrusion, a catalyst is desired which will dissociate slowly at room temperature and initiate polymerization with energy supplied through conductive heating or radio frequency radiation. Benzoyl peroxide used at 3% gives a pot

life of up to 7 days, and a fast cure within the die when conductive heating or radio frequency excitation is applied. Benzoyl peroxide dissociates to form aromatic radicals.



Resistance of Polyester to Environmental Effects

Hydrolysis is the main cause of chemical attack of polyester resins in an aqueous environment, resulting in chemical decomposition and resultant rupture of ester linkages in the polymer chain. Polyester resins possessing increased chemical resistance and thermal stability (and which also permit blending with a higher proportion of styrene) may be produced by condensing isophthalic-based formulations to higher molecular weight. Such polyester resin systems are now being used in the pultrusion process. Another chemically resistant polyester consists of hydrogenated bisphenol A combined with maleic, fumaric, and phthalic acids, and propylene glycol. The increased ring structure helps add chemical resistance; possibly, absence of tack during curing is imparted by the addition of bisphenol A. This resin also exhibits a high heat deflection temperature, low density, higher viscosity, low shrinkage during cure, and good adhesion to glass reinforcement, all of which contribute to resistance to hydrolysis.

APPENDIX C

DERIVATION OF STRUCTURAL EFFICIENCY EQUATIONS

Webcore Compression Panel

The mathematical models for the webcore panel considered both overall stability and strength under a uniaxially applied compressive load in the narrow direction of the panel. Overall stability was described using orthotropic sandwich plate theory[15] for a panel with simply supported edges. A maximum strain criterion was used to describe the strength limitations of the panel. The assumptions made were as follows:

1. Plane sections remain plane
2. Only small deflections admissable
3. The panel faces and webs are homogeneous and orthotropic.
4. The thickness of the web and faces are equal

Refer to Figure 43 for a diagram of dimensions used.

The equation for overall stability of an orthotropic sandwich panel as given in Reference 8 page 2.2.2-34 is:

$$N_x = \frac{K\pi^2}{b^2}\sqrt{D_{11}D_{22}} \qquad \text{(C-1)}$$

To express (C-1) in the form of a structural efficiency parameter it is convenient to divide both sides of the equation by the panel width b and replace the elastic constants D_{11} and D_{22} with equivalent expressions involving the elastic properties of the material and the panel dimensions. The result is:

$$\frac{N_x}{b} = \frac{a^2}{b\,m^2\pi^2}\left(a_{31} + a'_{31}\right) \qquad \text{(C-2)}$$

where a_{31} and a'_{31} are defined on page 2.2.2-34. The expressions for a_{31} and a'_{31} require some modification, however, since the dimensions of the panel are to be given as $\frac{a}{b}$, $\frac{t}{d}$ and $\frac{d}{a}$.

The factor a'_{31} is given in terms of eight expressions. The first simplification, as indicated on page 2.2.2-36, is to set ω equal to zero. Then by noting that $a_{22} \propto a_{13}$, $a_{32} \propto a_{11}$ and $a_{33} \propto a_{21}$, these eight expressions can be reduced to five. Factoring out common constants and substituting into (C-2), the final result is:

$$\frac{N_x}{b} = \frac{\pi^2 E_x}{2 m^2}\left(\frac{1 + t/d}{1 - \nu_{xy}\nu_{yx}}\right) \frac{t}{d}\left(\frac{d}{a}\right)^3\left(\frac{a}{b}\right)^5 (A + B) \tag{C-3}$$

where

$$A = m^4\left(\frac{b}{a}\right)^4 + 2 m^2\left(\frac{b}{a}\right)^2 n^2\left[\nu_{yx} + \frac{2 G_{xy}}{E_x}(1 - \nu_{xy}\nu_{yx})\right] + n^4 \frac{E_y}{E_x} \tag{C-4}$$

$$B = \frac{\pi^2 E_x}{2}\left(\frac{1 + t/d}{1 - \nu_{xy}\nu_{yx}}\right) \frac{t}{d}\left(\frac{d}{a}\right)^2 \left(\frac{a_{21}^2 a_{12} + 2 a_{11} a_{21} a_{13} - a_{11}^2 a_{23}}{a_{12} a_{23} + a_{13}^2}\right) \tag{C-5}$$

and

$$a_{11} = -m^3\left(\frac{b}{a}\right) - mn^2\left[\nu_{yx} + \frac{2 G_{xy}}{E_x}\left(1 - \nu_{xy}\nu_{yx}\right)\right] \tag{C-6}$$

$$a_{12} = G'_{cx} + \frac{\pi^2}{2}\left(1 + t/d\right)\frac{t}{d}\left(\frac{d}{a}\right)^2\left[\frac{m^2 E_x}{1 - \nu_{xy}\nu_{yx}} + n^2\left(\frac{a}{b}\right)^2 G_{xy}\right] \tag{C-7}$$

$$a_{13} = \frac{mn\pi^2}{2}\left(1 + t/d\right)\frac{t}{d}\left(\frac{d}{a}\right)^2\left[\frac{E_x \nu_{yx}}{1 - \nu_{xy}\nu_{yx}} + G_{xy}\right] \tag{C-8}$$

$$a_{21} = n^3 \frac{E_y}{E_x} + nm^2\left(\frac{b}{a}\right)^2\left[-\nu_{yx} + \frac{2 G_{xy}}{E_x}(1 - \nu_{xy}\nu_{yx})\right] \tag{C-9}$$

$$a_{23} = -\left(\frac{b}{a}\right)^2 G'_{cy} - \frac{\pi^2}{2}\left(1 + t/d\right)\frac{t}{d}\left(\frac{d}{a}\right)^2\left(\frac{b}{a}\right)^2\left[m^2 G_{xy} + n^2\left(\frac{a}{b}\right)^2 \frac{E_y}{1 - \nu_{xy}\nu_{yx}}\right] \tag{C-10}$$

The moduli of the face sheets are calculated by using laminated plate theory, and then with the assumption of homogeneity of the face material, equivalent moduli are calculated. The shear modulus for the webcore in the xz direction, G'_{cx}, was derived by reducing the web shear modulus G'_{xz} by the ratio of web thickness to panel unit width t/w:

$$G'_{cx} = G'_{xz}\left(\frac{t}{w}\right) \tag{C-11}$$

To relate panel unit width w to web width d, it is assumed that the face between the webs fails by local instability at the same strain as the webs. Using the equation for the local stability failure criteria from Reference 8 page 2.2.1-1, the critical strain for the face is:

$$\varepsilon_f = \frac{G_{xy}}{E_x}\left(\frac{t}{w}\right)^2 \tag{C-12}$$

and for the web:

$$\varepsilon_r = \frac{G'_{cx}}{E'_x}\left(\frac{t}{d}\right)^2 \tag{C-13}$$

Equating (C-12) and (C-13) gives

$$\frac{t}{w} = \sqrt{\frac{E_x}{E'_x}\frac{G'_{cx}}{G_{xy}}}\left(\frac{t}{d}\right) \tag{C-14}$$

Substituting (C-14) into (C-11) gives:

$$G'_{cx} = \frac{G'^2_{xz}}{G_{xy}}\frac{E_x}{E'_x}\left(\frac{t}{d}\right)^2 \tag{C-15}$$

For G'_{cy}, the web is modelled as a beam clamped at both ends with equal and opposite forces P perpendicular to the beam at each end. Then, the total displacement of the ends is the same as the apparent shear strain giving:

$$\gamma = \frac{Pd^2}{E'_z lt} \tag{C-16}$$

The apparent shear stress is:

$$\tau = \frac{P}{\ell t} \tag{C-17}$$

The shear modulus is τ/γ and by using (C-14) the shear modulus is:

$$G'_{cy} = \left(\frac{t}{d}\right)^3 \sqrt{\frac{G'_{cx}}{G_{xy}} \frac{E_x}{E'_x}}\ E'_z \tag{C-18}$$

The above expressions for the various moduli are substituted into (C-3). The integer values of m and n are then sought which minimize Nx/b where m and n denote the number of half wavelengths of the buckled panel in the x and y directions respectively.

The structural efficiency parameter for strength can be derived by writing an equation for the running load N_x in terms of strain:

$$N_x = 2E_x \varepsilon_f w \frac{t}{w} + E'_x \varepsilon_r d \frac{t}{w} \tag{C-19}$$

Typically the minimum compressive strain to failure is for a unidirectional layer loaded parallel to the fibers. By assuming that the panel fails when any one layer fails, the unidirectional ultimate strain $\varepsilon_{0^\circ}^{cu}$ can be substituted in (C-19). Dividing by b and using (C-14) gives:

$$\frac{N_x}{b} = \varepsilon_{0^\circ}^{cu} \frac{t}{d} \frac{d}{b} \left(2E_x + E'_x \sqrt{\frac{G'_{cx}}{G_{xy}} \frac{E_x}{E'_x}} \right) \tag{C-20}$$

The weight parameter used was W/ab^2. The total weight of the panel can be expressed as:

$$W = 2abt\rho_f + adt \frac{b}{w} \rho_r \tag{C-21}$$

Then dividing by ab^2 and using (C-14), the weight parameter equation becomes:

$$\frac{W}{ab^2} = \frac{t}{d} \frac{d}{b} \left(2\rho_f + \rho_r \sqrt{\frac{G'_{cx}}{G_{xy}} \frac{E_x}{E'_x}} \right) \tag{C-22}$$

The local instability structural efficiency parameter for the web is:

$$\sigma_{cr} = G'_{cx}\left(\frac{t}{d}\right)^2 = \frac{P_r}{dt} \qquad \text{(C-23)}$$

The load carried by the web then becomes:

$$P_r = G'_{cx}\,\frac{t^3}{d} \qquad \text{(C-24)}$$

The total load carried by the panel is:

$$P_{TOTAL} = 2P_f + P_r\,\frac{b}{w} \qquad \text{(C-25)}$$

The strains in the face and web are given by:

$$\varepsilon_f = \frac{P_f}{bt\,E_x} \qquad \text{(C-26)}$$

$$\varepsilon_r = \frac{P_r}{dt\,E'_x} \qquad \text{(C-27)}$$

Because of the Assumption 1, ε_f is equal to ε_r. Therefore P_f in terms of P_r is:

$$P_f = P_r\,\frac{b}{d}\,\frac{E_x}{E'_x} \qquad \text{(C-28)}$$

Substituting (C-24), (C-28) and (C-14) into (C-25) and dividing by b^2 gives:

$$\frac{N_x}{b} = \left(\frac{t}{d}\right)^3 \frac{d}{b}\,G'_{cx}\left(2\,\frac{E_x}{E'_x} + \sqrt{\frac{G'_{cx}}{G_{xy}}\,\frac{E_x}{E'_x}}\right) \qquad \text{(C-29)}$$

Single-Face Corrugated Compression Panel

An approximate solution to the stability problem for an isotropic plate with longitudinal stringers was obtained by Timoshenko[19] by energy methods. By application of the same method, Lekhnitski[15] also obtained an approximate solution for the case of a special orthotropic plate ($D_{16} = D_{26} = 0$).

The following assumptions were made:

1. Plane sections remain plane
2. Small deflections
3. The plate and stringers are homogeneous and orthotropic
4. The plate deflects and the stringer deflects and twists

Refer to Figure 44 for a diagram of dimensions used. By equating the increased potential energy of the system to the work done by the external forces, an equation for the running load N_x is obtained as:

$$N_x = \sqrt{D_{11} D_{22}}\ \frac{\int_0^b \phi\, dy + b \sum_{i=1}^{N} \left[\gamma_i \beta^4 f^2(\eta_i) + \chi_i \beta^2 f'^2(\eta_i) \right]}{\beta^2 \left[\int_0^b f^2 dy + b \sum_{i=1}^{N} \delta_i f(\eta_i) \right]} \qquad \text{(C-30)}$$

where

$$\phi = \sqrt{\frac{D_{22}}{D_{11}}} f''^2 - 2\beta^2 \nu_{yx} \sqrt{\frac{D_{11}}{D_{22}}} f f'' + \beta^4 \sqrt{\frac{D_{11}}{D_{22}}} f^2 + \frac{4 D_{66} \beta^2 f'^2}{\sqrt{D_{11} D_{22}}} \qquad \text{(C-31)}$$

$$\delta_i = \frac{A_s E'_x}{b t E_x} \qquad \text{(C-32)}$$

$$\gamma_i = \frac{E'_x I_s}{b \sqrt{D_{11} D_{22}}} \qquad \text{(C-33)}$$

$$\chi_i = \frac{J_s G'_{xy}}{b \sqrt{D_{11} D_{22}}} \qquad \text{(C-34)}$$

$$\beta = \frac{m\pi}{a}, \quad m = 1, 2, 3 \ldots \tag{C-35}$$

$$\eta_i = (i - 1/2)(w + d) \tag{C-36}$$

In deriving (C-30), conditions on the supported (loaded) edges and at the end of the stringers were met by assuming that deflections are given by:

$$\Delta = f(y) \sin \beta x \tag{C-37}$$

$$\Delta_i = f(\eta_i) \sin \beta x \tag{C-38}$$

$$\theta = f'(\eta_i) \sin \beta x \tag{C-39}$$

To solve the equation, an expression for functions in the form of a series with undetermined coefficients was introduced as follows:

$$f = \sum_m A_{mn} f_n(y) \tag{C-40}$$

A nontrivial solution requires that the determinant of the coefficients be zero. The smallest root of these homogeneous equations gives the critical load. For a plate with simply supported sides

$$f = \sum_m A_{mn} \sin \frac{n\pi y}{b} = \sum A_{mn} \sin \alpha y \tag{C-41}$$

The above expressions are now substituted into (C-30). Dividing by b^2 the result is:

$$\frac{N_x}{b} = \frac{R + S}{\frac{1}{2} + \frac{A_s E'_x}{bt E_x} \sum \sin^2(\alpha \eta)} \tag{C-42}$$

where

$$R = \frac{t^3}{24\,b(1-\nu_{xy}\nu_{yx})}\left[E_y\frac{\alpha^4}{\beta^2} + E_x\left[2\nu_{yx}\alpha^2+\beta^2\right] + 4G_{xy}(1-\nu_{xy}\nu_{yx})\alpha^2\right] \tag{C-43}$$

$$S = \frac{\beta^2 E'_x I_s}{b^2}\sum_{i=1}^{N}\sin(\alpha\eta_i) + \frac{G'_{xy}J_s\alpha^2}{b^2}\sum_{i=1}^{N}\cos(\alpha\eta) \tag{C-44}$$

I_s is the moment of inertia of the stringer. According to Reference 19 page 399, this should be taken with respect to the outer surface of the stringer to account for the stiffening effect of the plate.

J_s is a factor like the polar moment of inertia in the torsion of a non-circular shaft. A table of values for various cross-sections can be found in Reference 20. A_s is the cross-sectional area of the stringer.

The panel dimensions chosen for this analysis are shown in Figure 44. This results in the following values:

$$I_s = {}^2/_3\,A t d^3 \tag{C-45}$$

$$J_s = d A^3 t^3 \tag{C-46}$$

$$A_s = 3 A t d \tag{C-47}$$

These expressions are now substituted into (C-42). Furthermore, panel dimensions are rearranged so that all are expressed as t/d, d/b and b/a. The final result is:

$$\frac{N_x}{b} = \frac{K+L}{\frac{1}{2} + 3A\frac{d}{b}\frac{E'_x}{E_x}\sum_{i=1}^{N}\sin^2\left(\frac{n\pi}{b}\eta_i\right)} \tag{C-48}$$

where

$$K = \frac{\pi^2}{12(1-\nu_{xy}\nu_{yx})}\left(\frac{t}{d}\right)^3\left(\frac{d}{b}\right)^3\left[\frac{E_y}{2}\left(\frac{a}{b}\right)^2\frac{n^4}{m^2} + E_x\left(\nu_{yx}n^2 + \frac{1}{2}m^2\left(\frac{b}{a}\right)^2\right) + 2G_{xy}n^2(1-\nu_{xy}\nu_{yx})\right] \tag{C-49}$$

$$L = A\pi^2\left(\frac{t}{d}\right)^3\left(\frac{d}{b}\right)^4 n^2 \left[\frac{2}{3}\left(\frac{b}{a}\right)^2\left(\frac{m}{n}\right)^2\left(\frac{d}{t}\right)^2 E_x' \sum_{i=1}^{N} \sin^2\left(\frac{n\pi}{b}\eta_i\right) + A^2 G_{xy}' \sum_{i=1}^{N} \cos^2\left(\frac{n\pi}{b}\eta_i\right)\right] \quad \text{(C-50)}$$

The number of stringers N must be expressed in terms of panel dimension ratios and elastic moduli to be used in these expressions. First of all,

$$N = \frac{t}{d+w} \quad \text{(C-51)}$$

Unit plate width d + w must be related to unit stringer width d. Employing the same method used in deriving (C-14)

$$\epsilon_s = \frac{G_{xy}'}{E_x'}\left(\frac{At}{d}\right)^2 \quad \text{(C-52)}$$

$$\epsilon_p = \frac{G_{xy}}{E_x}\left(\frac{t}{d+w}\right)^2 \quad \text{(C-53)}$$

Equating ϵ_s and ϵ_p

$$\frac{t}{d+w} = \sqrt{\frac{E_x}{E_x'}\frac{G_{xy}'}{G_{xy}}}\,\frac{At}{d} \quad \text{(C-54)}$$

Substituting (C-54) into (C-51) and simplifying gives

$$N = A\frac{b}{d}\sqrt{\frac{E_x}{E_x'}\frac{G_{xy}'}{G_{xy}}} \quad \text{(C-55)}$$

This expression for N is substituted into (C-48) and the expression minimized with respect to integer values of m and n. The lowest value is the critical load.

The local stability structural efficiency parameter is derived by considering the total load carried by the panel as the sum of the plate load and the stringer loads as follows:

$$P_{TOTAL} = P_p + N P_s \tag{C-56}$$

However, the stringer is made of three equal elements that carry equal loads P_e. The strain in the plate and stringer elements can be expressed as:

$$\epsilon_p = \frac{P_p}{bt E_x} \tag{C-57}$$

$$\epsilon_s = \frac{P_e}{dAt E'_x} \tag{C-58}$$

Because of Assumption 1, the strains in the plate and stringer element are equal. Setting $\epsilon_p = \epsilon_s$ and solving for P_p gives:

$$P_p = \frac{b}{d} \frac{P_e E_x}{A E'_x} \tag{C-59}$$

The local stability failure criteria for the stringer element is:

$$P_e = A^3 G'_{xy} \frac{t^2}{d} \tag{C-60}$$

Considering that $3P_e = P_s$, substitute (C-59), (C-60) and (C-55) into (C-56). Divide this by b^2 to obtain the local stability parameter as

$$\frac{N_x}{b} = G'_{xy} \left(\frac{t}{d}\right)^3 \frac{d}{b} \left[A^2 \frac{E_x}{E'_x} + 3A^4 \sqrt{\frac{G'_{xy}}{G_{xy}} \frac{E_x}{E'_x}} \right] \tag{C-61}$$

The ultimate compressive strength parameter is based on the minimum strain criterion. The minimum strain to failure in compression is for a unidirectional layer loaded parallel to the fibers. The loads carried by the plate and a stringer respectively are:

$$P_p = E_x \varepsilon_p b t \tag{C-62}$$

$$P_s = 3 E'_x \varepsilon_s dA t \tag{C-63}$$

Then the total load carried by the panel is:

$$P_{TOTAL} = E_x \varepsilon_p b t + 3 N E'_x \varepsilon_s dA t \tag{C-64}$$

Again using Assumption 1, the minimum strain criterion is $\varepsilon_p = \varepsilon_s = \varepsilon_{0^\circ}^{cu}$. Dividing (C-64) by b^2 and substituting in (C-55) gives, for the strength parameter

$$\frac{N_x}{b} = \frac{t}{d} \frac{d}{b} \varepsilon_{0^\circ}^{cu} \left[E_x + 3 E'_x A^2 \sqrt{\frac{G'_{xy}}{G_{xy}} \frac{E_x}{E'_x}} \right] \tag{C-65}$$

The weight parameter is W/ab^2. The total weight of the panel can be expressed as:

$$W = abt\rho_p + 3NadtA\rho_s \tag{C-66}$$

Dividing by b^2 and using (C-55) the weight parameter equation becomes:

$$\frac{W}{ab} = \frac{t}{d} \frac{d}{b} \left[\rho_p + 3 A^2 \rho_s \sqrt{\frac{G'_{xy}}{G_{xy}} \frac{E_x}{E'_x}} \right] \tag{C-67}$$

LIST OF SYMBOLS

A	constant. Also used to relate stringer thickness to plate thickness
B	constant
D	term in constitutive equation
E	Youngs modulus
G	shear modulus
I	moment of inertia
K,L	constants
N	no. of stringers
P	load
R,S	constants
T	torque
W	structural weight
X	design allowable
a,b,c	dimensions of panel
d	depth (core)
l	unit length (webcore panel)
m,n	half wave lengths
t	panel thickness
w	web or stringer spacing
γ	shear strain
ϵ	strain
ρ	density
τ	shear stress
ν	Poisson's ratio
θ	rotation

Subscripts

cr	critical
cx	web-core
e	P_c refers to 1/3 of total stringer load
f	face (web-core panel)
o	direction with load axis
p	plate (single-face corrugated panel)
r	rib (in web-core panel)
s	stringer (single-face corrugated panel)
x,y,z	coordinate system referred to arbitrary axes
1,2,3	coordinate system referred to material principal axes

Superscripts

'	*web or stringer*
cu	compressive ultimate